“SAPIENZA” UNIVERSITY OF ROME

“The Role of NFI-A in Hematopoietic Lineage Specification and Differentiation”

A Thesis by

Linda Marie Starnes

SUBMITTED TO THE DEPARTMENT OF HISTOLOGY AND MEDICAL EMBRYOLOGY

IN PARTIAL FULFILMENT OF THE REQUIREMENTS FOR THE DEGREE OF DOCTOR OF PHILOSOPHY IN CELL SCIENCE AND MORPHOGENESIS (XXII CYCLE)

ROME, ITALY

October, 2009

Table of Contents

Acknowledgements *4*

Abstract *5*

Chapter One: Introduction *6*

1.1 Primitive hematopoiesis **7**

1.2 Embryonic definitive hematopoiesis **9**

1.3 Adult definitive hematopoiesis **14**

1.3.1 Extrinsic factors regulating self renewal and differentiation of HSCs & HPCs 15

1.3.2 Intrinsic Factors Regulating self renewal and differentiation of HSCs & HPCs 18

1.3.3 Role of TFs in leukemia 23

1.3.4 microRNAs add to the complexity of intrinsic regulation by regulating key TFs 25

1.3.5 Nuclear Factor I (NFI) TFs 28

RESEARCH AIMS *30*

Chapter Two: MATERIALS AND METHODS *31*

2.1 Cell culture **31**

2.1.1 AML Cell Lines 31

2.1.2 Human cord blood (CB) hematopoietic progenitor cell (HPC) purification, suspension culture and clonogenic assay. 31

2.1.3 Primitive erythroid progenitor (EryP-CFC) assay 32

2.1.4 Embryonic definitive colony assay 33

2.2 Mouse Tissues **34**

2.2.1 Embryonic Tissues 34

2.2.2 Adult Tissues 34

2.3 Cellular Morphologic analysis **35**

2.4 Flow cytometry **36**

2.5 Indirect Immunofluorescence **36**

2.6 Immunoblotting **36**

2.7 RNA extraction and analysis **37**

2.8 Chromatin Immunoprecipitation (ChIP) assay **39**

2.9 Plasmids and constructs **40**

2.10 Luciferase Assay **42**

2.11 Lentiviral production and infection **42**

2.12 Statistical analysis **44**

Chapter Three: RESULTS *45*

3.1 AIM I: To examine if deregulated miR-223 expression is associated with differentiation block underlying the pathogenesis of distinct leukemia subtypes, and to determine regulating factors involved. **45**

3.2 AIM II: To determine the function of TF NFI-A in normal human adult definitive hematopoiesis using both leukemic cell lines and primary culture of HPCs. **47**

3.2.1 NFI expression patterns in HL-60 and K562 leukemia cells and during unilineage E and G culture of human hematopoietic progenitor cells (HPCs). 47
3.2.2 NFI-A expression is upmodulated during erythropoiesis, while shut off during granulopoiesis. 49
3.2.3 NFI-A upregulation is required for erythroid differentiation of HPCs 51
3.2.4 NFI-A accelerates erythroid differentiation of K562 cells, HPCs, and it restores erythropoiesis of HPCs in the presence of suboptimal or minimal erythropoietin (Epo) stimulus. 53
3.2.5 NFI-A downmodulation is necessary to permit granulocytic differentiation/ maturation 56
3.2.6 NFI-A is a regulator of the erythro-granulocytic lineage decision 59
3.2.7 A functional relationship between NFI-A levels and two lineage-associated genes: β-globin and G-CSFR 64
3.2.8 NFI-A directly activates β-Globin and represses G-CSFR proximal promoters, exhibiting a dual transcriptional activity in a lineage-specific context 66

3.3 AIM III: To determine the role of TF NFI-A during both embryonic primitive and definitive hematopoiesis using the mouse as a model system. 71

Chapter Four: DISCUSSION & FUTURE DIRECTIONS 82

REFERENCES 92

APPENDIX I 102

Acknowledgements

I would like to first acknowledge my supervisor Dr. Clara Nervi for giving me the opportunity to complete a Ph.D. within her lab, and for her guidance over the past four years. I also give thanks to all of the Nervi lab members for their support and making my time in the lab enjoyable, and to my coordinator of the Ph.D. program Dr. Mario Molinaro. I would also like to thank all of the collaborators of Dr. Cesare Peschle's lab in particular Dr. Antonio Sorrentino as well as collaborators Dr. Elisabetta Vivarelli and Dr. Luciana De Angelis.

Abstract

Hematopoietic lineage commitment and differentiation is governed largely by a selective combination of transcription factors (TFs). The TF Nuclear Factor I-A (NFI-A) is a member of the NFI TF family that are known for their positive and negative transcriptional regulatory roles in a cell type and promoter specific context. NFI-A has a major role in brain development, and shows a unique pattern of expression in the developing mouse embryo. NFI-A was previously noted by our group as a relevant target of the myeloid regulator microRNA-223, whereas nothing is known on its role in normal human erythro-granulopoiesis. Here we have identified NFI-A as being necessary for directing hematopoietic progenitors (HPCs) to the erythroid (E) or granulocytic (G) lineage. In cord blood $CD34^+$ HPCs placed in hematopoietic unilineage culture differentiation systems, we demonstrated a lineage specific expression pattern of NFI-A: during E differentiation it is strongly upregulated whereas during G differentiation is markedly downregulated. Using lentiviral vectors encoding NFI-A and siNFI-A for expression in myeloid cell lines and in $CD34^+$ HPCs, we showed that NFI-A is required for E differentiation and its overexpression enhances E differentiation under suboptimal erythropoietin concentrations. Conversely, the silencing of NFI-A during unilineage G differentiation is required as its overexpression blocks G differentiation. Using an (E+G) bilineage culture system exogenous manipulation of NFI-A was found to direct HPCs to the E or G fate. Finally, a dual and opposite transcriptional action of NFI-A was identified by activating the β-globin promoter and repressing G-CSF receptor expression. Our current microarray based studies implicate NFI-A in upregulating a subset of erythroid genes in $CD34^+$ transduced HPCs (related to globin and heme biosynthesis and important erythrocyte membrane structural proteins). Ongoing characterization of NFI-A during hematopoietic ontogeny in the mouse implicates it in possibly having a role in primitive erythropoiesis and future studies using NFI-$A^{-/-}$ mice in combination with lentiviral technology will allow a deep examination of NFI-A function during both primitive and definitive embryonic hematopoiesis. Our data indicating the necessity of proper levels of NFI-A during hematopoietic differentiation of erythroid and granulocytic compartments indicates that NFI-A could be involved in the pathogenesis of haematological diseases further underlying its importance in hematopoietic development.

Chapter One: Introduction

Hematopoiesis (from Ancient Greek: *haima* blood; *poiesis* to make) refers to the production of the cellular component of blood, which is necessary throughout vertebrate life as mature blood cell types have a limited lifespan. The key to the maintenance of hematopoietic homeostasis is the pluripotent long-term hematopoietic stem cell (LT-HSC) with the dual capacity of self-renewal to produce additional LT-HSCs as well as differentiation to form all blood cell lineages and is defined by its capability to reconstitute the entire blood system of sequential adult recipients indefinitely. The HSCs that we are endowed with in life arise during embryonic development. Within the mammalian conceptus the hematopoietic system is one of the first complex tissues to be formed during ontogeny, derived from the mesodermal germ layer, with the allocation and specification of distinct blood cells in sequential overlapping sites including the yolk sac, an area including and surrounding the dorsal aorta termed the aorta-gonad-mesonephros (AGM) region, the placenta, fetal liver and finally the spleen and bone marrow [1] (Figure 1-1). To date HSC development has been characterized in most detail in the mouse, which serves as a model for human hematopoiesis [2-4]. The term hematopoiesis can be further diverged into two terms ‘primitive’ and ‘definitive’ hematopoiesis.

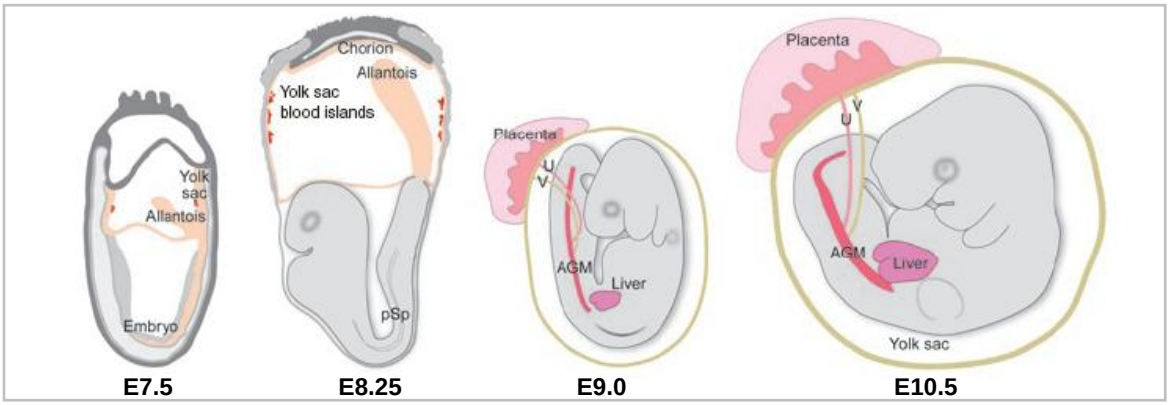

Figure 1-1 Sequential generation of hematopoietic cells within the mouse conceptus. E7.5 (Embryonic day 7.5 post coitus) shows the formation of the yolk sac being the site of primitive hematopoiesis within yolk sac blood islands at E8.25. The outgrowth of the allantois in E7.5 and E8.25 fuses with the chorion to form the placenta at E9.0. The circulation is established at E8.25-8.5. The E9.0 embryo has turned and is enveloped in the yolk sac. Hematopoietic colonization of the fetal liver begins at E9.0 which serves as a maturation and expansion site for HSCs and progenitors until birth. The E10.5 conceptus has hematopoietic clusters in the AGM region, the vitelline (V) and umbilical (U) arteries, and placenta where the first adult HSCs are formed. *[Modified from Dzierzak, E. & Speck, N.A. Of lineage and legacy: the development of mammalian hematopoietic stem cells. Nature Immunology. 9, 129-136 (2008)].*

1.1 Primitive hematopoiesis

During mammalian embryonic development, the earliest set of mesodermal cells enriched for Bry^+ $Flk1^+$ and $Flk1^+$ Scl^+ emigrating from the posterior primitive streak (E6.5-E7.0) termed 'hemangioblasts' [5] migrate to form the extraembryonic yolk sac, and slightly later the allantois (Figure 1-2).

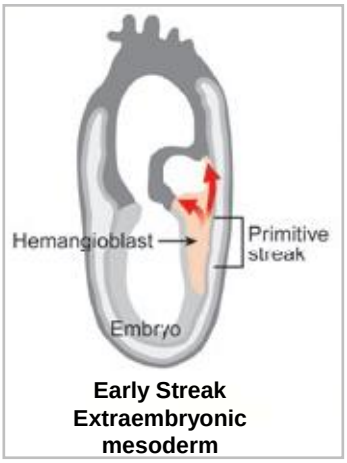

Figure 1-2 Mesodermal migration during early-streak stage in the mouse conceptus to form extraembryonic mesoderm. Emerging from the posterior primitive streak are waves of yolk sac mesoderm migrating to form this extraembryonic tissue. Hemangioblasts are found in the posterior primitive streak. Red arrows indicate emigration of mesoderm after egression from the primitive streak. *[Modified from Dzierzak, E. & Speck, N.A. Of lineage and legacy: the development of mammalian hematopoietic stem cells. Nature Immunology. 9, 129-136 (2008)].*

Hemangioblasts can give rise to both endothelial and hematopoietic progenitors, several of which contribute to the formation of each blood island [6, 7]. Yolk sac blood islands begin to form at E7.5, with primitive erythroblast progenitors (EryP-CFCs) present in the yolk sac

transiently from E7.25 to E9.0 giving rise to primitive erythroblasts (EryPs) that enter circulation by E8.5 whose function is to provide oxygenation to the rapidly growing embryo (Figure 1-3).

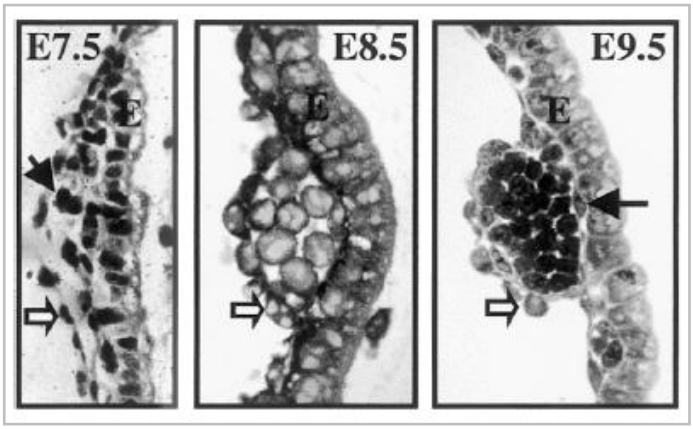

Figure 1-3 Yolk sac blood islands develop between E7.5 and E9.5. Yolk sac blood islands develop from undifferentiated mesoderm cells (E7.5 closed arrow) that give rise to inner blood cells (primitive erythroblasts) and outer endothelial lining (E9.5 closed arrow). Yolk Sac blood islands form between a single layer of endoderm cells (E) and mesothelial cells (open arrow). Primitive erythroblasts within each island are called primitive due to their resemblance to nucleated non-mammalian erythroblasts. *[Palis, J. & Yoder, M.C. Yolk-sac hematopoiesis: The first blood cells of mouse and man. Experimental Hematology. 29, 927-936 (2001).]*

Over the next 8 days the EryPs mature in the circulation whereas definitive erythroblasts mature in the fetal liver and post-natal bone marrow within erythroblastic islands [8]. In circulation EryPs undergo changes well recognized in maturing definitive erythroid progenitors of the adult-type in the fetal liver and adult bone marrow: their number of cell divisions is limited, hemoglobin concentration increases, nuclear condensation occurs, progressive decrease in cell size and enucleation follows [9]. Distinguishing them from definitive erythroid cells are their large size (approximately six fold larger) and nearly four times the amount of hemoglobin content (80pg/cell) [10]. Definitive erythroid cells in the mouse express adult globins, whereas primitive erythroblasts initially express embryonic (ζ, βH1, and εγ) globins and during maturation also synthesize adult (α1,α2, β1, and β2) globins [10]. Primitive hematopoiesis is not limited to cells of the erythroid lineage, for example, Klimchenko and colleagues recently defined a novel bipotential hematopoietic progenitor (MEP-P) from the hemangioblast that gives rise to both primitive erythrocytes and primitive megakaryocytes [11]. Also, in the past careful analysis of staged embryos indicated the

emergence of macrophage progenitors associated temporally and spatially with primitive erythroid progenitors at E7.25 [12]. Therefore the term 'primitive' erythropoiesis should be used to describe cellular lineages arising temporally and spatially with the EryPs in the presomitic yolk sac [13].

1.2 Embryonic definitive hematopoiesis

The term definitive hematopoiesis can be used to describe the hematopoietic lineages that emerge with the definitive erythroid lineage in the somite stage yolk sac, the AGM, fetal liver, and postnatal bone marrow [13].

Within the yolk sac definitive erythroid progenitors burst forming units-erythroid (BFU-E) are found at the beginning of somitogenesis at E8.25, and expand in the yolk sac. They are found in increasing numbers in the bloodstream between E9.5 and E10.5 and expand exponentially and differentiate in the liver soon after it emerges as a hematopoietic organ (E10.0). Unipotential mast cell progenitors, bipotential granulocyte-macrophage progenitors, as well as macrophage and megakaryocyte progenitors expand in the yolk sac with the same temporal kinetics as BFU-E, subsequently being found in the bloodstream and fetal liver [12]. A potent neonatal engrafting HSC was identified in the E9.0 mouse yolk sac, and that when injected into the liver of neonatal recipient mice can yield considerable multilineage engraftment, however, these cells are not capable of engrafting adult mice [14] indicating an additional *in vivo* maturation step is needed for them to acquire adult type definitive HSC properties. Recent cell tracing experiments also indicate that some HSCs arising from the yolk sac colonize the umbilical cord, AGM and embryonic liver [15]. Thus, it is clear that the yolk sac is not only an organ of primitive erythropoiesis, but also provides the first committed progenitors and may provide HSCs which their exact role in contributing to the adult HSC pool remains to be determined.

During the mid to late streak stage mesoderm emerging from the anterior primitive streak forms the paraxial and lateral mesoderm of the trunk region of the embryo. The para-aortic splanchnopleura (P-SP) region in the mouse develops from the intraembryonic lateral plate mesoderm contacting the endoderm. The aorta first develops from the P-SP, and primordiums of the mesonephros, mesentery and gonads soon become apparent after E10.0; this region has thus been named the AGM (Figure 1-4).

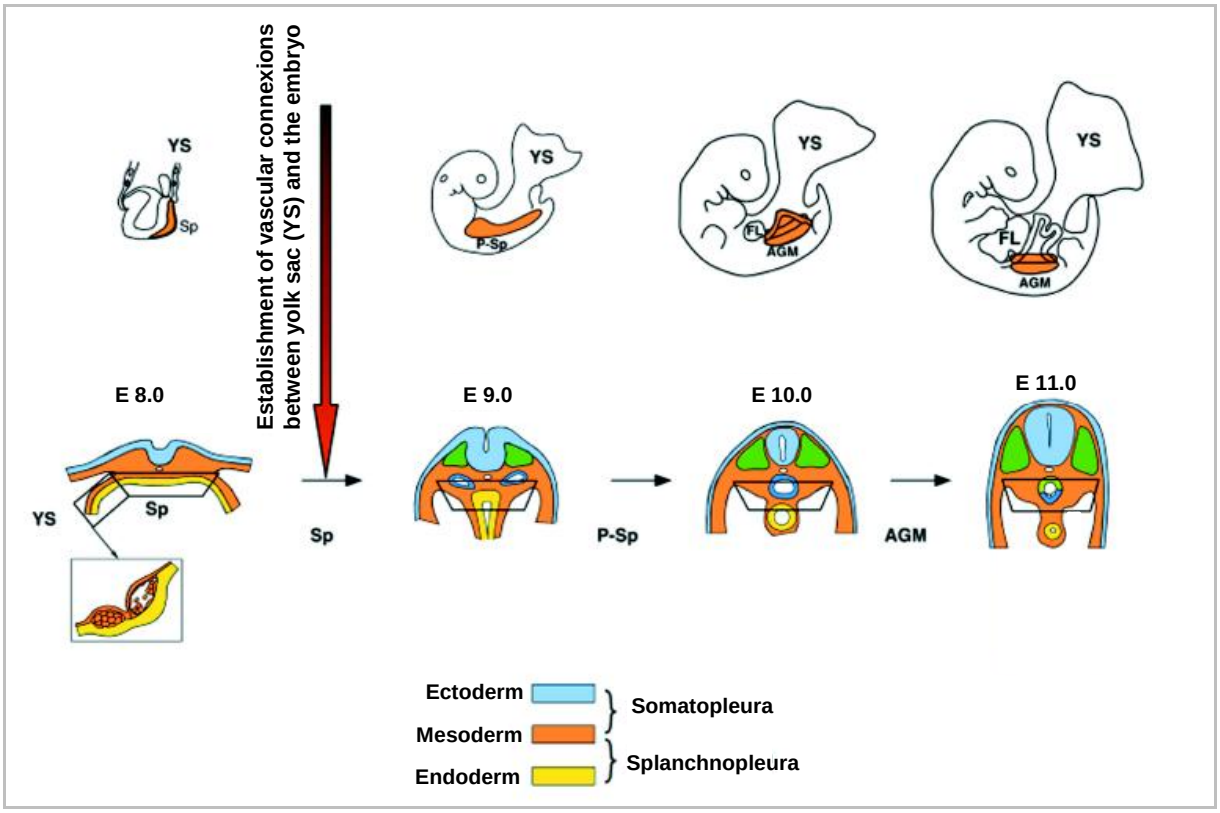

Figure 1-4 Localization and evolution of the intra-embryonic hemogenic site in the mouse embryo. Shown above in whole embryos is the presumptive intra-embryonic hemogenic site at E8.0 before the connexion of the extra- and intra- embryonic vessels: SP, and later the hemogenic site derived from it, the P-SP (E8.5-10.0), and then the AGM (E10.0-12.0). In the lower part the boxed areas indicate the structure of the presumptive hemogenic site (SP), and later the tissue composition between E8.5-11.0 known to contain HSCs within the P-SP/AGM. *[Modified from Godin, I. & Cumano, A. Of birds and mice. Hematopoietic stem cell development. Int. J. Dev. Biol. 49, 251-257 (2005)].*

Transplantation of various regions of the E8.0-E12.0 mouse conceptus has shown that LT-HSCs conferring complete, long term, hematopoietic reconstitution of adult irradiated recipients appear only at E10.5-E11.5 in the AGM region of the embryo body, and in the vitelline and umbilical arteries [16-18]. The ventral wall of the aorta as well as the vitelline and

umbilical arteries contain specialized vascular cells called ‘hemogenic endothelium’. It is thought that from the hemogenic endothelium, HSCs arise as intra-arterial hematopoietic clusters [19] (Figure 1-5C). Significant numbers of HSCs are also found in the mouse placenta as early as E9.0 [20, 21] nearly coincident with the appearance of HSCs in the AGM region. The relative contribution of the AGM, vitelline and umbilical arteries, and placenta to the final pool of adult HSCs is largely unknown [22].

It is clear from studies of knockout animals that HSC specification involves known developmental signaling pathways (ventralizing factors such as bFGF, TGFβ, VEGF-Flk-1, as well as BMP4 signaling) [23-25] that converge on the expression of a few pivotal transcription factors (TFs). The CBFA2/AML1/RUNX1 TF is required for definitive hematopoiesis [26, 27]. RUNX1 is pivotal to HSC generation in the vascular regions of the mouse conceptus- the aorta, vitelline and umbilical arteries, and placenta [28], and was recently shown that AML1 function is essential in endothelial cells for hematopoietic progenitor and HSC formation from the vasculature [29] (Figure 1-5A,B). GATA-2 TF deficient mice suffer from impaired primitive erythropoiesis and a complete lack of committed progenitors and HSCs and die by E10.5 [30]. GATA-2 is also expressed in the aortic endothelium and is thought to affect the expansion of the hemogenic population emerging from these cells [31]. SCL/Tal-1 and LMO2 deficient mice die embryonically with defects in both primitive and definitive hematopoiesis [32, 33].

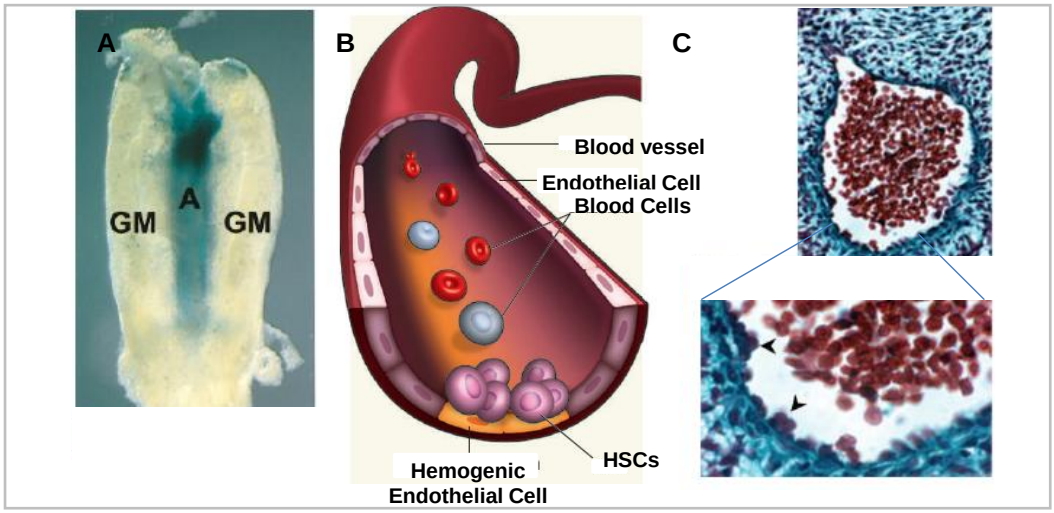

Figure 1-5 AML1 expression in the *Cbfa2-lacZ* knockin mouse conceptus at E11.0 and a schematic and histology of the dorsal aorta intraaortic clusters. (A). AML1 expression in sub regions of the AGM showing abundant staining in the area containing the dorsal aorta and mesenchyme (A), with only few cells stained in the gonad-mesonephros region (GM). **(B)** A schematic of the relationship between endothelial cells and blood cells where a subset of endothelial cells = hemogenic endothelium give rise to HSCs within blood vessels of the embryo **(C)** Trichrome staining showing intra-aortic hematopoietic clusters in the E11.5 dorsal aorta arising from hemogenic endothelium. Close up: ventral intraaortic clusters attached to the endothelial lining of the aorta (arrowheads) of a normal mouse dorsal aorta. *[Modified from: (A) de Bruijn, M., et al. Definitive hematopoietic stem cells first develop within the major arterial regions of the mouse embryo. EMBO J 19(11), 2465-2474 (2000). (B) Yoshimoto, M. & Yoder, M.C. Birth of the blood cell. Nature News and Views 457, 801-803 (2009). (C) Taoudi, S. & Medvinsky, A. Functional identification of the hematopoietic stem cell niche in the ventral domain of the embryonic dorsal aorta. PNAS 104 (22), 9399-9403 (2007)]*

The liver becomes the predominant hematopoietic site by E11.5 in the mouse, and instead of *de novo* generation of HSCs or progenitors serves as a site for their maturation, until their final seeding of the bone marrow late in fetal life [34, 35]. The first phase of fetal liver seeding is initiated at E9.5-E10.5 as the fetal liver rudiment becomes colonized by myelo-erythroid progenitors that generate definitive erythroid cells. This first wave of seeding is probably derived from the yolk sac's numerous definitive progenitors as the first vascular connections to the fetal liver through vitelline vessels are established [36]. HSCs arising from the embryonic regions at E10.5 mentioned above, migrate to the liver at E11.5 and proliferate between E13.0-E15.0 to considerably increase their numbers [37]. It is likely that the majority of HSCs colonizing the liver derive from the AGM and placenta via the umbilical vessels-the second major vascular circuit that connects to the fetal liver [36]. Fetal liver HSCs appear to follow the same differentiation hierarchy as bone marrow derived HSCs (discussed in "Adult

definitive hematopoiesis" below), but they show a higher proliferative capacity [38], have unique surface markers compared to bone marrow HSCs (Figure 1-6) [39] are less strictly lineage restricted [40], and erythroid progenitors are more readily obtained from precursors [41]. The early fetal liver is rich in colony-forming unit erythroid (CFU-Es) and proerythroblasts reflecting active definitive erythropoiesis, whereas myeloid and lymphoid progenitors accumulate with developmental age [36]. Little is known about the fetal liver HSC niche that promotes signals of symmetric self-renewal to expand the fetal HSC pool, whereas more is known about the adult bone marrow HSC niche. By day E15.0 the fetal spleen becomes hematopoietic and remains an extramedullary hematopoietic organ in adult life [37], followed by the skeletal system which develops during the third week of mouse gestation, concomitantly establishing a unique micro-environment within the bone marrow for the pool of HSCs found here at E17.5 onwards that are responsible for maintenance of adult definitive hematopoiesis [20, 42] (Figure 1-6).

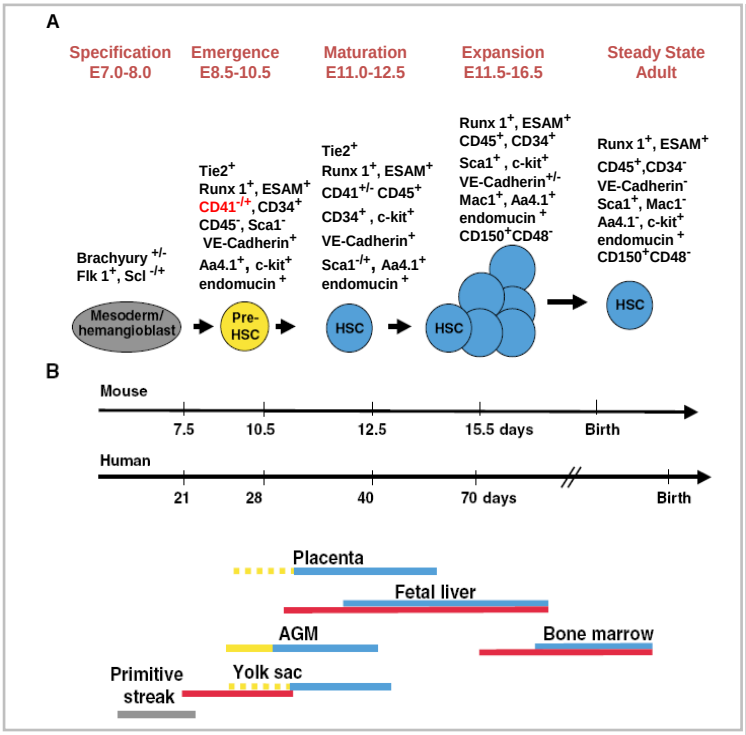

Figure 1-6 Establishment of definitive HSC pools in mouse and human embryos. (A). Hematopoietic development begins with specification of primitive streak mesoderm to hematopoietic and vascular fates. Nascent HSCs mature (blue) that allows them to engraft, survive, and self renew in future hematopoietic niches. Fetal HSCs expand rapidly after which a steady state is established in which HSCs reside in a relatively quiescent state in bone marrow. HSC markers at specific stages of mouse development are indicated; CD41 is indicated in red since its expression defines hematopoietic commitment. **(B)** The ages at which mouse and human hematopoietic sites are active. Gray bars indicate mesoderm; red bars active hematopoietic differentiation; yellow bars HSC genesis; blue bars presence of functional adult-type HSCs. Broken yellow bars for yolk sac and placenta indicate that *de novo* HSC genesis remains to be proven experimentally. *[Modified from Mikkola, H.K & Orkin, S.H. The journey of developing hematopoietic stem cells. Development 133, 3733-3744 (2006)]*

1.3 Adult definitive hematopoiesis

Rare LT-HSCs residing in the bone marrow of adult mammals, sit atop a hierarchy of more mature and increasingly lineage-restricted progenitors. They are characterized by unique surface markers within the mouse listed in Figure 1-6, and in humans are characterized as a $CD34^{+}$ $CD38^{-}$ population. During lineage commitment and restriction of LT-HSCs, they reduce their replicative potential as they form short-term hematopoietic stem cells (ST-HSCs) capable of repopulating bone marrow of a recipient only short term. ST-HSCs become more lineage restricted giving rise to hematopoietic progenitor cells (HPCs) of the myeloid or lymphoid compartments. The multipotent progenitor termed the common myeloid progenitor (CMP) [the functional equivalent of colony forming unit-granulocyte erythroid macrophage megakaryocyte (CFU-GEMM)] becomes more committed as the bipotent megakaryocyte/erythrocyte progenitor (MEP) or the granulocyte/monocyte progenitor (GMP). The genetic programs of the descendents of these progenitor types becomes fixed towards a single lineage producing unilineage precursors of the erythroid (E), megakaryocytic (Mk), granulocytic (G), and monocytic (M) lineages [respectively termed BFU-E and BFU-Mk, CFU-G and CFU-M] that give rise to mature circulating blood cells [22] (Figure 1-7).

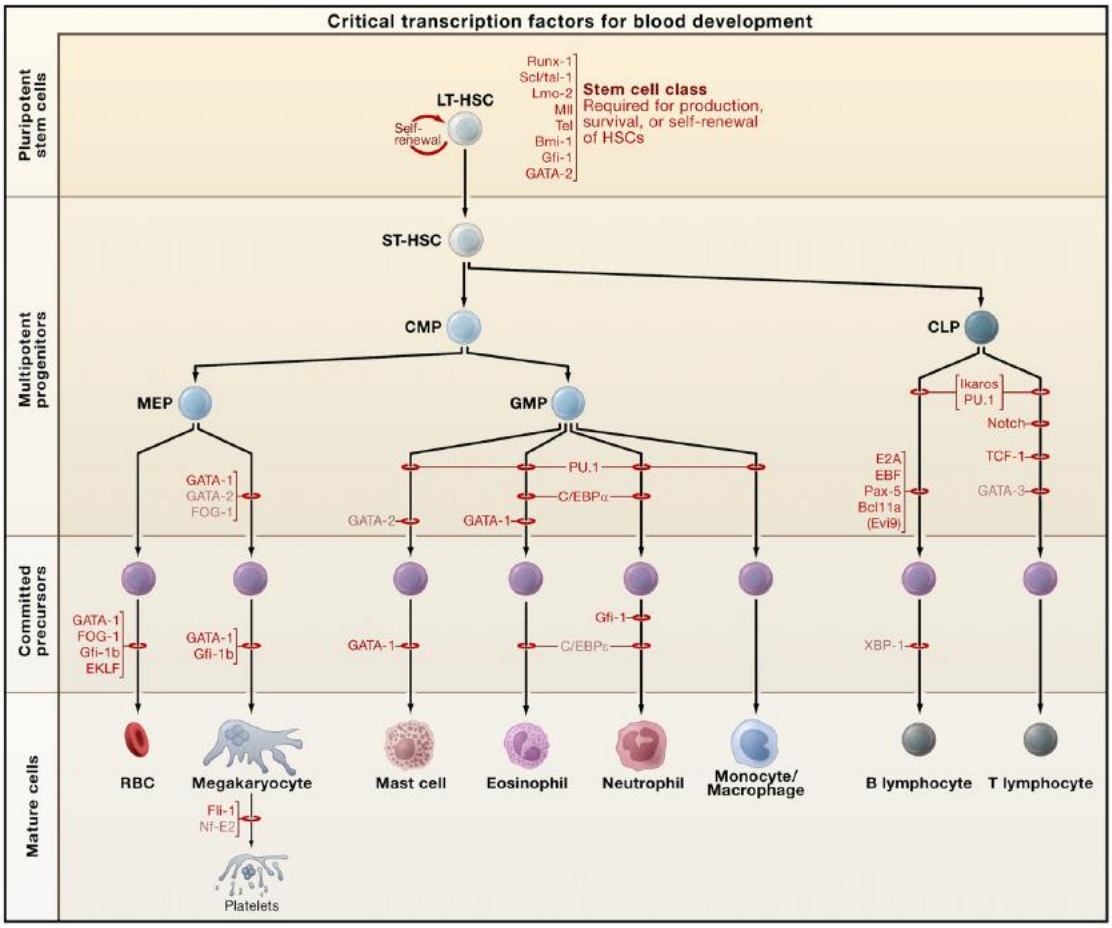

Figure 1-7. The hierarchy of hematopoiesis from the pluripotent LT-HSC to the differentiation of mature blood cells. Critical TFs for blood development are shown as identified through conventional gene knockout studies in mice. TFs important during embryonic development for the production and self renewal of the LT-HSC are highlighted in red. Those TFs important for specific lineage determination and differentiation are shown next to red loops- being the point in blockage of differentiation if the factor is absent. *[Orkin, S.H. & Zon, L.I. Hematopoiesis: an evolving paradigm for stem cell biology. Cell 132, 631-644 (2008)]*

1.3.1 Extrinsic factors regulating self renewal and differentiation of HSCs & HPCs

HSC quiescence, self renewal and differentiation are governed in part by extrinsic cytokines, growth factors, cell-cell and cell-matrix interactions within their particular location in bone marrow specialized micro-environments called HSC niches. In the literature HSCs have been found in close proximity to the endosteal surface of bone (endosteal niche) as well as adjacent to sinusoidal blood vessels (vascular or perivascular niches) and therefore the

combination of bone cells, vascular cells and hematopoietic cells likely regulate bone formation and hematopoiesis [43] (Figure 1-8).

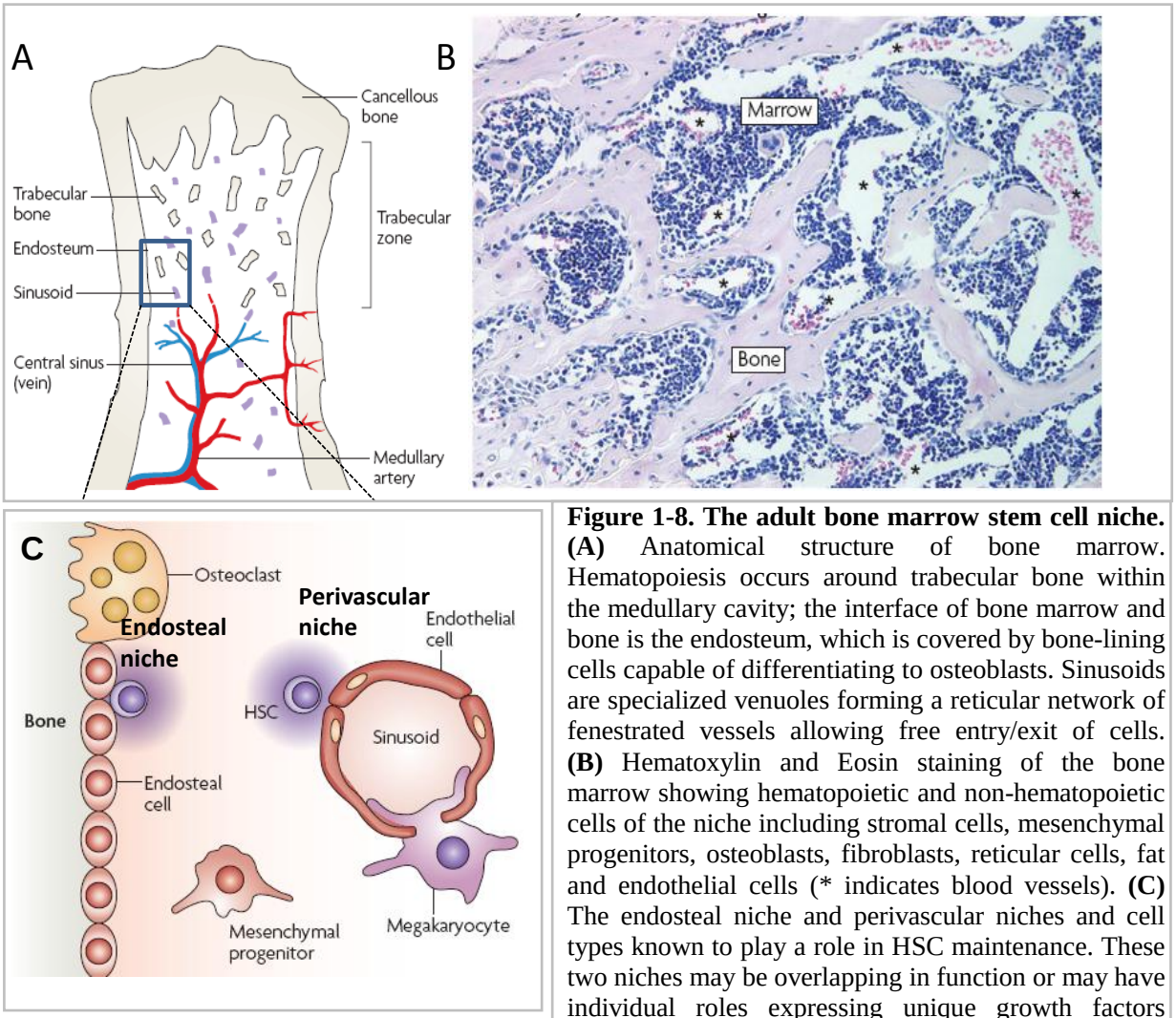

Figure 1-8. The adult bone marrow stem cell niche. **(A)** Anatomical structure of bone marrow. Hematopoiesis occurs around trabecular bone within the medullary cavity; the interface of bone marrow and bone is the endosteum, which is covered by bone-lining cells capable of differentiating to osteoblasts. Sinusoids are specialized venuoles forming a reticular network of fenestrated vessels allowing free entry/exit of cells. **(B)** Hematoxylin and Eosin staining of the bone marrow showing hematopoietic and non-hematopoietic cells of the niche including stromal cells, mesenchymal progenitors, osteoblasts, fibroblasts, reticular cells, fat and endothelial cells (* indicates blood vessels). **(C)** The endosteal niche and perivascular niches and cell types known to play a role in HSC maintenance. These two niches may be overlapping in function or may have individual roles expressing unique growth factors required by HSCs during quiescence versus active self-renewal. *[Modified from Kiel, M.J. & Morrison S.J. Uncertainty in the niches that maintain hematopoietic stem cells. Nature Reviews 8, 290-301 (2008)].*

Perivascular reticular cells in bone marrow express very high levels of CXCL12; a factor required for the maintenance of HSCs [44], and their migration [45]. Recent reports show that thrombopoietin (TPO) producing osteoblasts [46] and the interaction of Tie2-expressing HSCs with Ang-1 expressing osteoblasts [47] maintain HSCs in the quiescent state therefore preserve self renewal capability. Notch receptors and N-cadherin are also produced by osteoblasts

although their exact function in HSC maintanence *in vivo* remains to be elucidated [22, 48, 49]. Other developmental pathways such as Wnt, Sonic hedgehog, and BMP signaling have also been implicated as important environmental signals governing HSC self-renewal [50].

Osteoblasts play an important role during differentiation of more lineage restricted HPCs specifically in monocytopoiesis and lymphopoiesis. They release granulocyte colony stimulating factor (G-CSF) a cytokine necessary for granulocytic differentiation; the loss of osteoblasts *in vivo* reduces the number of c-Kit$^+$ promyelocytes as well as more mature granulocytes and monocytes [51]. The release of IL7 from osteoblasts is also critical for B-cell development [52]. Previously it was known that cytokines and growth factors are necessary and sufficient for the production of specific blood cell types (Figure 1-9) but it was uncertain if they simply allowed the survival or proliferation of cells that had already decided a certain lineage therefore selecting 'fated' cells. A recent elegant study by Schroeder *et al.* has demonstrated that macrophage colony stimulating factor (M-CSF) and G-CSF can instruct lineage choice of murine GMPs without the occurrence of cell death and induce and enhance their differentiation [53]. They used bioimaging approaches that allow continuous long-term observation at the single cell level therefore demonstrating that the signal transduction pathways initiated by cytokines influence the intrinsic determinants (TFs, cell cycle regulators, chromatin modifiers and microRNAs) of cellular phenotype.

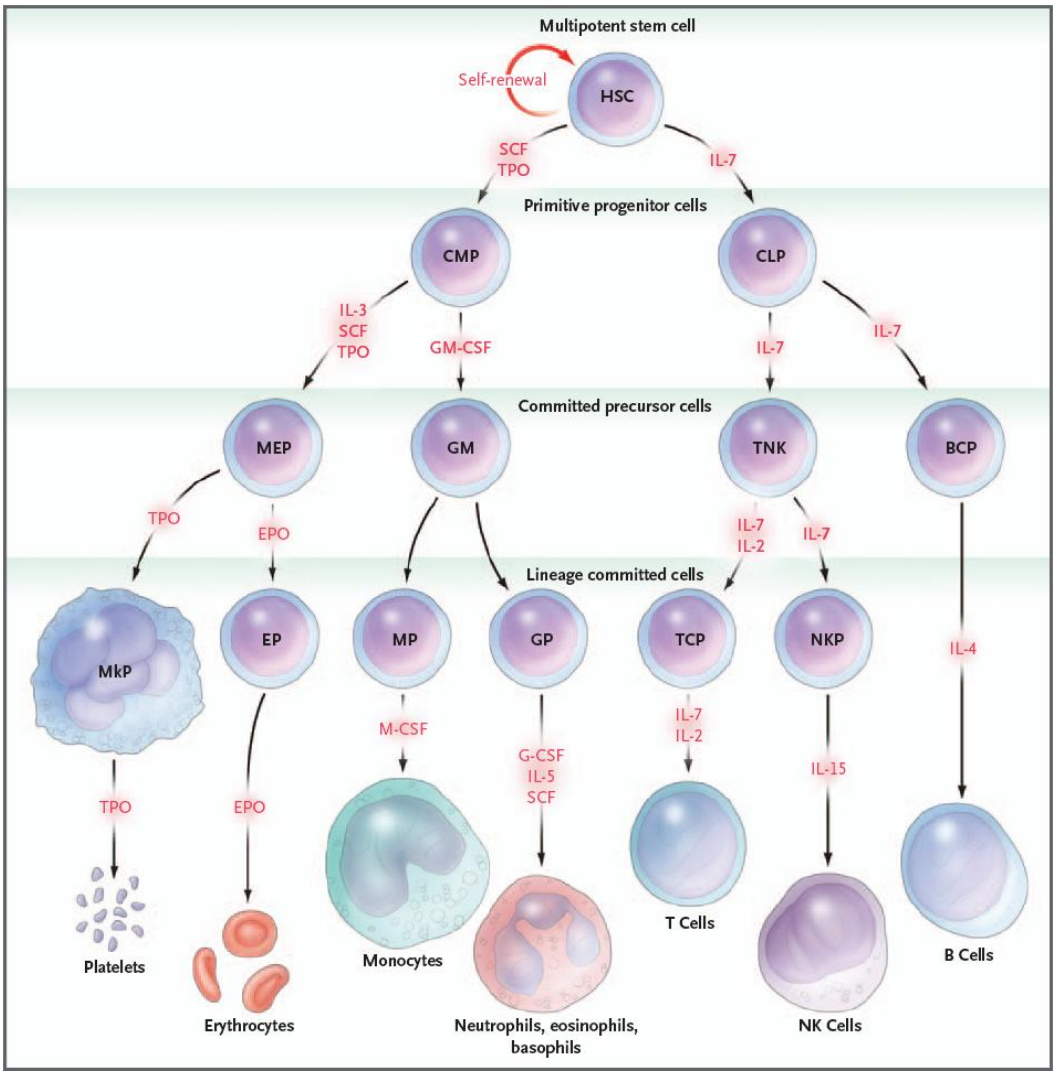

Figure 1-9 Cytokines and growth factors of hematopoiesis. The cytokines and growth factors that support the survival, proliferation, or differentiation of each type of cell are shown in red. IL denotes interleukin, stem-cell factor (SCF), thrombopoietin (TPO), macrophage colony–stimulating factor (M-CSF), granulocyte-macrophage CSF (GM-CSF), and erythropoietin (EPO). [*Kaushansky, K. Lineage-specific hematopoietic growth factors. N Engl J Med 354, 2034-45 (2006).]*

1.3.2 Intrinsic Factors Regulating self renewal and differentiation of HSCs & HPCs

The extrinsic environmental signals of the HSC niche, as mentioned above, must be integrated with the intrinsic molecular machinery to control cell fate of individual HSCs. Through gain and loss functional studies several TFs have been identified as important for the generation of HSCs (Figure 1-7) as discussed above in “Embryonic definitive hematopoiesis”. Additional TFs are important for HSC maintenance: TF Translocation Ets leukemia (Tel) is necessary for HSC maintenance as conditional inactivation in HSCs leads to their depletion,

although its inactivation in other hematopoietic lineages doesn't affect their survival or differentiation [54]. Growth factor independence 1 (Gfi1) is a zinc-finger repressor, and *Gfi1*-deficient HSCs display increased proliferation, and decreased capacity for repopulation of irradiated recipients [55, 56]. Recently the polycomb group (PcG) proteins have been implicated in maintaining the undifferentiated state of HSCs by repression of genes that promote lineage specification, cell death and senescence. Bmi1 is a member of the polycomb repression complex 1 (PRC1) and is required for self-renewal of adult HSCs [57], and increases their ability to repopulate bone marrow *in vivo* [58].

Lineage commitment and subsequent differentiation is controlled by the activation of and repression of selective sets of genes, and that the initiation of these genetic programs are ultimately under the control of TFs [59] (Figure 1-7) through their interaction with cofactors, co-repressors, chromatin modifying enzymes, and the basal transcriptional machinery at *cis*-acting elements within target gene promoters. In early hematopoietic progenitors an open chromatin state is maintained enabling multilineage differentiation programs to be readily accessible [60]. In fact, multipotent progenitors promiscuously transcribe a multitude of lineage-associated genes. In the myeloid compartment the majority of CMPs coexpress granulocyte and monocyte (GM)- (G-CSFR, myeloperoxidase and PU.1) and megakaryocyte/erythroid (MegE)-related genes (EpoR, β-globin, and GATA-2), whereas virtually all GMPs and MEPs express only GM- or MegE-related genes respectively [61]. This is hypothesized to allow flexibility in lineage choice at the multipotent stage, and allow rapid response to external cues from the environment [59]. Therefore, the timing of induction of expression of key TFs above a certain threshold i.e. their quantity within the cell, the ability for auto-regulating their own expression and their interplay (either competitive or collaborative) is key to lineage commitment and differentiation. The paradigm example is the interplay between PU.1 and GATA-1 TFs. PU.1 can bind the DNA binding domain of GATA-1 and block its

transcriptional abilities key to erythroid differentiation. Conversely, GATA-1 can bind and displace c-Jun, a key PU.1 cofactor, reducing the expression of PU.1 target genes and subsequent myeloid development [62, 63]. As these TFs contain autoregulatory loops, subtle changes in their expression levels lead to significant effects in the GM vs. MegE lineage commitment and gene expression (Figure 1-10).

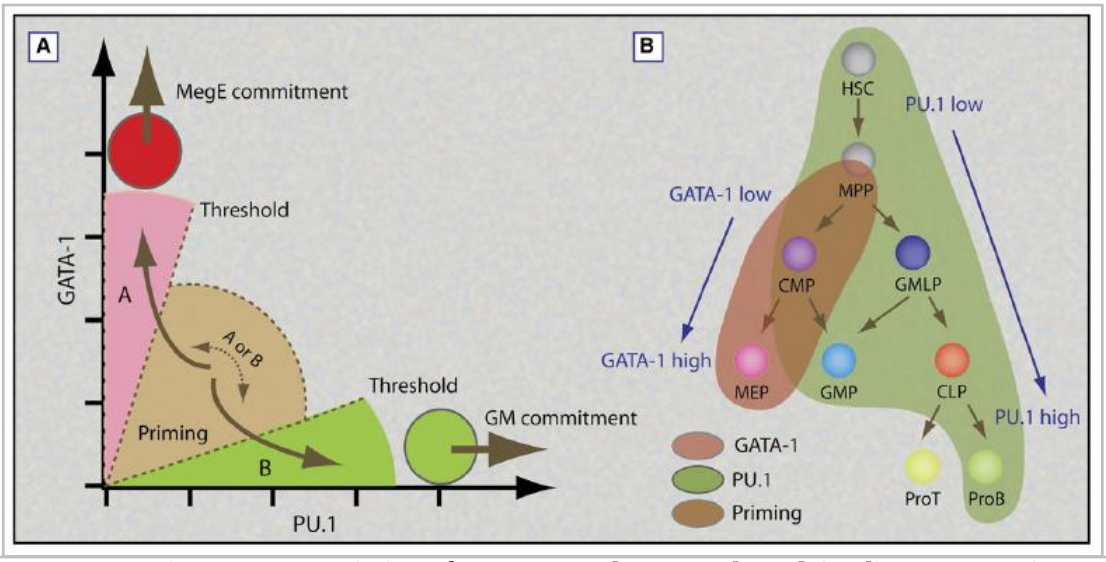

Figure 1-10 Promiscuous gene priming of GATA-1 and PU.1 and resolving lineage commitment. (A) GATA-1 and PU.1 are simultaneously expressed at 'primed' amounts (dashed line). When commitment occurs the dominant TF upregulates its expression via an auto regulatory loop and at the same time suppresses the other's transcription via direct protein contact inhibition. **(B)** The distribution of GATA-1 and PU.1 in definitive hematopoiesis. PU.1 is primed at low levels in HSCs but not GATA-1. GATA-1 is upregulated at the CMP stage where both GATA-1 and PU.1 are primed to have both GM and MegE potential. Higher levels of GATA-1 promote MEP development excluding GM potential whereas higher PU.1 promotes GMP and B-cell development. [*Iwasaki, H., Akashi, K. Myeloid lineage commitment from the hematopoietic stem cell. Immunity Reviews 26, 726-740 (2007).]*

1.3.2.1 GATA-1, EKLF and the TAL1/SCL/LMO2/Ldb1/E2A complex of TFs are critical for erythropoiesis

GATA-1

The sequence [(A/T)GATA(A/G)] (GATA) motifs exist within the *cis*-elements of most, if not all, erythroid cell specific genes. The dual zinc finger TF GATA-1 is the founding member of the GATA family of TFs and is a critical TF for erythroid differentiation and megakaryocytic maturation being expressed in erythroid, megakaryocytic, eosinophil and

mast cell lineages, while absent in myeloid and lymphoid cells [64]. GATA-1 knockout mice die at E10.5-11.5 due to profound anemia [65], as GATA-1 null cells are unable to differentiate beyond the proerythroblast stage due to apoptotic cell death [66]. Ectopic expression of GATA-1 in purified murine progenitors (myeloid or lymphoid) "instructed" their differentiation towards the erythroid and megakaryocytic lineage [67,68] as it is responsible for the activation as well as repression of several genes implicated in erythroid maturation (activation of α and β globins, heme biosynthesis enzymes and repression of GATA-2) [69], as well as the inhibition of PU.1 function as described above.

EKLF

Erythroid Krüppel-Like Factor (EKLF) is an erythroid specific zinc finger TF that binds to (NCNCNCCCN) CACC box motifs present in the β-globin promoter and many erythroid specific genes [70-72]. Naturally occurring mutations in the CACC element of the β-globin promoter lead to β-thalassemia in humans [73]. EKLF has many GATA-1 elements within its promoter and a 5' enhancer region implicating it as an upstream regulator of EKLF, and GATA-1 and EKLF can interact via direct protein-protein interactions [71]. EKLF knockout mice exhibit embryonic lethality at E14.0-15.0 due to lethal anemia [74, 75]. Gene expression profiling has shown impaired expression of genes involved in hemoglobin biosynthesis pathways and in the stability of the erythrocyte membrane [70, 76], and recently defects in cell cycle regulation [77] in EKLF$^{-/-}$ cells.

SCL/LMO2/Ldb1/E2A Complex

SCL/Tal-1 as mentioned earlier is essential for the generation of HSCs, but not their function and it also has a critical role in erythroid differentiation as demonstrated by a conditional knockout in adult hematopoiesis [78]. It is a basic helix-loop-helix (bHLH) TF that binds to the (CANNTG) E-box consensus motif. Its expression resembles that of GATA-1 being expressed in erythroid, megakaryoctye and mast cells. In erythroid cells SCL/Tal-1

forms a multiprotein complex with the ubiquitous E47E2A bHLH partner and with LMO2 and ubiquitous Ldb1 LIM domain containing cofactors [79-82]. This SCL complex is found in cells representing different stages of erythropoiesis and it preferentially binds a composite motif consisting of a GATA motif and a neighbouring E-box found in many erythroid genes and in the SCL/Tal-1 and GATA-1 genes themselves [82]. LMO2 acts as a bridge between SCL/Tal-1 and GATA-1 complex, and it is critical as the LMO2 knockout phenotype in mice is identical to that of the SCL/Tal-1 knockout [83].

1.3.2.2 PU.1 and C/EBPα TFs are critical for myelopoiesis

PU.1

PU.1 is a member of the (E twenty six) ETS TF family, and binds DNA as a monomer at the consensus sequence (5'AAAG(A/C/G)GGAAG-3'). PU.1 is found at low levels in HSCs and multipotent progenitors, it is present in granulocytes and eosinophils and is highly expressed in macrophages and B-lymphocytes [84]. PU.1 $^{-/-}$ mice die peri-natally and lack B lymphoid cells, mature monocytes/macrophages and have reduced neutrophil development [85, 86]. Through ectopic expression studies in murine fetal liver HPCs it was found that high levels of PU.1 drive macrophage development, while a lower level preferentially directs B-cell development [87]. Binding sites for PU.1 are found on almost all myeloid specific promoters including CD11b [88], receptors for M-CSF, GM-CSF, and G-CSF [89-91].

CCAAT/enhancer binding proteins (C/EBPα)

C/EBPα is the founding C/EBP family member which bind to DNA as dimers to the consensus motif 5'-T(T/G)NNGNAA(T/G)-3'. It's expression is upregulated during early granulocytic differentiation but then decreases upon later stages, and decreases during monocyte/macrophage differentiation as well [92]. In fact, C/EBPα disruption in mice disrupts granulopoiesis, and eosinophil development but maintains monocyte/macrophage development, erythroid and lymphoid cells [93]. Identified targets include defensins, lactoferrin,

myeloperoxidase, neutrophil elastase, M-CSF receptor, GM-CSF and G-CSF receptors, and PU.1. C/EBPα like PU.1 and GATA-1 autoregulates its own promoter [84]. Interestingly, C/EBPα can bind to PU.1 displacing its critical cofactor c-Jun, and inhibiting its activity, as well as transcriptionally repressing c-Jun expression [94]. The granulocyte monocyte lineage commitment branchpoint is controlled by the competitive interplay of TFs C/EBPα and PU.1 [95].

1.3.3 Role of TFs in leukemia

Acute Myeloid Leukemia (AML) is a genetically and phenotypically heterogeneous disease characterized by the overproduction of immature myeloid cells (blasts) with a block in differentiation. AML is classified into seven French-American-British (FAB) subtypes corresponding to the maturation stage of the leukemia as assessed by the expression of lineage differentiation makers, and morphology of blast populations [96]. Figure 1-11 shows the stages of differentiation block of different FAB classifications and the morphological series of differentiating normal cells of the myeloid compartment. Emerging evidence supports a stem cell model of leukemogenesis, where leukemia stem cells (LSCs) have limitless self-renewal ability and can propagate and maintain the AML phenotype [97-100]. Transforming events could take place in HSCs, or in more committed progenitors in the form of mutations, epigenetic changes and/or selective gene expression that allow unlimited self-renewal. Little is known about LSCs and identifying LSCs for each type of leukemia and their aberrant pathways remains an important objective for identifying new therapeutic approaches for leukemia, as recent evidence suggests that LSC persistence could be responsible for disease maintenance and/or recurrence [101] (Figure 1-11).

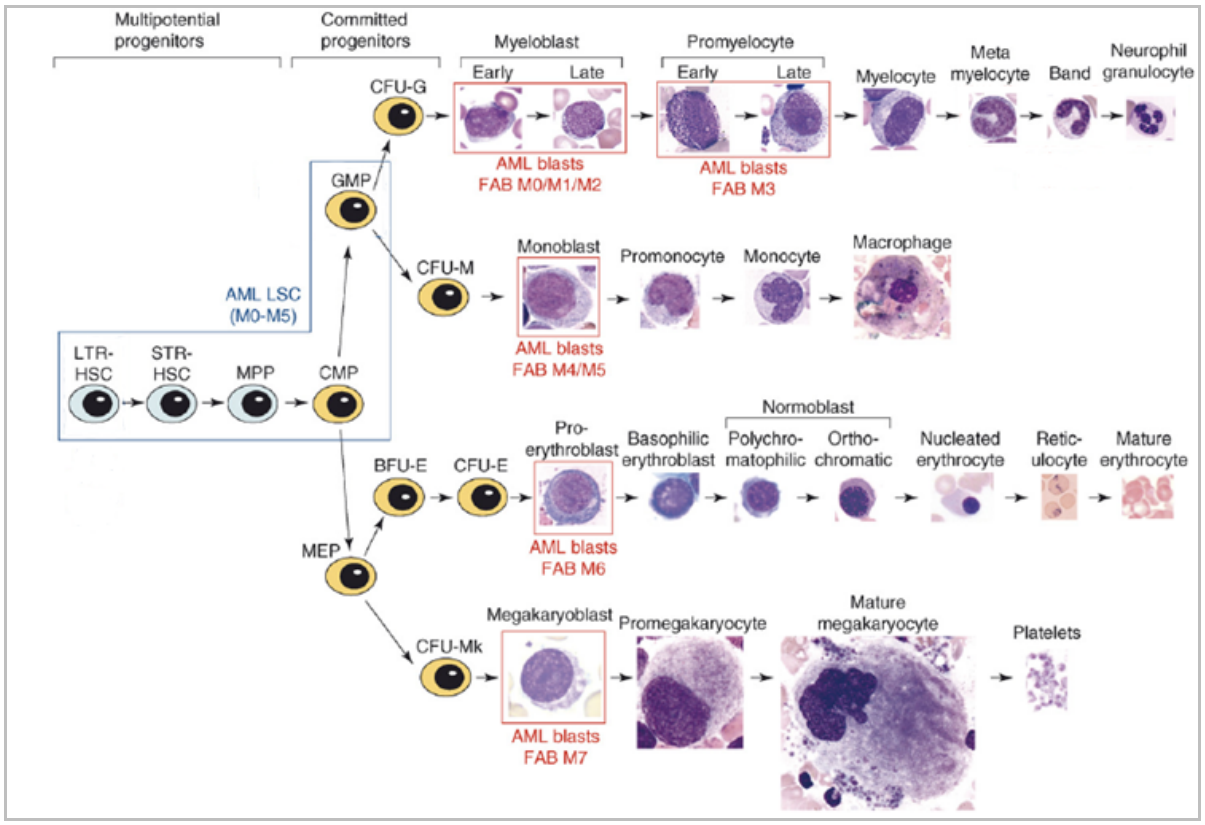

Figure 1-11 Diagram of normal myeloid development and the relationship to leukemic cells and LSCs. Differentiating myeloid cells recognizable by their distinct morphology are shown at the right. Malignant cells of AML are indicated by red boxes where the leukemic blasts for the different FAB classes of AML (M0-M7) correspond approximately to the different normal blasts in each lineage. LSCs are shown restricted to rare stem cells, multipotent or committed progenitors as indicated by a blue box. *[Modified from Krause, D.S., & Van Etten, R.A. Right on target: eradicating leukemic stem cells. Trends in Mol. Med. 13(11) 470-481 (2007)]*.

AML like other cancers is the consequence of more than one mutation: mutant genes that confer proliferative and/or survival advantage, usually as a result of aberrant activation of signal transduction pathways (e.g. activating mutations in RAS family members, receptor tyrosine kinases Kit and FLT3), cooperate with mutations affecting TF function (direct mutation, direct involvement by formation of fusion proteins or by interference of TF function via other translocation proteins) [102-105]. For example, in Acute Promeylocytic Leukemia (APL) characterized by the fusion protein PML-RARα (t15;17), expression of PU.1 is reduced [106], and its downregulation increases the penetrance of APL in PML-RARα transgenic mice [107]. All-trans-retinoic acid (RA) can induce the differentiation of PML/RARα positive APL blasts *in vivo* and *in vitro* [108, 109] in part through relief of C/EBPα and C/EBPε repression [110].

Recently, Tenen *et al*. have demonstrated in a murine model of APL a distinct population of cells representing the APL cancer initiating cell (LSC), and that downregulation of C/EBPα contributes to the transformation of APL cancer initiating cells [111]. C/EBPα has also been shown to be mutated [112, 113] or downregulated by expression of the fusion protein AML1-ETO [114], or methylation of its promoter [115].

1.3.4 microRNAs add to the complexity of intrinsic regulation by regulating key TFs

MicroRNA (miRs) are small ~22 nt endogenous non-coding RNAs (ncRNAs) transcribed by RNA polymerase (Pol) II that modulate mRNA levels post-transcriptionally by binding to target mRNA 3'-UTRs leading to translational repression; decapping, deadenylation and/or cleavage of the target mRNA. A single miRNA can regulate many mRNA targets and several miRNAs can regulate a single mRNA (Figure 1-12).

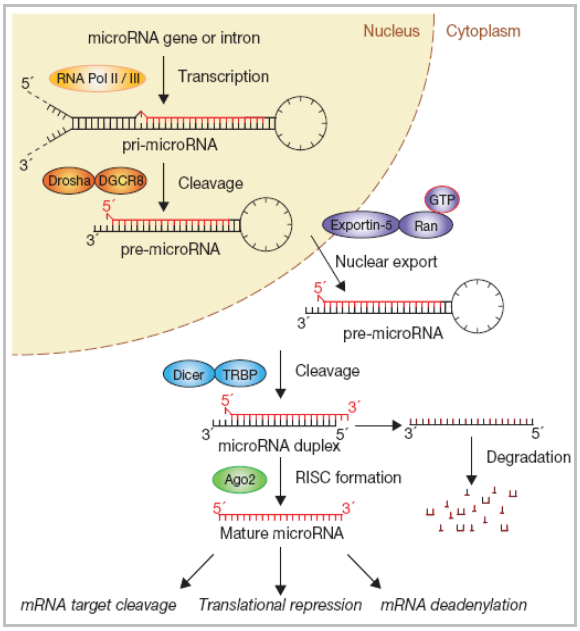

Figure 1-12. miRNA Biogenesis. A pri-miRNA is transcribed by RNA Pol II, which is cleaved by the microprocessor complex Drosha-DGCR8 (Pasha) within the nucleus. The resulting pre-miRNA is then exported to the nucleus where the RNase Dicer in complex with the double-stranded RNA-binding protein TRBP cleaves the pre-miRNA to its mature length ~ 22 nt. Only one of the strands of the miRNA duplex is loaded onto the RNA-induced silencing complex (RISC) and the strand selection is based on thermodynamic stability with loading of the strand with the less stable base pair at its 5' end. RISC containing the mature miRNA and Argonaute (Ago2) proteins then acts to silence target mRNA through mRNA cleavage, translational repression or deadenylation. [*Winter, J. et al. Many roads to maturity: microRNA biogenesis pathways and their regulation. Nature Cell Biology Review 11(3), 228-234 (2009).]*

MiRs have key roles in developmental control, neural development, apoptosis, cell proliferation, organ development and hematopoietic cell differentiation [116]. Recent data indicate that miRs are deregulated in diseases such as diabetes, heart disease and cancer [117-119], and further research established that miRs can behave as tumour suppressors or oncogenes [120, 121]. Current miR expression profiling has been associated with cytogenetic and molecular subtypes of AML [122, 123] and the functional role of these miRs in AML is an active area of ongoing research. During normal human hematopoiesis levels of miRs change during hematopoietic differentiation of specific lineages [124] (Figure 1-13) and it was found that human $CD34^+$ cell populations (enriched for HSCs and HPCs) have expression of 34 different miRs [125].

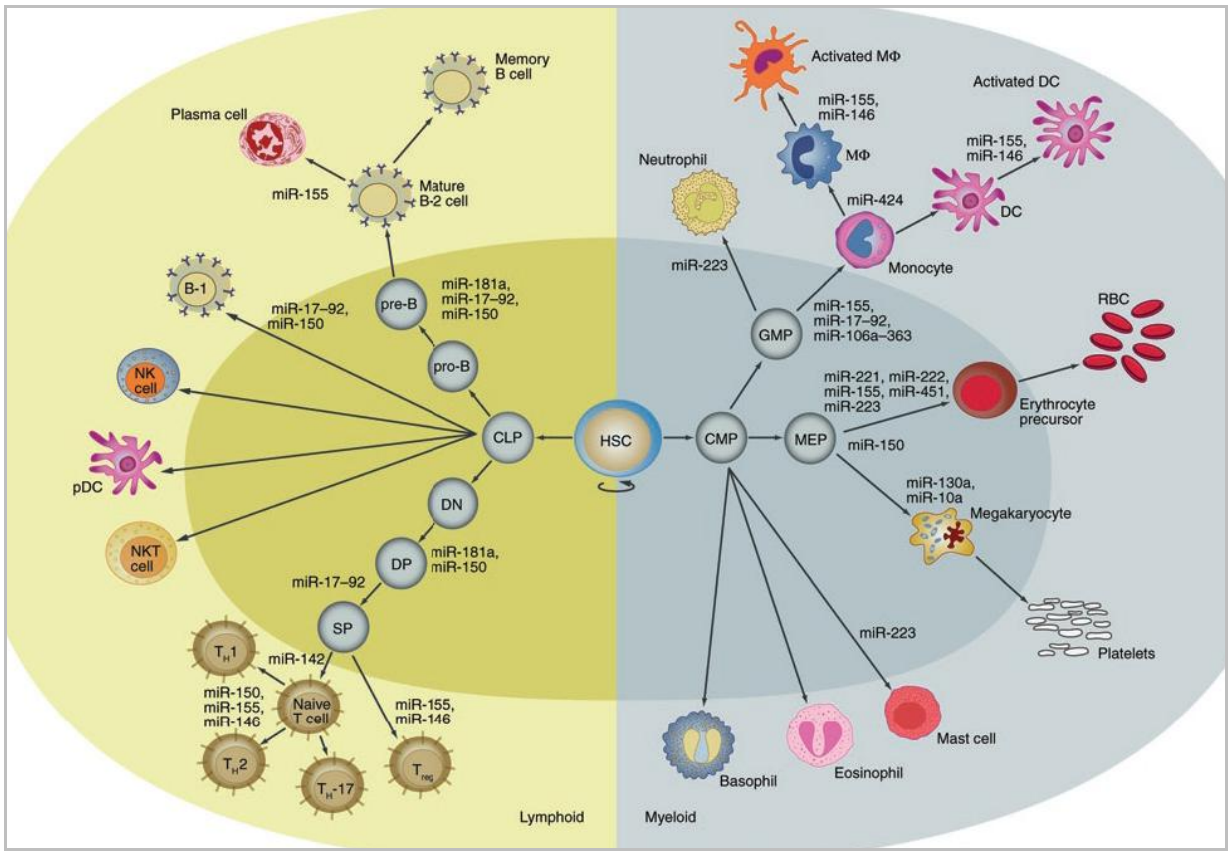

Figure 1-13. miRNAs in the myeloid and lymphoid compartments. miRNAs near arrows indicate an involvement in lineage differentiation in the specified cell type. [*Baltimore, D. et al. MicroRNAs: new regulators of immune cell development and function. Nature Immunology 9(8), 839-845 (2008).]*

Previous work from our lab identified miR-223 as a being highly expressed in human bone marrow being highest expressed in the $CD34^-$ fraction (mainly myeloid cells at different stages of neutrophilic differentiation) and absent in lymphocytes [126] matching the previous literature in murine bone marrow where miR-223 expression is also high [127]. This work from our lab was the first description of a miR circuitry involving two transcription factors during leukemic hematopoietic differentiation. Specifically, upon RA treatment of APL patient blasts and the APL cell line NB4, C/EBPα is upregulated and binds to the miR-223 promoter increasing its expression and subsequent granulocytic differentiation. miR-223 lentiviral overexpression also lead to granulocytic differentiation of NB4 leukemic cells. In this work a TF identified as nuclear factor I-A (NFI-A) was found to be a target of miR-223, and was found to repress miR-223 expression in undifferentiated cells; the suppression of NFI-A was found to be necessary during the leukemic granulocytic differentiation [126] (Figure 1-14).

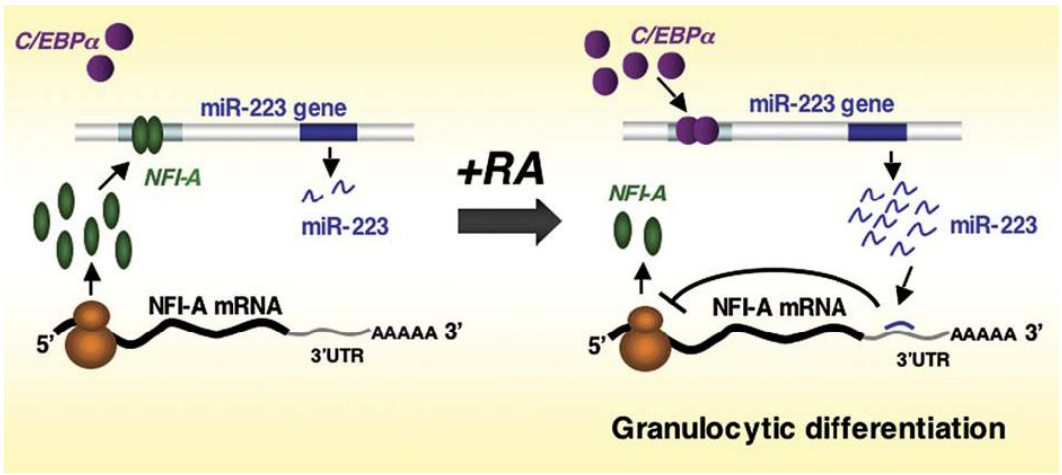

Figure 1-14 The circuitry of miR-223, C/EBPα and NFI-A during RA induced granulocytic differentiation of leukemic cells. In undifferentiated cells NFI-A binds to the miR-223 promoter to repress its transcription. Upon RA treatment C/EBPα expression increases displacing NFI-A from the miR-223 promoter and upregulating miR-223 expression. miR-223 in turn targets NFI-A to repress its expression. [*Fazi, F. et al. A minicircuitry comprised of microRNA-223 and transcription factors NFI-A and C/EBPα regulates human granulopoiesis. Cell 123, 819-831 (2005).]*

More recently, during monocytic-macrophage differentiation of human HPCs and leukemic APL blasts, PU.1 was found to induce the expression of miR-424, and that miR-424 targets

NFI-A, whose suppression was found also to be necessary for normal human monocytopoiesis [128].

1.3.5 Nuclear Factor I (NFI) TFs

NFI-A is a member of the nuclear factor I (NFI) family of TFs, which is comprised of four separate genes NFI-A, NFI-B, NFI-C and NFI-X that are highly conserved throughout vertebrate evolution [129]. NFI proteins consist of an N-terminal DNA binding/dimerization domain and a C-terminal transactivation or repression domain. NFI proteins bind as dimers to the sequence TTGGC/AN_5G/TCCAA on duplex DNA. NFI proteins can also bind to individual half-sites and the sequences flanking the consensus sequence and the number of nucleotides between the half sites can modulate NFI binding [130]. NFI-binding sites have been found in the promoter and enhancer regions of almost every organ system and tissue including promoters of the brain [131], muscle [132], lung [133], liver [134] and kidney [135], to name a few, where they act as transcriptional activators or repressors depending on the cell-type and promoter context. Knockout of NFI-A causes death of 95% of the mice at post-natal day 1 due to severe neurological defects including hydrocephalus, and agenesis of the corpus callosum [136]. NFI-B knockout mice die early postnatally and display neurological defects and severe lung hypoplasia [137]. NFI-C $^{-/-}$ mice show a prominent defect in tooth root development and NFI-X$^{-/-}$ mice show neurological defects similar to the NFI-A $^{-/-}$ mice and defects in bone ossification [138]. The NFI-A, B and X knockouts all exhibit brain malformations, indicating their importance for neural development and their non-redundant function. In fact, NFI genes are differentially expressed during mouse development and cellular differentiation, which suggests that these proteins could play important non-redundant roles in gene expression during development [139, 140]. Besides our previous findings [126] implicating a possible role for NFI-A in normal hematopoietic lineage differentiation, little is known on NFI function in blood development. Initial studies by Kulkarni *et al.* noted that NFI factor levels change

during phorbol ester induced differentiation of leukemic cells, and they noted that the NFI proteins may play distinct roles in hematopoietic development [140].

RESEARCH AIMS

It is becoming more evident in recent years that there must be tight control over the timing of expression of TFs in hematopoiesis, and especially in their concentration levels within cells at specific differentiation stages for normal correct hematopoietic development to occur. This fact also intertwines miRs, which can fine tune the expression levels of key TFs for hematopoiesis, into the complex scenario of hematopoietic lineage specification. Several key lineage determining TFs are aberrantly expressed or deregulated in AML. Previous work in the laboratory identified two new players governing leukemic granulocytic differentiation of APL blasts; miR-223 and NFI-A. It was found that during RA treatment of APL blasts that miR-223 levels increased, whereas the repression of NFI-A was a necessary step for leukemic granulocytic differentiation. We therefore decided to focus on the three following aims of research.

AIM I: To examine if deregulated miR-223 expression is associated with differentiation block underlying the pathogenesis of distinct leukemia subtypes, and to determine regulating factors involved.

AIM II: To determine the function of TF NFI-A in normal human adult definitive hematopoiesis using both leukemic cell lines and primary culture of human hematopoietic progenitors (HPCs).

AIM III: To determine the role of TF NFI-A during both embryonic primitive and definitive hematopoiesis using the mouse as a model system.

Chapter Two: MATERIALS AND METHODS

2.1 Cell culture

2.1.1 AML Cell Lines

AML cell lines including K562, and HL-60 were all maintained at a density of 0.5 x 10^6 cells/mL in Roswell park memorial institute (RPMI) 1640 + GlutaMax medium (Gibco-BRL, Grand Island, USA) supplemented with 10% fetal bovine serum (FBS) (Gibco-BRL), 50 µg/mL streptomycin and 50 IU penicillin in a fully humidified incubator with 5% CO_2 in air. To induce granulocytic differentiation HL-60 cells were treated with all-trans-retinoic acid (RA). For the induction of erythroid differentiation K562 cells were treated with cytosine β-D-arabino-furanoside (Ara-C). Both reagents were purchased from Sigma (St Louis, MO, USA) and utilized at a concentration of 1 µM, and 0.5 µM, respectively.

For benzidine staining, K562 cells (1 x 10^5) were washed twice with cold phosphate-buffered saline (PBS) and resuspended in 50 µl cold PBS supplemented with 10 µl of the freshly prepared benzidine solution (0.4% benzidine, 12% acetic acid, 1.8% H_2O_2). After incubation on ice for 2 minutes the percentage of benzidine positive cells (blue) was determined by light microscopic examination of at least 500 cells per sample.

2.1.2 Human cord blood (CB) hematopoietic progenitor cell (HPC) purification, suspension culture and clonogenic assay.

Cord Blood (CB) was obtained from healthy, full-term pregnancies according to institutional guidelines. From CB low-density mononuclear cells were isolated by Ficoll–Hypaque density gradient centrifugation (Pharmacia, Peapack, NJ, USA). $CD34^+$ cells were purified by positive selection using the midi-MACS immunomagnetic separation system (Miltenyi Biotech, Berisch Gladabach, Germany) in accordance with the manufacturer's recommendations. The purity of $CD34^+$ cells was assessed by flow cytometry using a monoclonal PE-conjugated anti-CD34 antibody and was routinely over 95%. $CD34^+$ HPCs were cultured in a fully humidified 5% CO_2, 5% O_2 atmosphere, in serum-free medium and

viable cells were counted every 2-3 days using Trypan Blue Staining (Sigma) and passaged at 2 x 10^5 cells/mL. Serum-free medium was prepared as follows: freshly prepared Iscove's modified Dulbecco's medium (IMDM) (Gibco BRL) was supplemented with: bovine serum albumin (10 mg/mL), pure human transferrin (700 μg/mL), human low-density lipoprotein (40 μg/mL), insulin (10 μg/mL), sodium pyruvate (10^{-4} mol/l), L-glutamine (2 x 10^{-3} mol/l), rare inorganic elements supplemented with iron sulfate (4 x 10^{-8} mol/l) and nucleosides (10 μg/mL each) (All purchased from Sigma). The following cytokines were added: Epo (3 U/mL), IL-3 (0.01 U/mL) and GM-CSF (0.001 ng/mL) for erythroid (E) unilineage culture and for granulocytic (G) culture serum free medium was supplemented with IL-3 (1 U/mL), GM-CSF (0.1 ng/mL), and G-CSF (500 U/mL). In bilineage E+G culture, serum-free medium was supplemented with IL-3 (1 U/mL), GM-CSF (0.1 ng/mL), Epo (0.6 U/mL) and G-CSF (500 U/mL). Human growth factors (HGFs) were purchased from Peprotech (Rocky Hill, NJ, USA), human erythropoietin (Epo) was provided by Amgen (Thousand Oaks, CA, USA).

In clonogenic assay, 10^2 $CD34^+$ cells were plated in duplicate in serum-free medium containing 0.9% methylcellulose MethoCult H4100 (StemCell Technologies, Vancouver, BC, CAN). The following cytokines were used; for *BFU-E assay*: Interleukin-3 (IL-3) (0.01 U/mL), GM-CSF (0.001 ng/mL) and Epo (3U/mL). For *CFU-G assay*: IL-3 (1 U/mL), GM-CSF (0.1 ng/mL) and G-CSF (500 U/mL). For *BFU-E/CFU-G assay:* IL-3 (1 U/mL), GM-CSF (0.1 ng/mL), Epo (0.6 U/mL) and G-CSF (500 U/mL).

2.1.3 Primitive erythroid progenitor (EryP-CFC) assay

Yolk sacs of E8.0 CD1 embryos were dissected, as written below, pooled together and placed in Dulbecco's modified eagle medium (DMEM) (Gibco-BRL) with 10% FBS. Yolk Sacs were pelleted by brief centrifugation and resuspended in 200 μl PBS and 0.25% collagenase (Sigma) and placed at 37°C for 30 min-1h after which single cells were obtained by vigorous pipetting. Excess cold PBS with 10% FBS was then added to the cells to stop the

collagenase reaction followed by centrifugation at 1200 rpm for 5 min at 4°C. Cells were resuspended in IMDM, 2% FBS (Gibco-BRL), and counted using Trypan Blue staining (Sigma). Cells were plated in triplicate at 1 x 10^5 cells/mL in 0.9% methylcellulose-based media MethoCult M3134 (StemCell Technologies, Vancouver BC, Canada) including IMDM, 2mM glutamine (Gibco-BRL), 1% penicillin/streptomycin (Gibco-BRL), 5% protein-free hybridoma medium II (PFHM-II; Gibco-BRL), 50 µg/mL ascorbic acid (Sigma), 450 µM monothioglycerol (MTG; Sigma), 200 µg/mL iron-saturated holo-transferrin (Sigma), 15% plasma-derived serum (Sera Laboratories International LTD, West Sussex, UK) and 4 U/mL rhEPO (PBL Biomedical Laboratories, New Brunswick, NJ, USA). Primitive colony numbers were scored after 7 days of culture in a fully humidified incubator at 37°C with 5% CO_2 in air.

2.1.4 Embryonic definitive colony assay

Tissues from individual embryos of CD1 mice of yolk sac E9.0, AGM E11.0-12.0, and Liver E11.0 and E14.0 were isolated from individual embryos and then pooled together as described below. Individual tissues were then placed in DMEM with 10% FBS. Tissues were pelleted by brief centrifugation and resuspended in 200-400 µl PBS and 0.25% collagenase (Sigma) and placed at 37°C for 30 min-1h after which single cells were obtained by vigorous pipetting. Excess cold PBS with 10% FBS was then added to the cells to stop the collagenase reaction followed by centrifugation at 1200 rpm for 5 min at 4°C. Cells were resuspended in IMDM, 2% FBS, and counted using Trypan Blue staining. Yolk Sac E9.0 cells were plated in triplicate at 12 x 10^3 cells/mL in methylcellulose based media MethoCult GF 3434 (StemCell Technologies). AGM cells from E11.0 and E12.0 were plated in triplicate at a concentration of 20 x 10^3 cells/mL and Liver E14.0 cells were plated in triplicate at a concentration of 30 x 10^3 cells/mL in MethoCult GF 3434. Embryonic definitive hematopoietic colonies (BFU-E, CFU-GM, CFU-G, CFU-M and CFU-GEMM) were scored after 7 days of culture in a fully humidified incubator at 37°C with 5% CO_2 in air.

2.2 Mouse Tissues

2.2.1 Embryonic Tissues

Timed pregnant CD1 mice were killed by cervical dislocation and uteri were removed from the peritoneum and washed with several changes of PBS. Decidual tissues and Reichert's membrane was dissected free of the embryos in PBS, 10% FBS solution. Presomite embryos (E7.0) were staged and grouped according to established morphological criteria [141], and somite stage embryos (E8.0-E14.0) were grouped according to somite number. Individual embryos were either kept whole or dissected to remove the yolk sac and amnion= yolk sac, AGM, dorsal Aorta, GM, and liver for further processing.

2.2.2 Adult Tissues

Adult CD1 mice were euthanized via CO_2 inhalation. Immediately after inhalation peripheral blood was collected by cardiac puncture of the heart using a 1mL syringe and 27G needle (Terumo, Leuven, Belgium). Blood was collected and placed in a collection tube containing ethylenediaminetetraacetic acid (EDTA) (Starsted, Nünbrecht, Germany) to prevent coagulation. Red blood cells (RBCs) were lysed using the Buffer EL erythrocyte lysis buffer (Qiagen, Hilden, Germany) according to the manufacturer's instructions. The resulting cell pellet was then used for either RNA extraction or lysed to obtain protein for western blotting.

To obtain spleen cells, spleens of adult mice were dissected from the euthanized mice and washed several times in cold PBS. Spleens were then mechanically dissociated in cold PBS and passed through a 70 µM filter (BD Biosciences, Franklin Lakes, NJ, USA). The resulting cells were pelleted by refrigerated centrifugation at 1200 rpm for 5 min at 4°C and the RBCs were lysed as described previously. The resulting pellet was then used for RNA extraction, or was lysed to obtain protein for western blotting.

For collection of bone marrow cells, whole legs were dissected free from the hip of a euthanized mouse, and muscle tissue was cleaned away from the femora and tibiae. The head of the femur or tibia was cut and a 5mL syringe with 26G needle containing cold IMDM medium and 10% FBS was used to flush bone cavities to collect bone marrow. The cells were centrifuged at 1200 RPM for 5 min at 4°C and the RBCs were lysed from the resulting pellet as above. Cell pellets were then used for RNA extraction or lysed to obtain protein for western blot.

2.3 Cellular Morphologic analysis

For morphological analysis of E unilineage, G unilineage, and E+G bilineage cultures cells (10-20 x 10^3) were harvested from day 3 to day 21-24 of suspension culture. HL-60 (60 x 10^3) and K562 (40 x 10^3) cells were harvested from exponentially growing cultures. For morphology of embryonic primitive colonies several EryP colonies were pooled, for definitive colony morphology individual colonies were picked. Collected types of cells were pelleted, washed 1X with cold PBS 1% BSA (Sigma), and were spotted onto glass slides by centrifugation using the Shandon Cytospin 4 (Thermo electron©, Waltham, MA, USA). Slides were stained with standard May-Grünwald-Giemsa (Sigma), and observed by conventional light field microscopy, to evaluate morphology (HL-60 and K562 cells) and cell differentiation through the erythroid (E unilineage and E+G bilineage culture) and granulocytic pathways (G unilineage and E+G bilineage culture). Proerythroblasts, Basophilic, Polychromatophilic and Orthochromatic cells were counted in the erythroid series. Myeloblasts, Promyelocytes, Myelocytes and Mature Cells (Meta/Band) in the granulocytic series were identified and their percentage value was obtained. At least 500 cells were counted per slide.

2.4 Flow cytometry

PE-conjugated anti-human Glycophorin-A (GPA), CD34, CD15, CD14, CD11b, CD114 antibodies were purchased from BD Biosciences Pharmigen (San Diego, CA, USA). G-CSFR total protein expression was assessed by immunostaining using a PE-conjugated anti-CD114 antibody in cells fixed and permeabilised with 100 μL of Cytofix/Cytoperm (BD Biosciences Pharmingen). Immunophenotype and 7-Amino-actinomycin D (Calbiochem, San Diego, CA, USA) cell viability staining (final concentration of 5μg/mL), performed according to manufacturer's instructions were analysed by flow cytometry using FACScan instrument (BD Biosciences).

2.5 Indirect Immunofluorescence

Slides containing EryPs were fixed in 4% paraformaldehyde (Sigma) at 4°C for 10 min and permeabilized using 1% BSA, 0.2% Triton X-100 (Sigma) in PBS (PBST). Slides were incubated with 10% goat serum (Abcam, Cambridge, UK) in PBS for 1 h to block nonspecific binding, then incubated with primary polyclonal anti-NFIA antibody (Abcam) diluted 1:200 in PBS, 1% goat serum. Cells were washed with PBST and incubated with a Cy-2 conjugated secondary IgG anti-rabbit antibody (Jackson Immunoresearch Laboratories Inc, Suffolk, UK) diluted 1:250 in PBS 1% goat serum for 1h at room temperature. Slides were washed with PBST and then stained with 4',6-diamidino-2- phenylindole (DAPI; Sigma) diluted 1:5000 in PBS for 10 min at room temperature, followed by washes with PBS and were mounted using Vectashield Mounting Medium (Vector Laboratories Inc, Burlington, CA, USA). Cells were examined with epifluorescence on a Nikon Eclipse TE-2000-E microscope.

2.6 Immunoblotting

Total protein was extracted using CelLytic M Lysis Reagent (Sigma) following the manufacturer's protocol, supplemented with Protease Inhibitor Cocktail (Sigma). Protein

concentration was determined by the Lowry Protein Assay [142]. Total cell extracts were fractionated under denaturating conditions by electrophoresis on NuPAGE® 10% Bis-Tris gels (Invitrogen) using NuPAGE® MOPS SDS running buffer (Invitrogen) followed by electroblotting onto a nitrocellulose membrane (Whatman PROTRAN® Dassel, Germany). Blots were probed with the following primary antibodies: polyclonal anti-NFI-A (Abcam), polyclonal anti-Hemoglobin ε (ProteinTech Group Inc., Chicago IL USA), monoclonal anti-β-actin (Calbiochem, San Diego, CA, USA), polyclonal anti-AML1/RHD (Calbiochem), polyclonal anti-HA, monoclonal anti-Hemoglobin β, monoclonal anti-Hemoglobin γ, polyclonal GATA-1 and polyclonal anti-G-CSFR all purchased from Santa Cruz Biotechnology (Santa Cruz CA USA). Secondary antibodies used were as follows: anti-mouse IgG peroxidase conjugate and anti-rabbit IgG peroxidase conjugate (Pierce, Rockford, IL, USA). Immunoreactivity was measured using the ECL method (Amersham Biosciences).

2.7 RNA extraction and analysis

Total RNA was isolated using the Trizol reagent (Invitrogen, Carlsbad, CA, USA) following the manufacturer's instructions for AML cell lines, unilineage and bilineage culture of human HPCs, and mouse whole tissues (yolk sac, AGM, spleen, liver, peripheral blood). For extraction of RNA from samples containing few cells (embryonic colonies), RNA was extracted using the RNeasy Plus Micro kit (Qiagen). First-strand cDNA of all samples was synthesized with the SuperScript® II (Invitrogen) reverse transcriptase enzyme using equivalent amounts of total RNA for each sample and oligo (dT) (Invitrogen) primers. mRNA quantification of samples was performed in triplicate by real-time PCR using the ABI PRISM 7700 Sequence Detection System (Applied Biosystems, Foster City, CA, USA) and either inventoried TaqMan gene expression assays (Applied Biosystems), or with SYBR Green PCR reaction mix (Applied Biosystems) with ΔC_t values normalized using endogenous GAPDH as control. Primers used for SYBR Green real-time PCR are listed in Table 2-1.

Semiquantitative PCR was performed on 1 µl of cDNA using the primers listed in Table 2-1, with the following mix: 1X PCR buffer (Invitrogen), Primer mix (0.2 pmol/ µl each), 2 x 10^{-4} dNTPs (Invitrogen), $MgCl_2$ 1.5 x 10^{-3} (Invitrogen), and 2.5 U Platinum® Taq DNA polymerase (Invitrogen).

Table 2-1 Primer name and sequence for primers employed during semiquantitative PCR, multiplex PCR for ChIP assay, real-time PCR and luciferase assay

Primer Use	Primer Name and Sequence
Semiquantitative PCR	Gapdh se 5' - ATCAGCAATGCCTCCTGCAC - 3' Gapdh as 5' - TGGCATGGACTGTGGTCATG - 3'
Semiquantitative PCR	mNFIA se 5' - TGGCATACTTTGTACATGCAGC -3' mNFIA as 5' - ACCTGATGTGACAAAGCTGTCC - 3'
Semiquantitative PCR	mNFIB se 5' - GTTTTTGGCATACTACGTGCAGG - 3' mNFIB as 5' - CTCTGATACATTGAAGACTCCG - 3'
Semiquantitative PCR	mNFIC se 5' - GACCTGTACCTGGTCTACTTTG - 3' mNFIC as 5' - CACACCTGACGTGACAAAGCTC - 3'
Semiquantitative PCR	mNFIX se 5' - CTGGCTTACTTTGTCCACACTC - 3' mNFIX as 5' - CCAGCTCTGTCACATTCCAGAC - 3'
Semiquantitative PCR	mRunx1 se 5' - GGCACTCTGGTCACCGTCAT - 3' mRunx1 as 5' - CGTTGAATCTCGCTACCTGGTT - 3'
Semiquantitative PCR	βh1 se 5’ - CCTGATTGTTTACCCATGGAC - 3' βh1 as 5’ - CAATCACCAACATGTTGCCCAG - 3'
Semiquantitative PCR	βmaj se 5’ - GGTGCACCTGACTGATG - 3' βmaj as 5’ - AGTGGTACTTGTGAGCC - 3'
Semiquantitative PCR	mGATA-1 se 5' - GGAGCCCTCTCAGCTCAGC - 3' mGATA-1 as 5’ - GCCACCAGCTGGTCCTTCAG - 3’
Semiquantitative PCR	m c-fms se 5’ - CTGAGTCAGAAGCCCTTCGACAAAG -3' m c-fms as 5’ - CTTTGCCCAGACCAAAGGCTGTAGC -3’
Semiquantitative PCR	mKLF1 se 5’ - GAGACTGTCTTACCCTCCAT - 3’ mKLF1 as 5’ - CCACGAAGGGTTCAGGGGCT - 3’
Multiplex PCR G-CSFR ChIP	G-Up as 5’- CTCCGGATTTCCTGAGCTCAAAGC - 3’ G-Dw se 5’- GAACCTGGAACACACCCTTCTGAG - 3’
Multiplex PCR β-Globin ChIP	B-Up se 5’- TATATCTTAGAGGGAGGGCTGAGGGT - 3’ B-Dw as 5’- TGTAAGCAATAGATGGCTCTGCCC - 3
Multiplex PCR Unrelated intergenic genomic Region ChIP	UR-Up as 5’- AAGGACACTAGGTGGTTGAGATCC - 3’ UR-Dw se 5’ – CCAGCTGATTGAGAATGCAGATGC – 3’
Real-time PCR ChIP G-CSFR	GCSFR se 5’ - GTGAAGATGTGGTCCCCAAG - 3’ GCSFR as 5’ - GGATTTCCTGAGCTCAAAGC - 3’
Real-time PCR ChIP β-Globin	HBBse 5’ - ATCACTTAGACCTCACCCTGTGGA - 3’ HBBas 5’ - AAGCAATAGATGGCTCTGCCCTGA - 3’
Luciferase assay β-Globin Wild-type promoter	HB-Wt For 5’- CCGAGGTAGAGTTTTCATCCA – 3’ HB-Wt Rev 5’ – TAGATGGCTCTGCCCTGACT- 3’
Luciferase assay β-Globin Mutant1 promoter	HB-Mut1 5’-GAGCCACACCCTAGGGTTGTAAAATCTACTCCCAGGAGCAG – 3’
Luciferase assay β-Globin Mutant2 promoter	HB-Mut2 5’-GGGTTTGAAGTCCAACTCCTAAGCCAGTTAAAGAAGAGCCAAGGAC – 3’

Table 2 Continued	
Luciferase assay β-Globin Mutant3 promoter	HB-Mut3 5'-AGCAATTTGTACTGATGGTATGGGTAAAAGAGATATATCTTAGAGGGAGGG-3'
Luciferase assay G-CSFR Wild-type promoter	GR-Wt For 5'– GCGGTACCTGGTCTATGGGCA - 3' GR-Wt Rev 5'- GAAGATCTGTCGTTAATGGCTC – 3'
Luciferase assay G-CSFR Mutant1 promoter	GR-Mut1 For 5'– GAGCCTGGGCCCTGCCCAGC – 3' GR-Mut1 Rev 5'– CTTATGCCCCCTGCCCTGGG – 3'
Luciferase G-CSFR Mutant2 promoter	GR-Mut2 For 5'– GTGATGCTCCCCCAGGGCA – 3' GR-Mut2 Rev 5'- CTGGCTGGAAGGCTCACCCG – 3'
Real-time PCR	OAS1 For 5' – CCAGGAAATTAGGAGACAGC - 3' OAS2 Rev 5' – GAGCGAACTCAGTACGAAGC – 3'
Real-time PCR	OAS2 For 5' – TCAGAAGAGAAGCCAACGTGA – 3' OAS2 Rev 5' – CGGAGACAGCGAGGGTAAAT – 3'
Real-time PCR	IFNB1 For 5' – TGCTTCTCCACGACAGCTCTT – 3' IFNB1 Rev 5' – TGACACTGACAATTGCTGCTTCT - 3'

2.8 Chromatin Immunoprecipitation (ChIP) assay

Formaldehyde was added to cultured cells (2×10^6) at a final concentration of 1% for 10 min at 37°C to cross-link DNA and protein complexes. Chromatin was sheared by sonication and immunoprecipitated with 3 µg of anti-NFI-A (Abcam). Putative NFI-A sites contained within the proximal promoters of interest were determined by using a combination of Chip-Mapper, Alibaba 2.1, and MatInspector Professional software programs (http://bio.chip.org/mapper/mapper-main, http://darwin.nmsu.edu/~molb470/fall2003/Projects/solorz/aliBaba_2_1.htm, http://www.genomatix.de/products/MatInspector/).

For ChIP assay of primary cells genomic regions of about 200 bp containing the NFI-A consensus site were amplified by multiplex PCR[143] in presence of [α-^{32}P] dATP using the primers listed in Table 2-1. PCR signals were quantified using Typhoon Trio Phosphoimager (Amersham Biosciences, Piscataway, NJ, USA) and ImageQuant software (Molecular Dynamics, Sunnywale, CA, USA). The relative occupancy of NFI-A present on the promoter (Prom) specific regions is normalized to the Input (I) signal, following the algorithm: $[(IP-BO)/I]_{PROM}/[(IP-BO)/I]_{UR.}$ IP represents chromatin immunoprecipitated by the NFI-A

antibody. BO (Beads Only) represents non-specific signal in absence of antibody. The co-amplification of Tubulin (mentioned as Unrelated genomic Region (UR)) within the same multiplex reaction serves as an internal control for background non-specific chromatin. PCRs were performed within the linear range of amplification.

Binding of NFI-A in K562 and HL-60 cells within the β-globin and G-CSFR promoters was verified by real-time PCR analysis using SYBR Green PCR Master Mix (Applied Biosystems, Foster City, CA, USA). The amount of product was determined relative to a standard curve of input chromatin, and quantified by the algorithm IP-BO/Input. Dissociation curves showed that the PCRs yielded a single product.

2.9 Plasmids and constructs

For expression of NFI-A within primary HPCs, HL-60 and K562 cells the lentiviral vector encoding HA-NFI-A was previously described [128]. For the ectopic expression of miR-223 the lentiviral vector was previously described [126].

The shRNA expressing lentiviral vector to knockdown human NFI-A within primary HPCs, HL-60 and K562 cells was designed as follows. siNFI-A was designed using siRNA advanced design tools from the MWG (http://www.mwg-biotech.com/) and Ambion (http://www.ambion.com/) websites: these tools employ various published criteria to obtain the most effective siRNA in terms of silencing efficiency and reduced off-targeting effects (including custom BLAST analysis). The shRNA encoding the siNFI-A sense 5'-AACCAGAGGTCAAGCAGAA-3' was subcloned into the pSUPER.retro.neo+GFP plasmid, from which the shRNA expression cassette was then cloned into the ClaI site of pRRLcPPT.hPGK.EGFP.WPRE lentiviral vector (named Vector) to generate the siNFI-A vector. After comparison to our previously published siNFI-A (here named siNFI-A-2), we selected the siNFI-A for subsequent studies as distinct shRNA producing a consistent phenotype are expected to have non-overlapping spectra of off-target effects[144] and did not

induce a non-specific interferon response as measured by Real-time PCR using OAS1, OAS2 and IFN primers listed in Table 2-1.

For the ectopic expression of NFI-A within murine embryo cells a cDNA encoding HA tagged mNFI-A was isolated from the expression plasmid pCHNFI-A1.1 (kindly provided by Dr. Richard Gronostajski) by digestion with Not I and Nhe I restriction enzymes (Promega, Madison, WI USA). The resulting cDNA fragment was subcloned by blunt ligation into the Sma I site of the pBlueskript KS plasmid (Stratagene, La Jolla, CA USA). The pBlueskript KS plasmid containing the HA-NFI-A with correct directionality was digested with Xho I and Xba I restriction enzymes (Promega) and the resulting HA-NFI-A cDNA fragment was cloned into the lentiviral vector pRRL.cPPT.hCMV.hPGK.GFP.WPRE within the Xho I and Xba I sites. This system allows expression of HA-NFI-A from the CMV promoter and simultaneous expression of the reporter GFP from the PGK promoter. cDNA encoding NFI-B, NFI-C, and NFI-X were also digested from pCHNFI-B2, pCHNFI-C2 and pCHNFI-X2 expression plasmids (kindly provided by Dr. Richard Gronostajski) using Not I and Nhe I restriction enzymes as above. These cDNA constructs were cloned blunt into the pBlueskript KS plasmid cut with EcoRV (Promega), and clones with correct directionality were cut with Xho I and Xba I enzymes and the resulting HA-tagged NFI proteins were cloned as above into the pRRL.cPPT.hCMV.hPGK.GFP.WPRE lentiviral vector.

A second construct was designed to to knockdown NFI-A within murine embryo cells as the NFI factors display 96-99% homology to human NFI factors at the protein level and 90-95% homology at the nucleotide sequence. A nBLAST (http://blast.ncbi.nlm.nih.gov/Blast.cgi) showed only 14 nucleotides out of 19 similar to the human siNFI-A designed above. Therefore cloning steps were performed as described above for the human siNFI-A using the msi-NFI-A sequence 5’- GCACACTGAAGAAGTCTGA-

3'. A negative control vector expressing a siRNA against luciferase was also cloned as above using the sequence 5' – CTTACGCTGAGTACTTCGA- 3'.

For promoter luciferase assays the G-CSFR promoter was PCR-amplified from human genomic DNA using the primers listed in Table 2-1, and cloned into the pGL3-Basic plasmid (Promega) using the *Kpn*I and *Bgl*II sites. Site-specific mutant constructs were generated by deleting the sites using the primers listed in Table 2-1. For promoter luciferase assays the β-Globin proximal promoter was PCR-amplified from human genomic DNA and inserted between the *Kpn*I / *Xho*I sites of the pGL3-Basic plasmid (Promega). NFI-A site-specific mutations were introduced using the QuikChange Multi Site-directed Mutagenesis kit (Stratagene) according to the Manufacturer's instructions. For the complete list of primers employed see Table 2-1.

2.10 Luciferase Assay

For the β-Globin promoter assay, K562 cells (1×10^5 cells/mL) were transfected using Lipofectamine LTK + PLUS Reagent (Invitrogen) with 0.5 μg of pGL3-HB-Wt plasmid or one of the mutant constructs (HB-Mut1, HB-Mut2, HB-Mut3, HB-Mut (1-2-3)), 2 μg of pCH-NFI-A1.1 and 50 ng of pRL-TK plasmid (Promega).

The G-CSFR promoter assay was performed as above using 1ug of pGL3-GR-Wt plasmid or one of the mutant constructs (GR-Mut1, GR-Mut2 or GR-Mut (1-2)) and 50 ng of pRL-TK plasmid (Promega). Cells were harvested 48 hr post-transfection and assayed with Dual Luciferase Assay (Promega) according to the manufacturer's instructions.

2.11 Lentiviral production and infection

HEK293T cells were maintained in IMDM containing 4.5 g/l D-glucose, and pyruvate plus 10% FBS and 1% penicillin/streptomycin (Invitrogen). For production of virus cells were seeded in 150 mm plates 24 h prior to transfection so that on the day of transfection the cells were between 50-60% confluent. Media was changed 4 hours prior to transfection of

HEK293T with the following plasmids: 20 µg of transfer lentiviral vector, 13 µg of the pCMVRΔ8.74 (encoding gag, pol, rev) packaging vector and 7 µg of the pMDG plasmid (expressing the VSV-G envelope). Plasmid mix was made in 1 mL of ddH_20 and 0.25M final $CaCl_2$ which was added dropwise to 1 mL of 2X HBS buffer [10 mM D-Glucose (Applichem GmbH, Darmstadt Germany), 10 mM KCl, 1.4 mM Na_2HPO_4, 38.4 mM HEPES sodium salt, 274 mM NaCl (all purchased from Sigma)] to form precipitates while bubbling air through the solution. Precipitates were added to the cells and the media was replaced after 14-16h. Virus was collected 48 h after transfection, filtered through a 45 µM filter, aliquoted and stored at -80°C. Transducing units measured by titration of virus on HeLa cells ranged from 0.5-1.0 x 10^8 TU/mL.

Cell lines and primary cells were infected by the spin-innoculation method. For infection of cell lines, cells were plated at a concentration of 1 x 10^5/mL of virus with 4 µg/mL polybrene (Sigma) in 12 or 24 well plates and centrifuged at 1800 RPM at 32°C for 45 min. Cells were then placed in a fully humidified incubator at 37°C, 5% CO_2 in air for 2-4 hours, after which the cells were washed with PBS and put in the appropriate culture media. The efficiency of transduction was examined by GFP expression 48 h after transfection by flow cytometry using the FACScan instrument (BD Biosciences, Franklin Lakes, NJ, USA), and resulted in efficiencies of 97-100%. For the infection of primary cells; $CD34^+$ cells were infected at day 1 of culture and were plated at a concentration of 1 x 10^5 cells/mL of virus with 4 µg/mL polybrene, and centrifuged at 32°C for 45 min after which the cells were incubated at 37°C 5% CO_2 in air for 1h 15 min followed by plating in fresh media. At 48h after infection the cells were monitored for GFP expression by flow cytometry, showing an average transduction efficiency ranging from 15-20% (for the HA-NFI-A construct) to 30-40% (for empty lentivirus (Vector) and human siNFI-A). At this time GFP^+ cells were sorted

using the FACSaria instrument (BD Biosciences) and placed in liquid phase culture or clonogenic medium.

2.12 Statistical analysis

Comparison between multiple groups was made by one-way analysis of variance (ANOVA) and the Tukey post test to analyse significance. Two-tailed *t-test* analysis for significance was used to compare individual data to control values. *p*-values legend: * $p < 0.05$, ** $p < 0.01$.

Chapter Three: RESULTS

3.1 AIM I: To examine if deregulated miR-223 expression is associated with differentiation block underlying the pathogenesis of distinct leukemia subtypes, and to determine regulating factors involved.

Results of AIM I are summarized below and these results were recently published in the paper located in APPENDIX I.

Fazi F., Racanicchi S., Zardo G., Starnes L.M., Mancini M., Travaglini L., Diverio D., Ammatuna E., Cimino G., Lo-Coco F., Grignani F., Nervi C. "Epigenetic silencing of the myelopoiesis-regulator microRNA-223 by the AML1/ETO oncoprotein". Cancer Cell. 2007 Nov;12(5):457-66.

To answer the above aim we first examined the miR-223 expression levels by quantitiative real-time PCR within peripheral blood (PB) an bone marrow (BM) samples of 31 leukemia patients and found that miR-223 was expressed at high levels in BM and PB from healthy donors (~50-70% committed/mature myeloid precursors) and was at lowest levels in immature $CD34^+$ HPCs isolated from normal PB or BM isolated from leukemias related to erythroblastic (M6) or lymphoid lineages, and in the most immature myeloid phenotype (M0 and M1) FAB classifications. Intermediate levels were found in primary samples expressing more mature AML phenotypes (M3, M4, and M5 representing acute-promyelocytic, myelomonocytic, and monoblastic leukemias, respectively). Interestingly, low levels of miR-223 expression were found in cases harbouring the AML1/ETO fusion protein expressed due to the t(8;21). miR-223 levels were found to be lowest in the SKNO-1 AML cell line harbouring constitutively active AML1/ETO when compared to other AML cell lines. In fact, silencing of AML1/ETO via siRNA lentiviral transduction of the SKNO-1 cell line proved to raise the levels of endogenous miR-223 while overexpression of AML1/ETO in U937 cells (representing the M5 subtype with higher levels of miR-223) silenced the miR-223 expression. This effect was further demonstrated to be specific to the AML1/ETO fusion protein as overexpression of PML/RARα, the AML-M3 associated fusion protein had no

effect on miR-223 expression within U937 cells. ChIP assay demonstrated that AML1/ETO specifically bound to an AML1 site present in the core-promoter sequence of the pre-miR-223 upstream region, which was further verified by luciferase reporter constructs. It is known that AML1/ETO interacts with histone deacetylases (HDACs) and DNA methyltransferases (DNMTs) rendering AML1/ETO a potent transcriptional silencer [145, 146]. ChIP assay and bisulfite sequencing demonstrated the presence of deacetylated histones and hypermethylated CpGs within the pre-miR-223 chromatin regions occupied by AML1/ETO within SKNO-1 cells, and U937 cells overexpressing AML1/ETO but not in U937 mock cells expressing empty lentiviral vector, or in HL-60 cells. Notably, when AML1/ETO was knocked down in SKNO-1 cells via siRNA, the histone acetylation was restored and the CpGs methylation was decreased. At the same time, upon AML1/ETO knockdown via siRNA, or treatment with a demethylating agent 5-azacytidine, the miR-223 levels of expression in these cells increased 2-3 fold while NFI-A protein levels, a target of miR-223, decreased and cells also increased the expression of CD11b being an early myeloid differentiation marker. Importantly, I was able to contribute to this study by transducing HL-60 cells and fresh primary blasts isolated from PB of two consecutive newly diagnosed AML patients of the M3 and M4-M5 subtype with a lentiviral vector ectopically expressing miR-223. From this experiment it was shown that overexpression of miR-223 led to the re-installment of the granulocytic differentiation program in these cells as measured by morphology and immunophenotype by flow cytometry analysis showing an increase in CD11b expression (Figure 5 and 6 of the attached paper: “Epigenetic silencing of the myelopoiesis regulator microRNA-223 by the AML1/ETO oncoprotein” located in APPENDIX I.

3.2 AIM II: To determine the function of TF NFI-A in normal human adult definitive hematopoiesis using both leukemic cell lines and primary culture of HPCs.

The results for AIM II have recently been published in the following paper that can be found in APPENDIX I.

*Starnes L.M. *Sorrentino A., Pelosi E., Ballarino M., Morsilli O., Biffoni M., Santoro S., Felli N., Castelli G., De Marchis M.L., Mastroberardino G., Gabbianelli M., Fatica A., Bozzoni I., Nervi C., Peschle C. "NFI-A directs the fate of hematopoietic progenitors to the erythroid or granulocytic lineage and controls β-globin and G-CSF receptor expression". Blood. 2009 Aug;114(9):1753-63.(* Equal contribution)

3.2.1 NFI expression patterns in HL-60 and K562 leukemia cells and during unilineage E and G culture of human hematopoietic progenitor cells (HPCs).

HL-60 cells are a myeloblastic cell line representing the M2 FAB classification, and are capable of granulocytic differentiation in the presence of RA and monocytic differentiation in the presence of $VitD_3$ [147]. K562 cells were isolated from a chronic myelogenous leukemia (CML) patient in blast crisis [148]. These cells are capable of erythroid differentiation in the presence of Ara-C [149] and megakaryocytic-monocytic differentiation in the presence of phorbol esters [150]. Initial examination by real-time PCR analysis shows that the NFI factors (A, C and X) are expressed at higher levels within K562 cells than HL-60 and that this difference is greatest for the factor NFI-A, and NFI-B is not expressed (Figure 3-1A). Factors important for erythroid differentiation include GATA-1 and LMO2, and for granulocytic differentiation; C/EBPα. NFI-A mRNA expression pattern is similar to GATA-1, being a key factor for erythroid differentiation (Figure 3-1B). Upon collaboration with Dr. Cesare Peschle NFI levels were examined in $CD34^+$ HPCs isolated from cord blood and put into either Granulocytic (G) unilineage culture or Erythroid (E) unilineage differentiation culture to induce granulocytic and erythroid differentiation respectively. During granulocytic differentiation NFI-A, B, and X factors are downregulated at the mRNA level during later stages of granulocytic differentiation whereas NFI-C levels remain relatively the same (Figure

3-1C,E). During erythroid differentiation NFI-B and C are barely expressed (Figure 3-1D), and NFI-X is upregulated slightly during early culture days and then is downregulated at later times when compared to NFI-A (Figure 3-1E). Of the NFI factors, NFI-A is drastically upregulated during erythroid differentiation at the mRNA level (Figure 3-1D, E). Based on these preliminary findings we decided to further study specifically NFI-A.

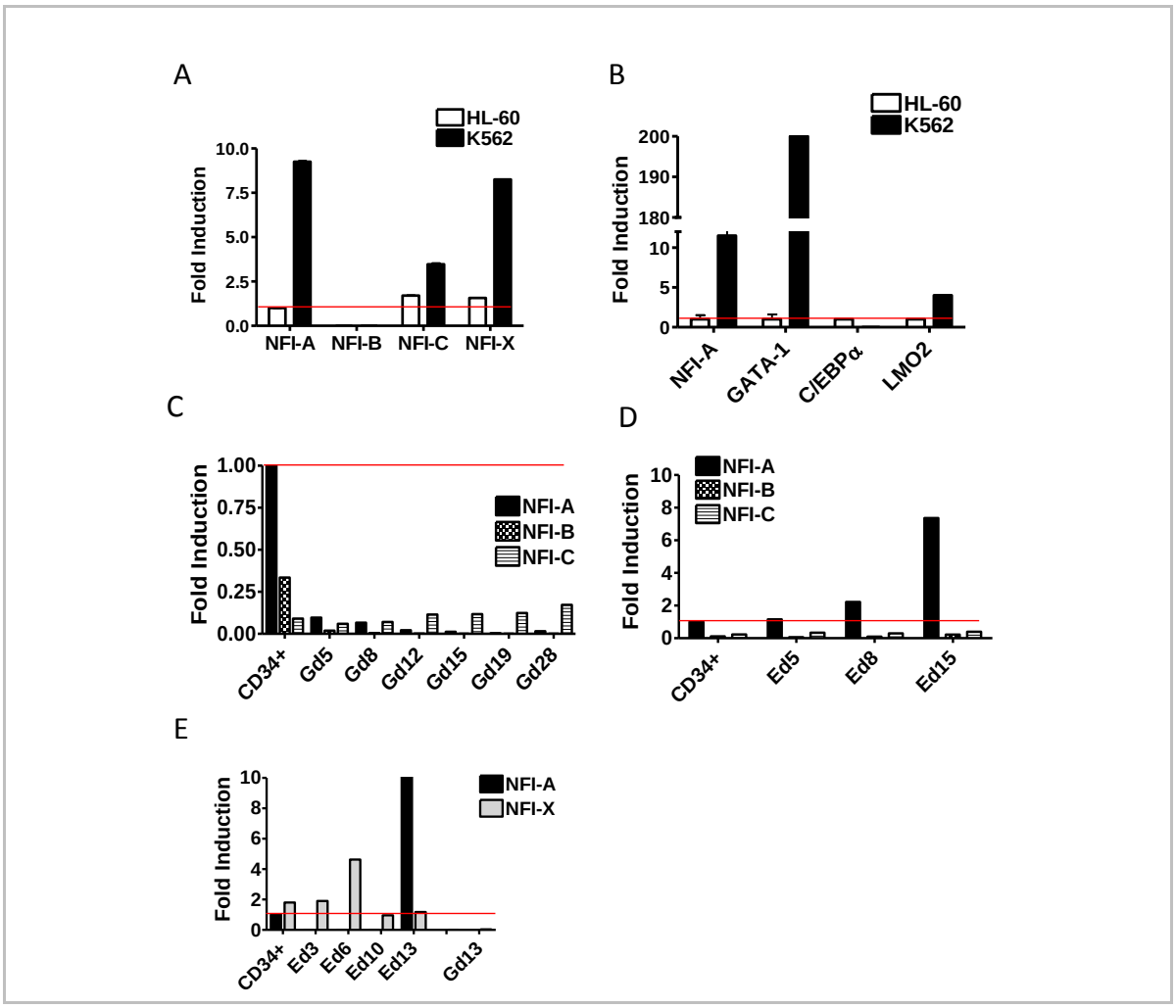

Figure 3-1 Real-Time PCR analysis of NFI factor expression. (A) NFI-A, B, C, X mRNA expression in HL-60 and K562 cells relative to NFI-A levels in HL-60 cells. **(B)** NFI-A, GATA-1, C/EBPα, and LMO2 mRNA levels in HL-60 and K562 cells relative to HL-60 levels for each gene. **(C)** NFI-A, B, C mRNA levels relative to NFI-A levels in $CD34^+$ HPCs during unilineage granulocytic (G) differentiation. **(D)** NFI-A, B, C mRNA levels relative to NFI-A levels in $CD34^+$ cells during unilineage erythroid (E) differentiation. **(E)** NFI-X mRNA expression levels relative to NFI-A in $CD34^+$ HPCs during unilineage erythroid differentiation, and at a late day of granulocytic differentiation (Gd13). NFI-A samples were analyzed in CD34+ and Ed13 for comparison. Representative data out of 3 separate experiments.

3.2.2 NFI-A expression is upmodulated during erythropoiesis, while shut off during granulopoiesis.

Closer examination of NFI-A during unilineage culture systems revealed that in the E culture, NFI-A is sharply upmodulated at both the RNA and protein level (Figure 3-2C), in parallel with the increase of Glycophorin-A^+ (GPA) cells (a major sialoglycoprotein of the erythrocyte membrane) by flow cytometry analysis, and erythroblast differentiation/maturation (Figure 3-2Aii-iii) as measured by morphology analysis. Conversely, in G culture we observed a drastic decrease of NFI-A, reaching undetectable RNA and protein levels starting from day 10-13 (Figure 3-2D): this correlated with the increasing number of $CD15^+$ cells (a marker of more mature neutrophils) as measured by flow cytometry and G differentiation/maturation at the morphology level (Figure 3-2Bii-iii).

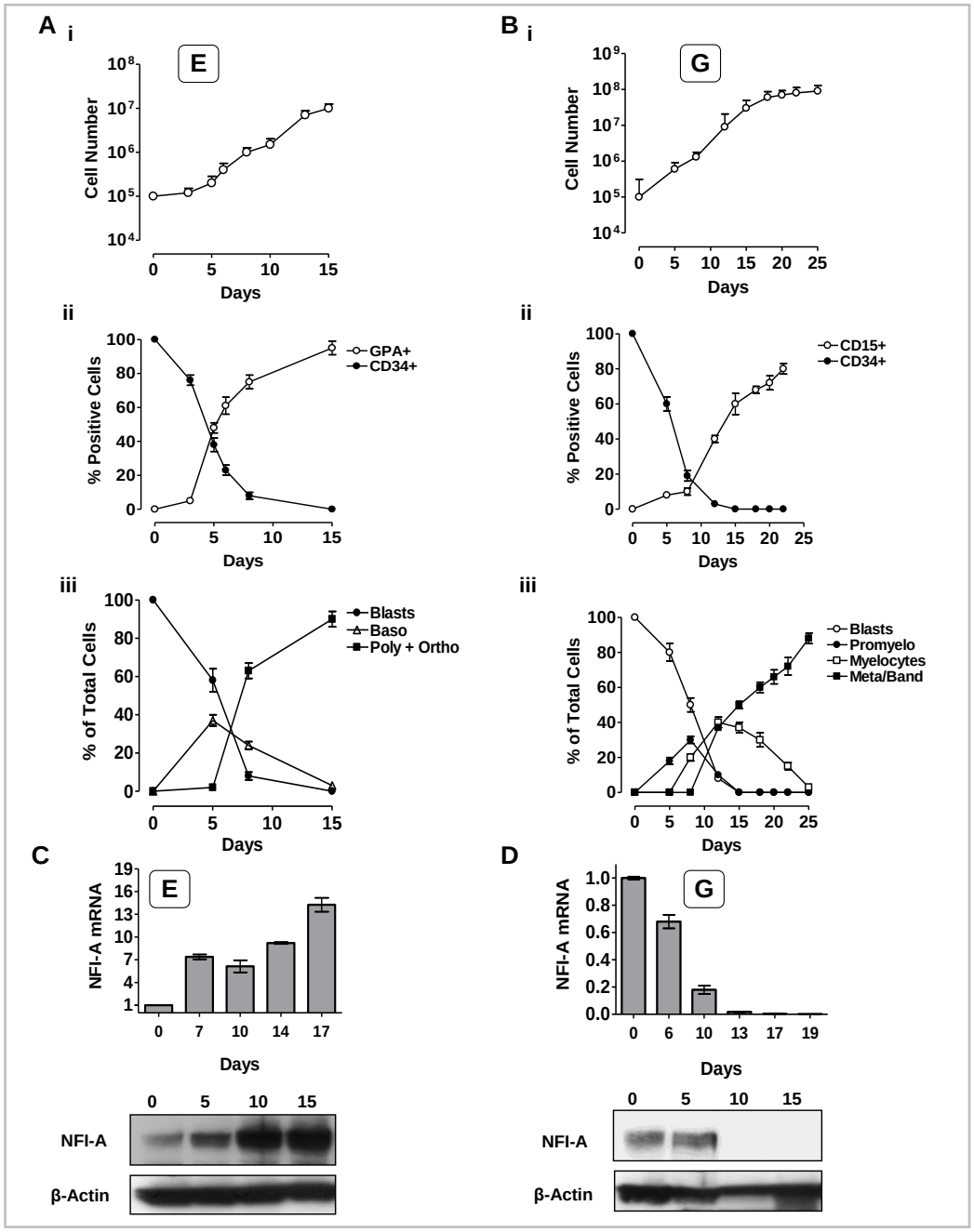

Figure 3-2 Unilineage erythroid (E) and granulocytic (G) culture of HPCs: NFI-A expression pattern during E and G differentiation/maturation. (A) Unilineage E culture of cord blood (CB) $CD34^+$ HPCs. **(i)** Growth curve, **(ii)** CD34 and GPA surface marker expression, and **(iii)** percentage of blasts, proerythroblasts (Blasts), basophilic (Baso), polychromatophilic (Poly) and orthochromatic (Ortho) erythroblasts (mean +/- SEM values (*n*=7)). **(B)** Unilineage G culture of CB $CD34^+$ HPCs. **(i)** Growth curve, **(ii)** CD34 and CD15 surface marker expression, and **(iii)** percentage of blasts, promyelocytes (Promyelo), myelocytes, mature metamyelocytes and band cells (Meta/band) (mean +/- SEM values (*n*=8)). **(C)** NFI-A increases in E culture. (Upper) Real-time PCR evaluation of NFI-A mRNA. Normalized mean +/- SEM values (*n*=3). (Lower) Immunoblot of NFI-A protein. β-Actin was used as loading control. **(D)** NFI-A decrease in G culture. (Upper) Real-time PCR evaluation NFI-A mRNA. Normalized mean +/- SEM values (*n*=3). (Lower) Immunoblot of NFI-A protein.

3.2.3 NFI-A upregulation is required for erythroid differentiation of HPCs

The dichotomy of NFI-A expression patterns in the E vs. G lineage suggested that this TF may exert opposite functional actions in these cell differentiation pathways. To verify this hypothesis, we first monitored the effects of NFI-A knockdown in HPCs seeded in E culture using a lentiviral construct encoding a shRNA targeting NFI-A mRNA (named siNFI-A). To exclude possible off-target effects, siNFI-A was compared to a previously published shRNA against NFI-A[126] (here named siNFI-A-2): both the constructs specifically knocked down NFI-A, and siNFI-A showed the maximum silencing efficiency (Figure 3-3A) without triggering an off-target interferon response (Figure 3-3B). In E culture, HPCs stably expressing siNFI-A showed an impaired growth capacity: by day 8 the majority of the cells were non-viable (Figure 3-3C-D). NFI-A protein knockdown in siNFI-A expressing cells was confirmed by western blot (Figure 3-3E). Moreover, E differentiation/maturation in siNFI-A cells was dramatically afflicted: at day 12, the residual cells were almost totally of granulocytic and monocytic type (Figure 3-3F-G). Similarly, clonogenic assays in E medium showed that siNFI-A transduction caused a drastic reduction of the BFU-E colony number (Figure 3-3H). These results indicate that NFI-A upmodulation is necessary to allow normal E differentiation/maturation of HPCs.

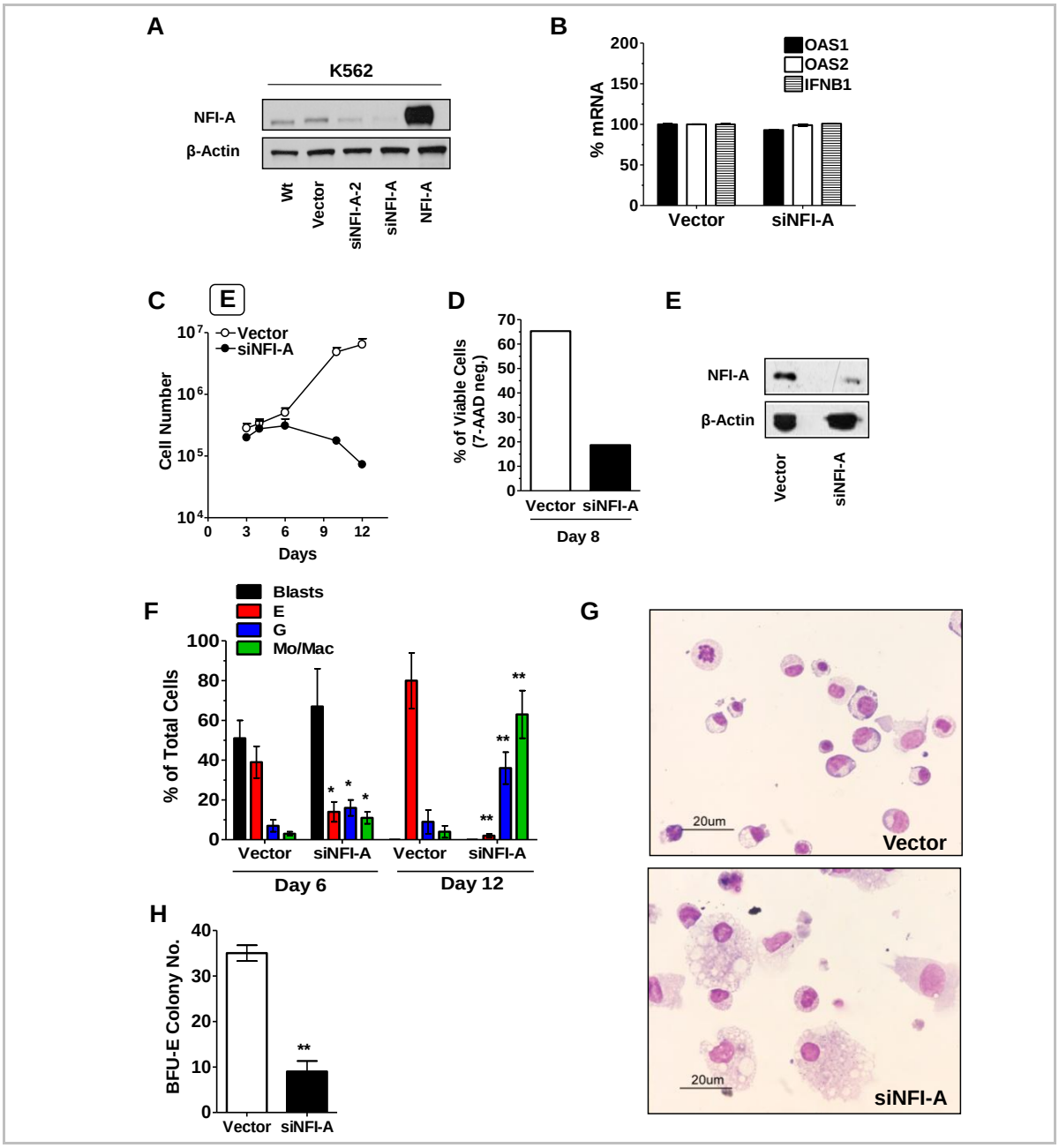

Figure 3-3. NFI-A knockdown impairs erythroid (E) differentiation of HPCs. (A) Immunoblot analysis of NFI-A in K562 wild type cells (wt) and control empty vector (Vector)-, siNFI-A-2-, siNFI-A-, NFI-A-overexpressing cells, showing the various degrees of knockdown and overexpression of the protein. **(B)** Real-time PCR of the interferon-response genes OAS1, OAS2 and IFNB1 in Vector- and siNFI-A-K562 cells. Mean +/- SEM from 2 paired experiments. **(C)** Growth curve of HPCs in unilineage E culture infected with control Vector or siNFI-A. Mean +/- SEM values of three independent experiments. **(D)** The histogram shows the percentage of viable (or 7-AAD-negative) cells detected by flow cytometry (Representative out of three). **(E)** Western blot analysis confirming NFI-A knockdown in siNFI-A expressing HPCs in unilineage E culture. **(F)** Wright-Giemsa staining of Vector- and siNFI-A-transduced cells. Percentage of blasts, erythroid (E), granulocytic (G) and monocytic/macrophage (Mo/Mac) cells. Mean +/- SEM values of three independent experiments. **(G)** Morphology of Vector and siNFI-A cells at day 12 of E culture (representative field, original magnification x 400). **(H)** Number of BFU-E colonies generated by Vector- and siNFI-A-infected HPCs. Mean +/- SEM values (*n*=3).

3.2.4 NFI-A accelerates erythroid differentiation of K562 cells, HPCs, and it restores erythropoiesis of HPCs in the presence of suboptimal or minimal erythropoietin (Epo) stimulus.

We then hypothesized that the enforced overexpression of NFI-A may favour E differentiation, as compared to empty Vector cells. NFI-A ectopic expression in K562 caused an increase in benzidine stained cells and GPA expression in both baseline conditions and Ara-C-induced E differentiation with no significant change in cell growth rates (Figure 3-4Ai-iii).

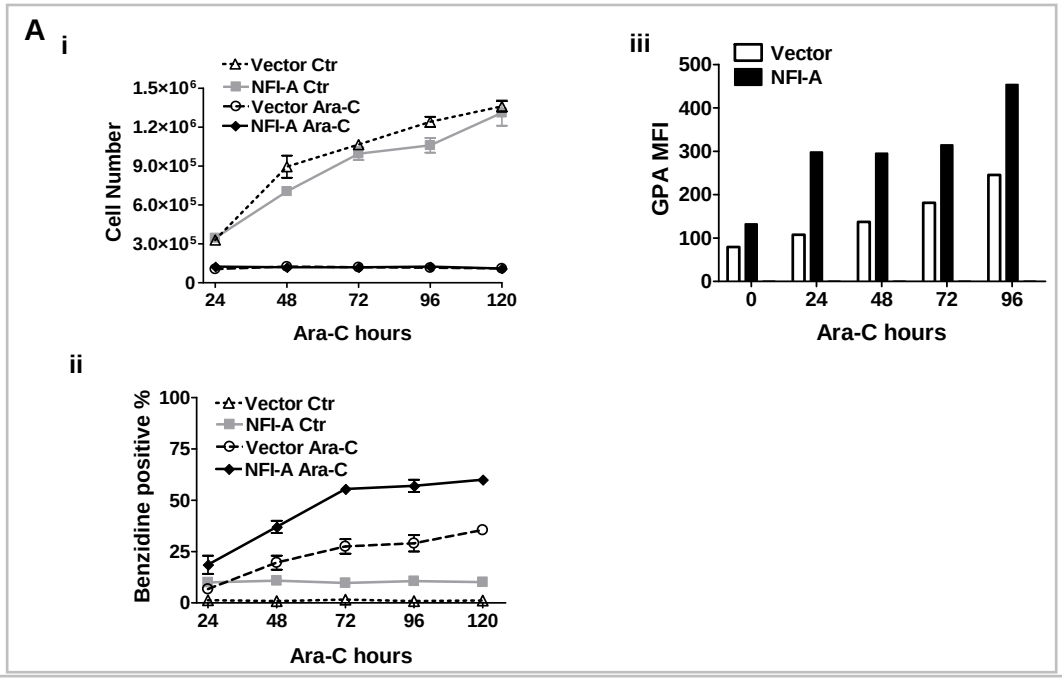

Figure 3-4 Differentiation status of Vector- and NFI-A-transduced K562 cells in the absence and presence of Ara-C. (A) (i) Growth curve and **(ii)** Benzidine counts and **(iii)** Glycophorin A Mean Fluorescence Intensity (MFI) of K562 cells transduced with either NFI-A- or empty Vector- lentivirus in untreated control (Ctr) cells or treated with Ara-C for 120 hours. Mean +/- SEM values are shown (n=3).

Lentiviral NFI-A overexpression in HPCs seeded in E culture (Figure 3-5Ai) resulted in an accelerated differentiation and maturation, as demonstrated by the increase of orthochromatic erythroblasts at day 8 (Figure 3-5Aii). Western blot analysis using anti-HA and anti-NFI-A antibodies confirmed the expression of exogenous NFI-A (Figure 3-5Aiii).

In standard E culture saturating levels of Epo (3 U/ml) are required to induce optimal erythroblast expansion and differentiation/maturation[151, 152]. We hypothesized that NFI-A overexpression may restore erythropoiesis in the presence of a suboptimal or minimal Epo

stimulus. To test this hypothesis, we supplemented E culture with a low or minimal Epo concentration, corresponding respectively to 1:20 (0.15 U) and 1:100 (0.03 U) of the saturating Epo level. When compared to control cells, NFI-A-transduced HPCs seeded in Epo 0.15 U medium displayed a similar proliferation rate (Figure 3-5Bi), while exhibiting enhanced differentiation/maturation as indicated by erythroblast morphology (Figure 3-5Bii), GPA expression and β-Globin mRNA level (Figure 3-5Biii). Interestingly, NFI-A enforced expression also increased BFU-E colony formation (Figure 3-5Biv). When Epo was lowered to 0.03 U, cell expansion was blocked (Figure 3-5Ci): importantly, erythroid cells were not present in control culture, while NFI-A overexpressing cells matured to the terminal stage, as shown by the increase of GPA^+ cells (Figure 3-5Cii) and morphology analysis (Figure 3-5Ciii-iv).

We conclude that NFI-A overexpression in HPCs promotes E differentiation and maturation, while inducing a more mature E phenotype in K562 cells. Furthermore, NFI-A overexpression restores erythroblast development in E culture supplemented with a suboptimal or minimal Epo stimulus.

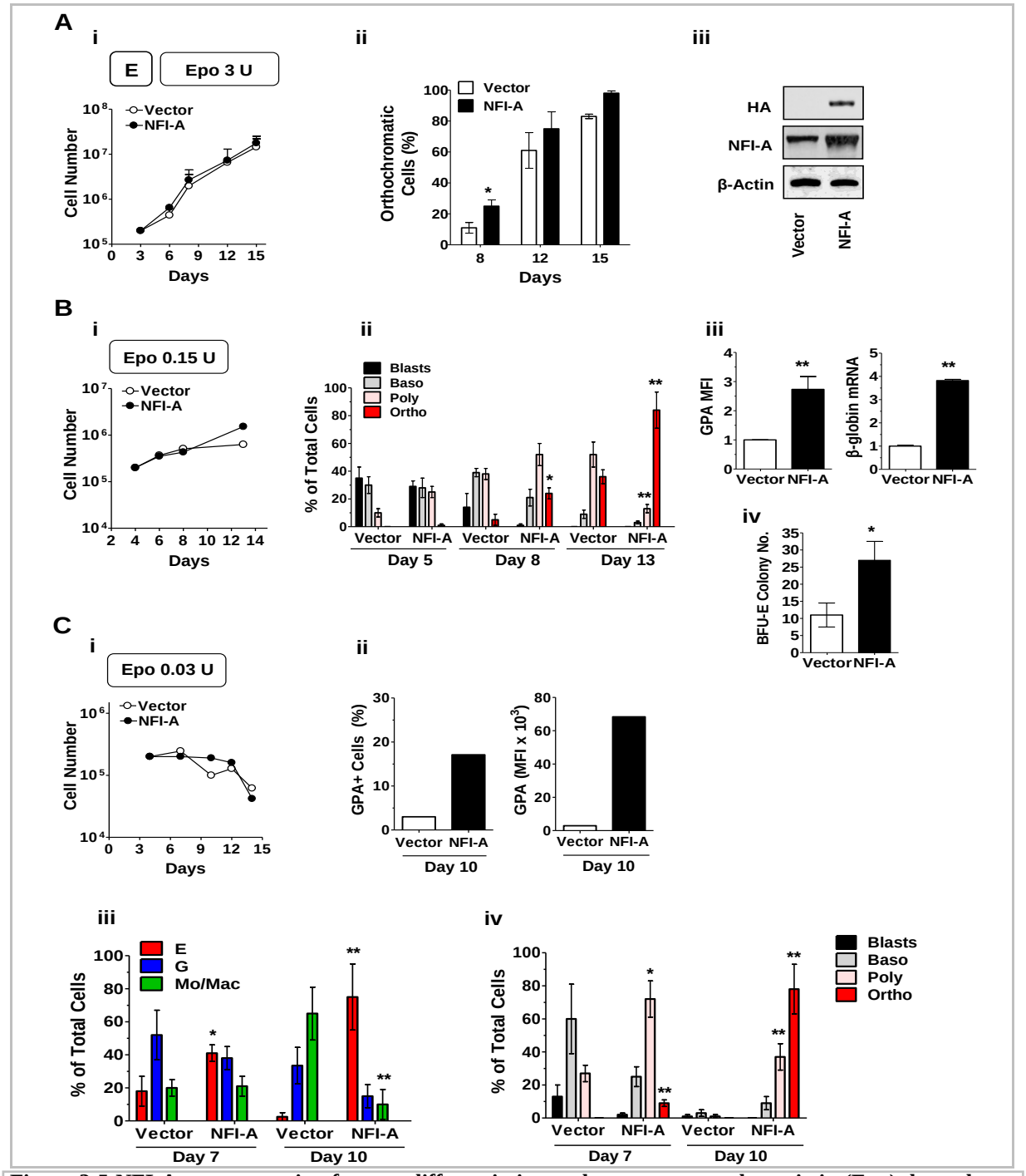

Figure 3-5 NFI-A overexpression favours differentiation and overcomes erythropoietin (Epo) dependence of erythroid (E) culture. (A) (i) Growth curve of Vector- and NFI-A-transduced HPCs in standard unilineage E culture (Epo 3 U/ml). Mean +/- SEM values (n=3). **(ii)** Percent of orthochromatic cells at sequential stages of E culture generated by Vector- and NFI-A-expressing HPCs. Mean +/- SEM values (*n*=3). **(iii)** Western blot showing ectopic expression of HA-tagged NFI-A in NFI-A-infected HPCs in E culture at day 8. **(B) (i)** Growth curve (A representative experiment out of three is shown) and **(ii)** Morphological evaluation (Mean +/- SEM values (*n*=3)) of E differentiation of Vector- and NFI-A- transduced HPCs seeded in E culture with suboptimal amounts of Epo (0.15U). **(iii)** Increase of GPA Mean Fluorescence Intensity (MFI) (Mean +/- SEM values (*n*=3)) and real-time PCR showing β-Globin mRNA expression (Mean +/- SEM values from two independent infections) **(iv)** Number of BFU-E colonies plated in Epo 0.15 clonogenic medium. Mean +/- SEM values of two paired experiments. **(C) (i)** Growth curve of Vector- and NFI-A-transduced HPCs in culture supplemented with minimal amounts of Epo (0.03 U). A representative experiment out of three is shown. **(ii)** Percentage of GPA^+ cells (left) and GPA MFI (right) at day 10. A representative experiment out of three is shown. **(iii-iv)** Morphology analysis of Vector- and NFI-A-infected HPCs (Mean +/- SEM values, *n*=3).

3.2.5 NFI-A downmodulation is necessary to permit granulocytic differentiation/ maturation

In the HL-60 cell line, ectopic expression of NFI-A (Figure 3-6A) decreased the RA effect on G differentiation, whereas NFI-A knockdown by siNFI-A (Figure 3-6A) increased the differentiation status of control cells as seen by morphology. In siNFI-A control cells there is a decreased cytosolic basophilia, appearance of paranuclear golgi region, and chromatin condensation with nuclear segmentation- that becomes more apparent with hypersegmented nuclei upon RA treatment at 96h (Figure 3-6B). On the contrary, NFI-A ectopic expressing cells remain less differentiated than empty Vector-transduced cells (Figure 3-6B). The decreased effect of RA on G differentiation of the NFI-A ectopic expressing HL-60 cells is also indicated by the lower level of differentiation markers (CD11b, CD15 and G-CSFR) (Figure 3-6Ci-ii,Di-ii). In fact, GCSF-R protein is not expressed in empty Vector-transduced cells, and becomes apparent only upon NFI-A knockdown (Figure 3-6Diii).

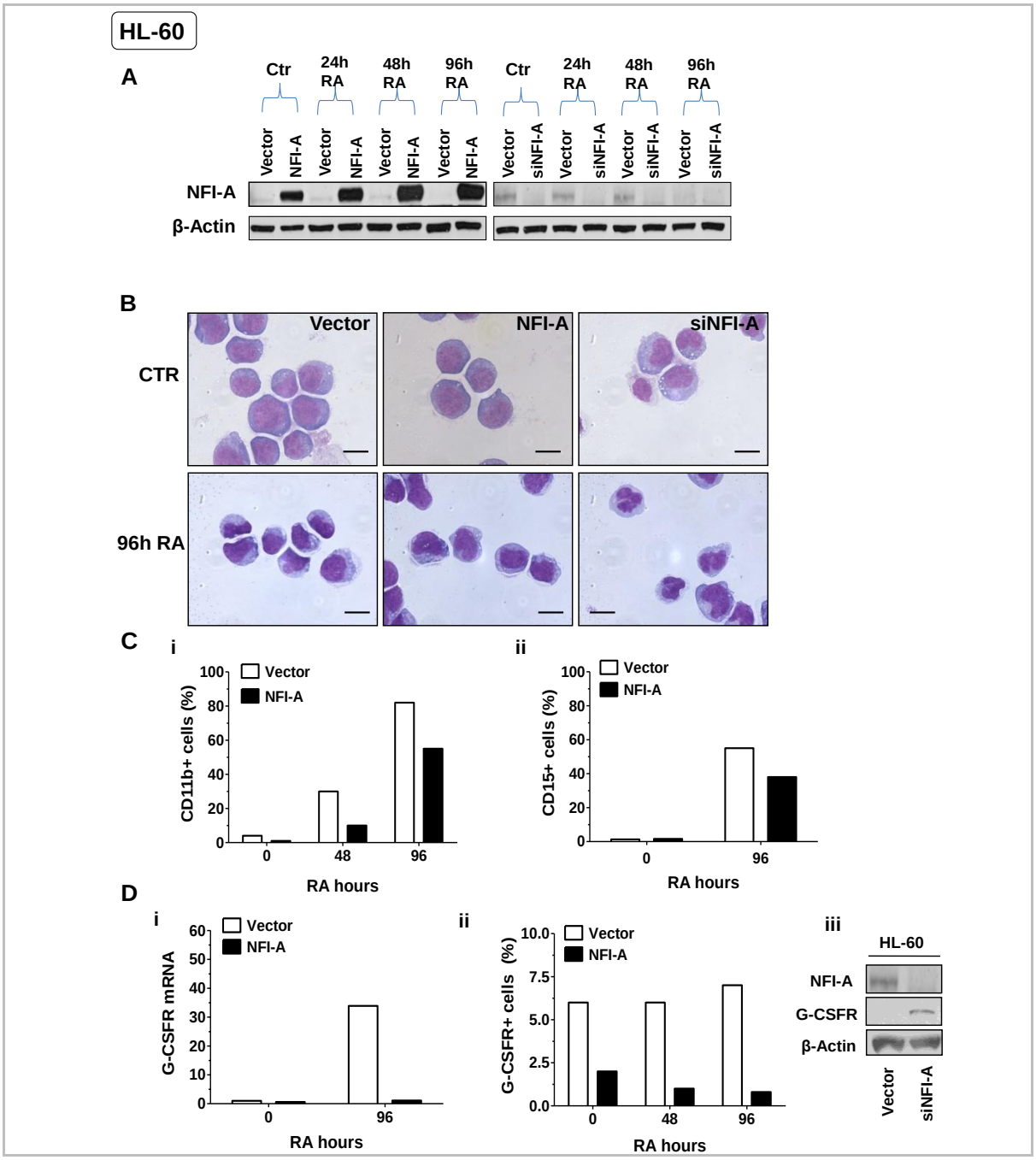

Figure 3-6 Ectopic expression of NFI-A in HL-60 cells blocks G differentiation whereas siNFI-A transduction accelerates G differentiation and induces G-CSFR expression. (A) Immunoblot of NFI-A expression showing ectopic NFI-A expression, and the effectiveness of siNFI-A in transduced HL-60 cells. β-actin was used as loading control. **(B)** Morphology of Vector, NFI-A and siNFI-A by Wright-Giemsa staining of cells with or without RA treatment for 96h (representative field, original magnification x 1000 scale bar=10 μM). **(C) (i)** Percentage of CD11b and **(ii)** CD15 positive HL-60 cells as detected by flow cytometry in the absence or presence of RA after 48 hours and 96 hours of treatment. **(D) (i)** G-CSFR mRNA levels as detected by real-time PCR in the absence and presence of RA at 96 hours after treatment. Values are relative to untreated (0 hours) cells. Mean +/- SEM values are shown (n=3). **(ii)** Surface G-CSFR expression as identified by flow cytometry in the absence or presence of RA after 48 and 96 hours of treatment. **(iii)** Immunoblot detection of endogenous NFI-A and G-CSFR expression in Vector- and siNFI-A-transduced HL-60 cells. β-actin was used as loading control.

To examine the functional role of NFI-A during normal granulopoiesis, HPCs transduced with a lentivirus encoding NFI-A were seeded in G culture. Control cells were transduced with the empty Vector. Cells expressing ectopic NFI-A had reduced viability (Figure 3-7Ai-ii) and showed a delayed entry in the G pathway (Figure 3-7Aiii). NFI-A cells displayed a significant reduction of G-CSFR mRNA (Figure 3-7Bi) and total protein expression (Figure 3-7Bii) in addition to a strong decrease in myeloid markers CD11b and CD14/15 (Figure 3-7Ci-ii). In a clonogenic G assay, Vector-transduced HPCs generated a significant number of CFU-G colonies of large size, while in cultures of NFI-A infected cells almost all G clones were abortive (Figure 3-7D).

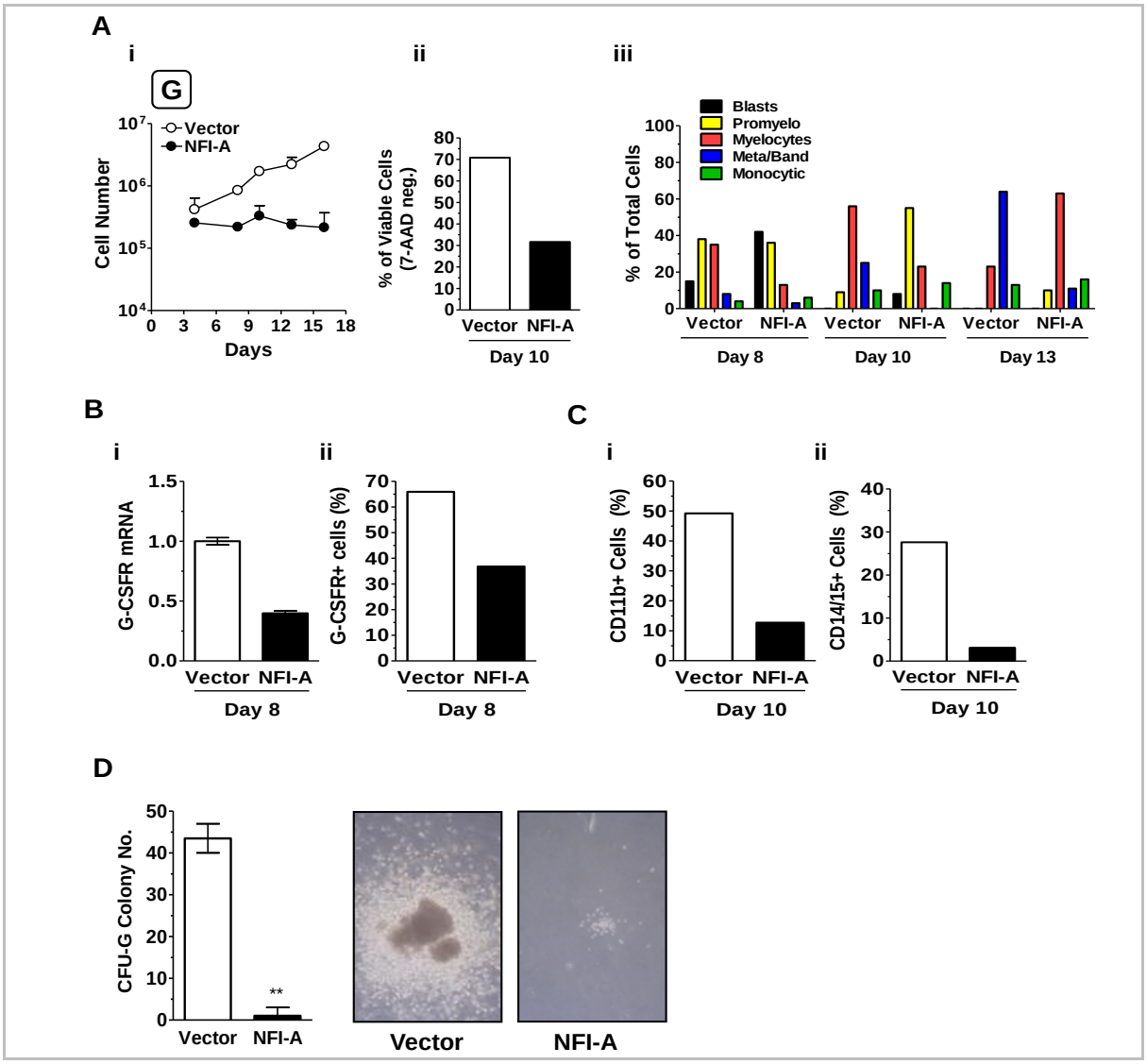

Figure 3-7 Ectopic expression of NFI-A blocks granulocytic (G) differentiation of HPCs. (A) (i) Growth curve of unilineage G cultures transduced with Vector or NFI-A lentivirus. Mean +/- SEM values of three independent experiments. **(ii)** The histogram shows the percentage of viable (or 7-AAD-negative) cells detected by flow cytometry (Representative out of three). **(iii)** Wright-Giemsa staining of infected cells, showing the percentage of cells at various stages of differentiation. A representative experiment out of three is shown. **(B) (i)** Real-time PCR analysis of G-CSFR mRNA and **(ii)** flow cytometry analysis of total G-CSFR protein expression in Vector and NFI-A cells at day 8. **(C)** Flow cytometry analysis of **(i)** CD11b and **(ii)** CD14/15 myeloid markers at day 10. **(D)** (Left) number of CFU-G colonies generated by transduced HPCs. Mean +/- SEM values (*n*=3). (Right) representative microphotographs of G colony or cluster in Vector or NFI-A culture respectively at day 14.

3.2.6 NFI-A is a regulator of the erythro-granulocytic lineage decision

Based on the above results, we hypothesized that NFI-A levels may function in directing HPCs into the E or G differentiation pathway. To test the hypothesis, we developed a culture system allowing HPCs to undergo bilineage E+G differentiation/maturation (Figure

3-8). This culture system is stimulated by an appropriate mixture of E and G growth factors (including Epo 0.6 U/mL and G-CSF 500 U/mL, see "Materials and Methods"): as a result, the proliferating cells are characterized by a balanced ratio of E and G cells undergoing differentiation and maturation up to the terminal stage, while including a small monocytic contaminant.

HPCs subjected to NFI-A enforced expression or knockdown were seeded into the E+G bilineage culture. Here again, control cells were infected with empty Vector. As shown in Figure 3-8Ai, NFI-A- and Vector transduced HPCs similarly proliferated and differentiated up to day 9. Thereafter, the E population significantly prevailed and matured more rapidly in NFI-A overexpressing cells (Figure 3-8Aii-iii). HPCs infected with siNFI-A proliferated similarly to control cells up to day 9, but then showed a blockage of cell expansion (Figure 3-8Bi). Notably, the siNFI-A-transduced cells displayed a predominant G morphology coupled with a more rapid maturation to mature granulocytes (Figure 3-8Bii-iii). Analysis of lineage-specific surface markers (GPA for the E and an equimolar mix of CD14/15 for the G lineage) at day 9 confirmed the morphological observations. NFI-A-infected cells express more GPA and no G markers, whereas siNFI-A-infected cells express with a greater intensity G markers and little or no GPA (Figure 3-8Ci). In addition, β-globin and G-CSFR mRNA (Figure 3-8Cii), along with G-CSFR protein expression analysed by flow cytometry (Figure 3-8Ciii) showed an opposite pattern of expression in the siNFI-A vs. NFI-A cells as compared to the Vector cells confirming the lineage-specific prevalence. At day 9 macroscopic observation of the control cell pellet showed a central core of red E cells, surrounded by white G cells, whereas the siNFI-A pellet is entirely G-white and NFI-A overexpressing cells are almost entirely E-red, as confirmed by microscopic morphological analysis of the same cell pellets (Figure 3-8D).

In a clonogenic E+G assay, GFP^+ colonies were scored after 14 to 18 days (Figure 3-8E). NFI-A overexpressing cells showed an increased proportion of BFU-E colonies and a dramatic reduction in CFU-G colonies compared to Vector colonies. In contrast, siNFI-A infected HPCs showed an opposite distribution of colony types, with a predominance of CFU-Gs.

Altogether, these experiments indicate that NFI-A plays a key role in the erythro-granulocytic lineage decision at the level of HPCs and possibly early precursors.

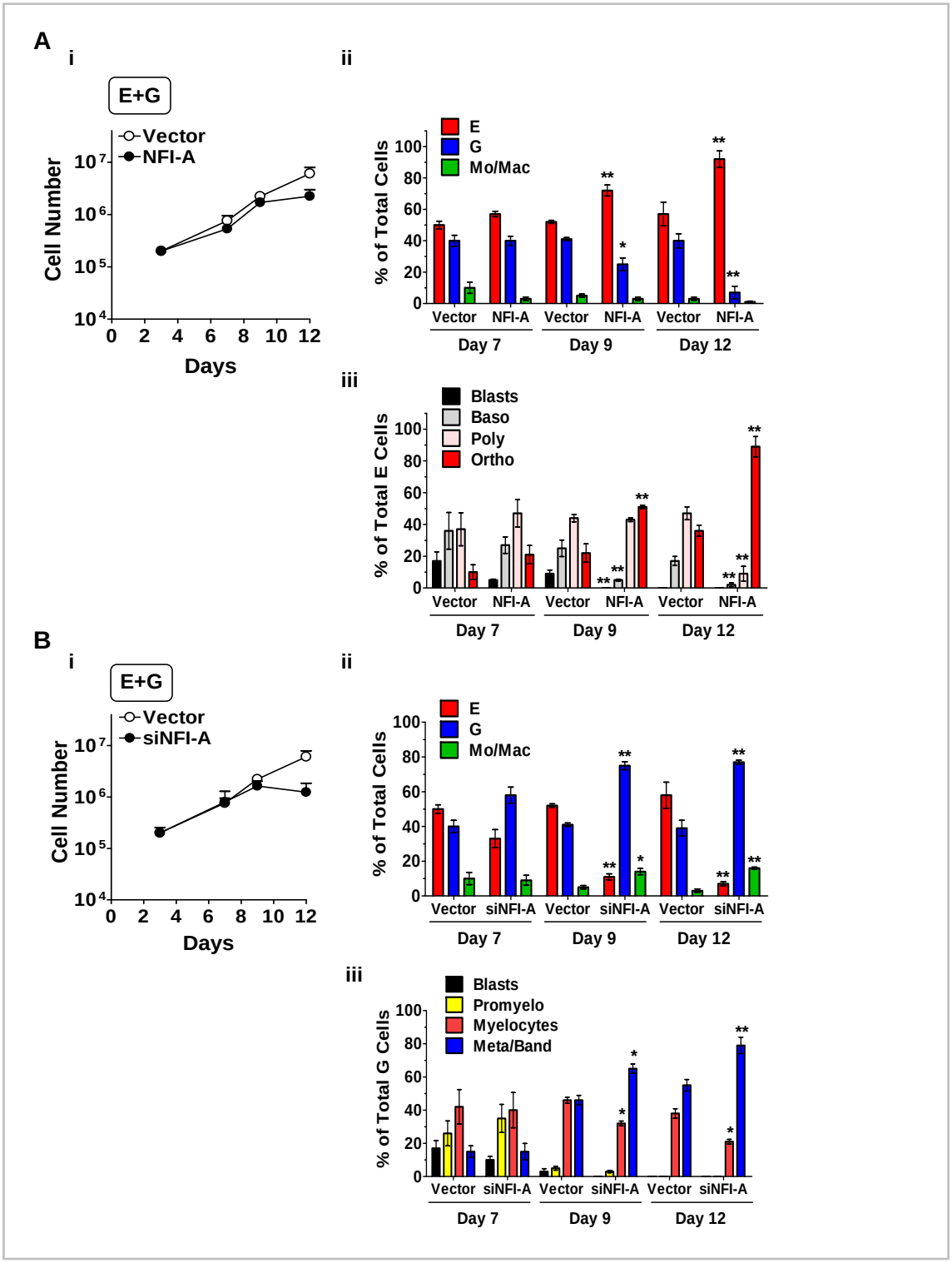

Figure 3.8 A,B (legend on following page).

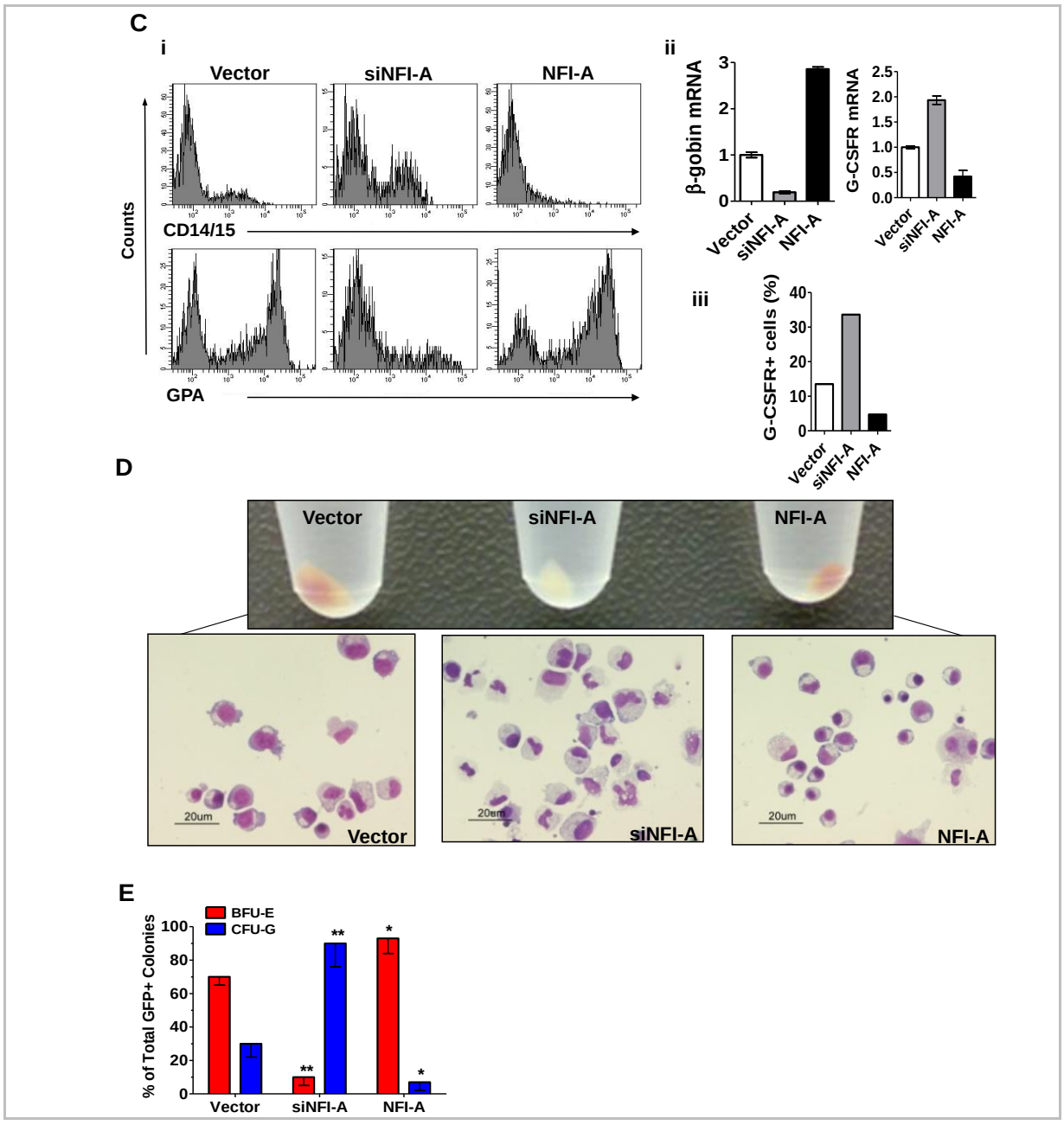

Figure 3-8 NFI-A regulates erythroid (E) versus granulocytic (G) lineage differentiation in bilineage E+G culture. Mean +/- SEM values from three independent experiments are presented. **(A)** Ectopic expression of NFI-A promotes E and inhibits G differentiation/maturation. **(i)** Growth curve, **(ii)** morphology analysis of the cellular composition at sequential culture times, and **(iii)** differentiation/maturation of the E population of Vector- and NFI-A-infected HPCs. **(B)** NFI-A knockdown blocks E and promotes G differentiation/maturation. **(i)** Growth curve, **(ii)** morphology analysis at sequential culture times, and **(iii)** differentiation/maturation of the G population in culture of Vector- and siNFI-A-infected HPCs. **(C)** Lineage-specific marker expression at early stage (day 9) of culture. **(i)** Representative flow cytometry analysis of Vector-, siNFI-A- and NFI-A-infected cells using the erythroid GPA and the myeloid CD14/15 markers, **(ii)** β-Globin and G-CSFR mRNA detected by real-time PCR, and **(iii)** percentage of cells expressing G-CSFR detected by flow cytometry (day 7). **(D)** Macroscopic and morphological changes of Vector-, siNFI-A- and NFI-A-infected cells at day 9 of E+G culture. (Upper) Macroscopic view of cellular pellets centrifuged from Vector culture (mixed population, erythroid red cells in the centre and peripheral myeloid-white cells in the surrounding ring), siNFI-A culture (only myeloid cells) and NFI-A culture (predominance of red cells). (Lower) Representative morphology fields (original magnification, x 400). **(E)** E+G clonogenic activity of HPCs transduced with Vector, siNFI-A or NFI-A viruses. Histograms represent the relative GFP^+ BFU-E and CFU-G colonies distribution. GFP^+ colony numbers were: Vector BFU-E 34,3+/-7, CFU-G 14,3 +/-5; siNFI-A BFU-E 4,6+/-1,5, CFU-G 31+/-9; NFI-A BFU-E 29,3 +/-6, CFU-G 3,5+/-1 (Mean +/- SEM values from three paired experiments is shown).

3.2.7 A functional relationship between NFI-A levels and two lineage-associated genes: β-globin and G-CSFR

We then attempted to explore the mechanism of NFI-A action by screening possible *cis*-acting elements interacting with NFI-A within promoter regions of E- and G-specific genes.

We selected the β-globin promoter as a target of NFI-A during E differentiation, since binding sites were noted in the proximal promoter region[153]. As expected, analysis of β-globin expression in E and G culture showed that the mRNA (not shown) and protein level greatly increased in the E series, while was absent in the G lineage (Figure 3-9A). Using a HPLC assay, we observed that in E culture NFI-A-overexpressing cells showed an increased β-chain content at both early and intermediate days of differentiation (Figure 3-9Bi). Conversely, real-time PCR showed a marked decrease of β-globin mRNA in siNFI-A-cells (Figure 3-9Bii). Results in K562 cells were striking (Figure 3-9Ci-ii). In empty Vector cells β-globin was not detectable in both control cultures and after Ara-C induced E differentiation, thus in line with previous reports[149, 154]. Conversely, β-globin mRNA and protein were strongly induced in NFI-A overexpressing cells in either control or Ara-C treated cultures (Figure 3-9Ci-ii). γ-globin and ε-globin were equally present in control Vector and NFI-A cells and both increased in a time dependent manner upon Ara-C treatment (Figure 3-9Ci). Altogether, these data show that ectopic expression of NFI-A specifically induces β-globin expression not only in E culture of HPCs, but also in K562 cells, which normally do not express β-globin.

Next, we focused on the G-CSFR, which contains two conserved putative NFI sites. In E culture the G-CSFR mRNA and protein levels dropped down to untraceable levels at terminal stages (Figure 3-9Di-ii). Conversely, in G culture the G-CSFR mRNA and protein level progressively increased through late maturation (Figure 3-9Ei-ii). In E cells, lentiviral knockdown of NFI-A was similarly associated with marked upmodulation of G-CSFR total protein and G-CSFR surface expression (Figure 3-9Fi-ii).

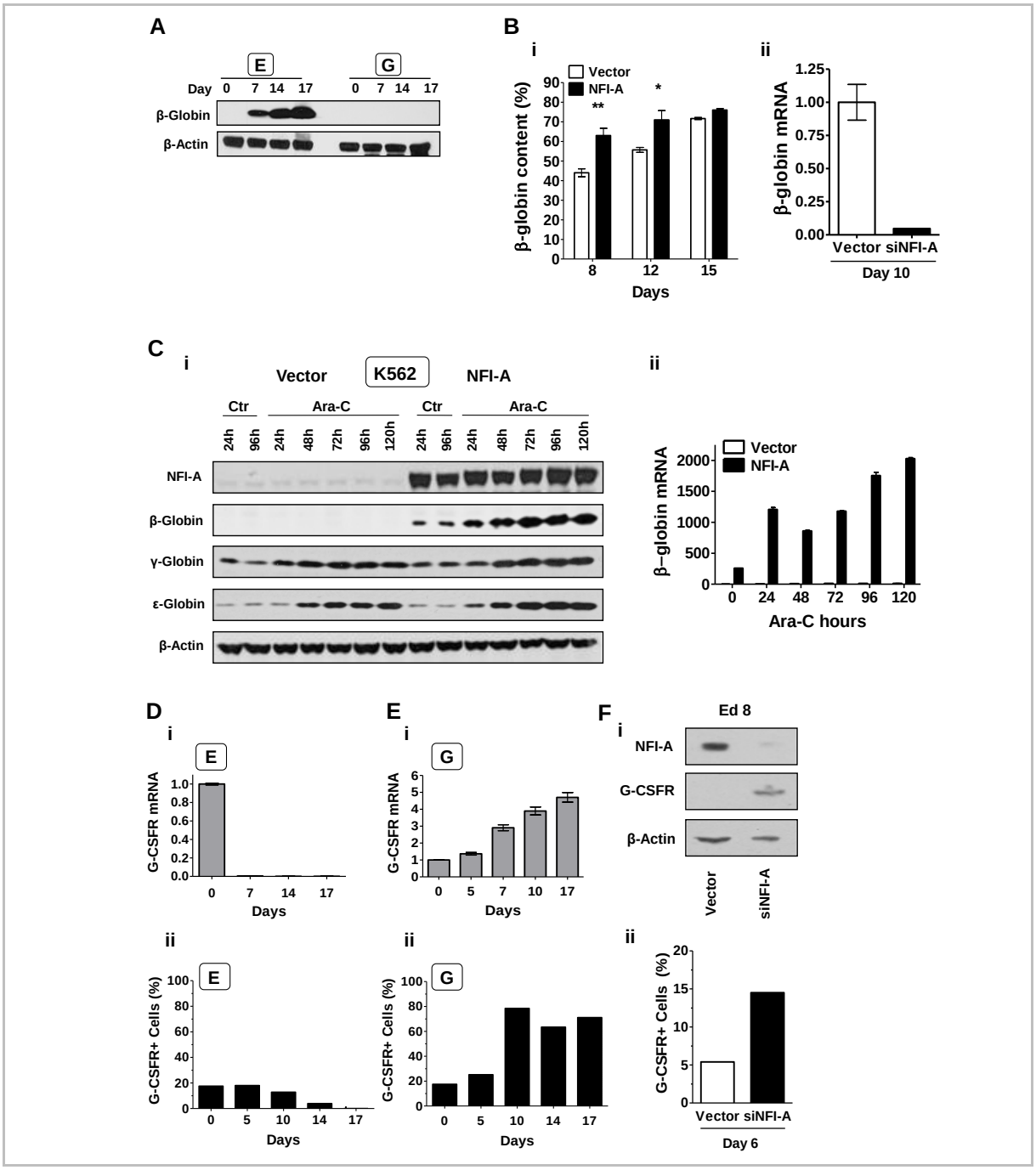

Figure 3-9 A functional relationship between NFI-A and two lineage-associated genes; β-globin and G-CSFR. **(A)** Immunoblot detection of β-globin at sequential stages of E and G culture. **(B) (i)** HPLC analysis of globin-chains content in unilineage E culture of HPCs transduced with empty Vector or NFI-A. The β-Globin chain content is expressed as the percentage of β-globin/non α-globin chain content (i.e., β/β+γ). Mean +/- SEM values (*n*=3). **(ii)** Real-time PCR of β-globin mRNA expression in siNFI-A-infected vs. empty Vector HPCs in E culture at day 10 (Mean +/- SEM values (*n*=3)). **(C)(i)** Western blot analysis of β-Globin, γ-Globin, ε-Globin and NFI-A protein expression in control (Ctr) and Ara-C treated Vector- and NFI-A- transduced K562 cells **(ii)** Real-time PCR showing β-Globin mRNA expression in Vector- and NFI-A-infected K562 cells during a time course of Ara-C. Values are relative to Vector-infected untreated cells (Ara-C 0 hours). Mean +/- SEM values are shown (*n*=3). **(D) (i)** G-CSFR mRNA during E culture detected by real-time PCR (Normalized mean +/- SEM values (n=3)) and **(ii)** percentage of G-CSFR$^+$ cells detected by flow cytometry that were permeabilised and stained with a PE-conjugated G-CSFR antibody. **(E) (i)** G-CSFR mRNA during G culture, and **(ii)** percentage of G-CSFR$^+$ cells detected by flow cytometry. **(F) (i)** Western blot analysis showing G-CSFR reactivation after NFI-A knockdown in siNFI-A-infected HPCs in unilineage E culture at day 8. **(ii)** Surface expression of G-CSFR detected by flow cytometry in siNFI-A infected E cells at day 6.

3.2.8 NFI-A directly activates β-Globin and represses G-CSFR proximal promoters, exhibiting a dual transcriptional activity in a lineage-specific context

Due to the functional role of NFI-A in β-globin induction, we attempted to map the *in vivo* binding of endogenous NFI-A to the β-globin promoter using chromatin-immunoprecipitation (ChIP). Computational analysis by Chip-Mapper, Alibaba 2.1 and Mat-Inspector Professional software programs[155-157] revealed three potential NFI binding sites in the β-globin proximal promoter region (Figure 3-10A): specifically, phylogenetic footprinting showed site 1 to be embedded in a highly evolutionary conserved region. Consequently, NFI-A chromatin occupancy in primary cells (physiological binding) was determined using genomic DNA isolated from $CD34^+$ HPCs, terminal E cells (E culture, d14) and intermediate G cells (G culture, d7) and immunoprecipitated using a NFI-A antibody. DNA was analysed by multiplex PCR using primers specific for the promoter region containing the NFI-A binding sites and an Unrelated genomic Region (UR) as an internal control. The linear range of amplification was confirmed by serial dilution of input DNA. Figure 3-10B shows that NFI-A at these sites was present in $CD34^+$ HPCs and greatly enriched in terminal E cells, characterized by elevated levels of both NFI-A and β-Globin. Intermediate G cells, which lack NFI-A protein, were used as a negative control (Figure 3-10B). We further extended ChIP analysis in K562 cells using real-time PCR to asses NFI-A binding. ChIP was performed in Vector- and NFI-A-transduced K562 cells in the absence or presence of Ara-C. Only NFI-A-transduced cells show NFI-A binding to the β-globin promoter and this occupancy increases in a time dependent manner in the presence of Ara-C (Figure 3-10C), complementing the trend observed in primary cells. As expected, real-time ChIP analysis in the HL-60 cell line shows no significant binding over the course of RA treatment (Figure 3-10D). To assess the contribution of individual NFI-A sites in β-globin transcription, we designed promoter-luciferase fusion constructs containing the wild-type β-Globin promoter and NFI-A site-specific mutants (Figure 3-10E). Figure 3-10E shows that co-transfection of HB-Wt with a

plasmid encoding NFI-A in K562 cells led to ~3-fold increase in transcription with respect to HB-Wt alone. In contrast, HB-Mut1 abolished transcriptional induction even in the presence of ectopic NFI-A. HB-Mut3 responded to NFI-A to a lesser extent, whereas HB-Mut2 behaved similarly to HB-Wt. The mutant construct, containing three mutated sites (HB-Mut(1-2-3)), exhibited no transcriptional induction upon NFI-A ectopic expression, as observed for HB-Mut1. In conclusion, the results indicate that NFI-A binds to and activates the β-globin promoter through primarily site 1 and secondarily site 3.

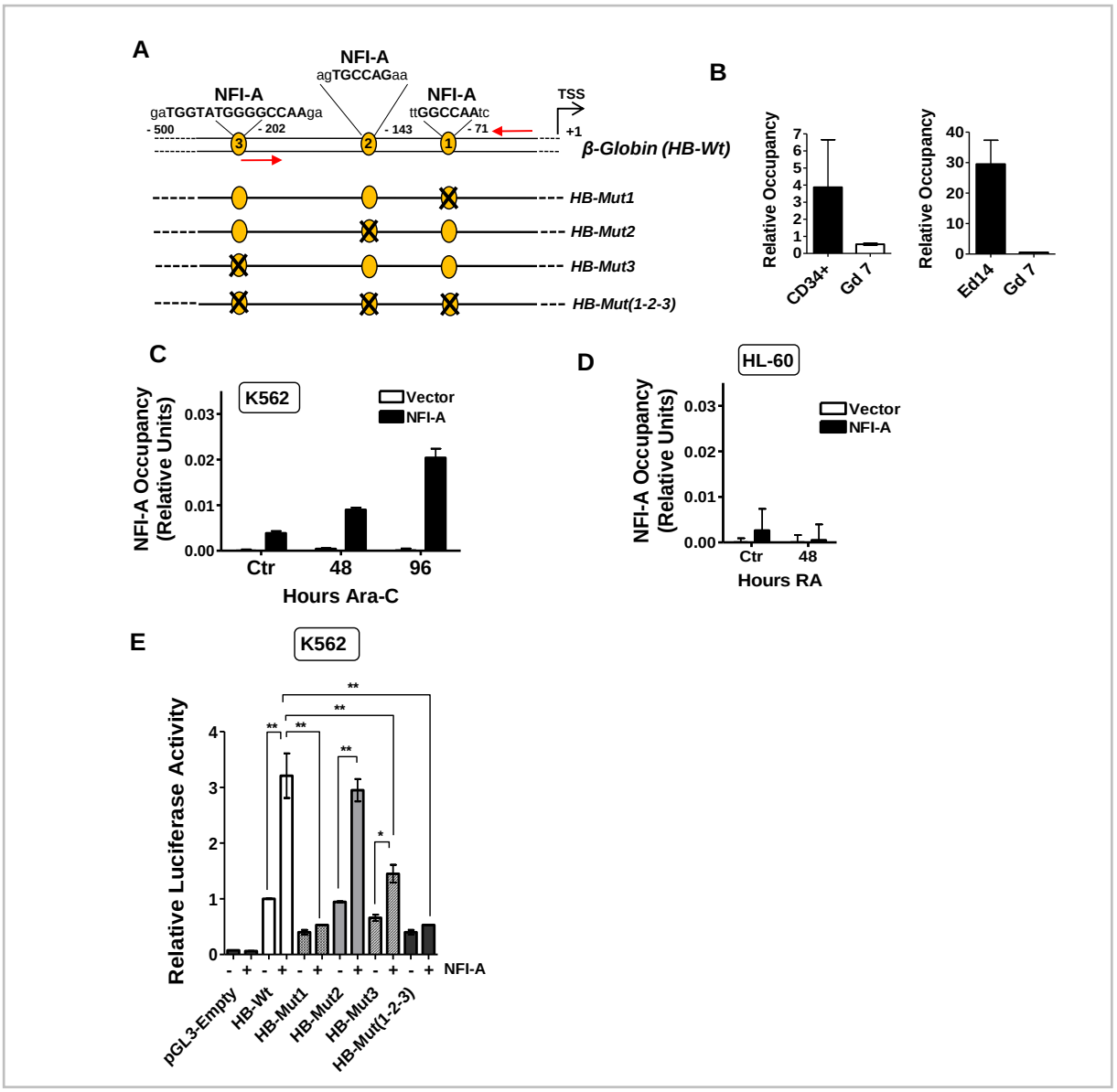

Figure 3-10 Binding of NFI-A on the β-Globin promoter *in vivo*. (A) Schematic representation of the β-Globin proximal promoter. NFI-A DNA binding site sequences are highlighted in bold characters. TSS indicates the Transcriptional Start Site and red arrows indicate the position of the primers employed for the ChIP analysis. Mutant sites are numbered according to their vicinity to the TSS. **(B)** Relative quantification of NFI-A occupancy on the β-Globin promoter in primary cells. Chromatin was immunoprecipitated with a NFI-A antibody, and the bound DNA was analysed by multiplex PCR using specific primers corresponding to the β-Globin promoter region containing the NFI-A binding sites and an Unrelated intergenic genomic Region (UR) as an internal control. Histograms represent the mean +/- SEM from three independent DNA preparations; PCR analyses were repeated at least 3 times. **(C)** Real-time PCR of NFI-A binding to the β-globin promoter of Vector- and NFI-A-transduced K562 cells treated with or without Ara-C. Mean +/- SEM (n=3). **(D)** Real-time PCR of NFI-A binding to the β-globin promoter in Vector- or NFI-A-transduced HL-60 cells in the absence or presence of RA. Mean +/- SEM (n=3). Three independent DNA preparations were used for the above ChIP analyses. **(E)** Promoter assay showing a positive role of NFI-A in β-Globin proximal promoter activation. Wild-type and mutant constructs were assayed for transcriptional activity relative to the endogenous NFI-A or in a co-transfection with a NFI-A expressing plasmid. The Firefly luciferase values were normalized to the Renilla luciferase values for each transfection, and the relative luciferase activity is represented as relative fold induction over the HB-Wt transfection. Mean +/- SEM values from 4 independent transfections. Each reading was repeated at least two times.

The G-CSFR promoter contains two conserved putative NFI binding sites. As a result, we performed multiplex ChIP analysis of the promoter using primers including both sites (Figure 3-11A). Genomic DNA from $CD34^+$ HPCs, intermediate E cells (Ed7), and intermediate G cells (Gd7) was immunoprecipitated using a NFI-A antibody. As shown in Figure 3-11B, we found binding of NFI-A to the G-CSFR sites in $CD34^+$ HPCs and E cells, but not in G cells. Binding of NFI-A to G-CSFR sites within NFI-A-transduced K562 cells was assessed by real-time PCR and increased with time upon exposure to Ara-C (Figure 3-11C). On the contrary, in the HL-60 cell line NFI-A is present on the G-CSFR promoter in both Vector- and NFI-A-transduced control cells, and rapidly falls off in Vector- cells upon RA treatment whereas it's occupancy is only slightly reduced in NFI-A-overexpressing cells upon RA treatment (Figure 3-11D).To further demonstrate that NFI-A transcriptionally represses the G-CSFR promoter, we performed a promoter assay in K562 cells, using a wild-type promoter construct and site-specific mutants (Figure 3-11A). As shown in Figure 3-11E, the basal activity of the G-CSFR wild-type promoter construct (GR-Wt) was enhanced by mutating site 2 (GR-Mut2), as shown by a rescue of transcription of ~2-fold. The mutant construct bearing a mutation in site 1 (GR-Mut1), did not affect its transcriptional activity; conversely, the double mutant construct (GR-Mut(1-2)) behaved similarly to GR-Mut2. In conclusion, we postulate that NFI-A binds and transcriptionally represses the G-CSFR promoter, specifically through site-2, while site-1 is inactive.

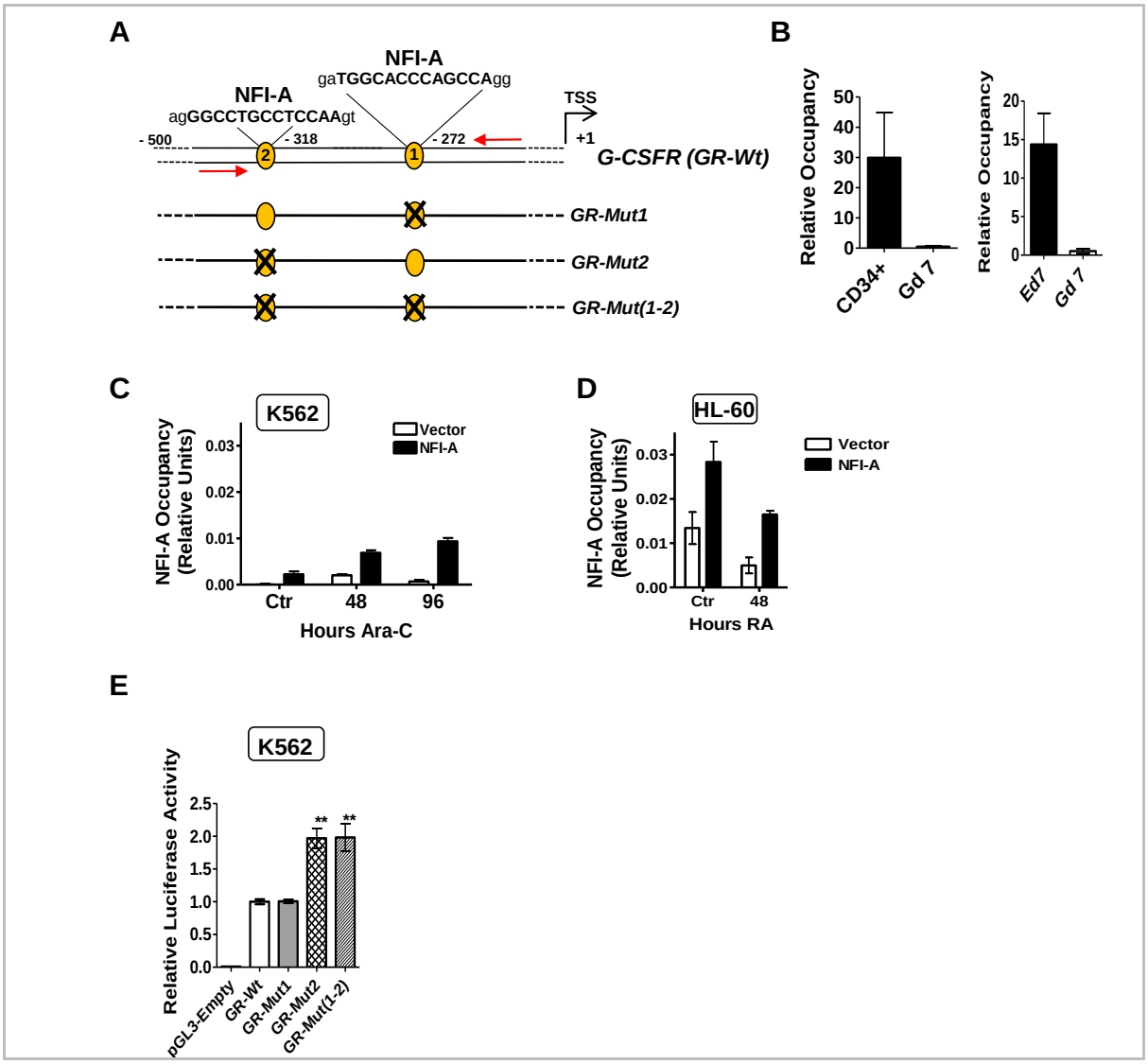

Figure 3-11 Binding of NFI-A on the G-CSFR promoter *in vivo*. (A) Schematic representation of the NFI-A binding sites on the G-CSFR promoter. **(B)** Relative quantification of NFI-A occupancy on the G-CSFR promoter in primary cells. Chromatins were immunoprecipitated with a NFI-A antibody, and the bound DNA was analysed by multiplex PCR using specific primers corresponding to the G-CSFR promoter region containing the NFI-A binding sites and an Unrelated intergenic genomic Region (UR) as an internal control. Histograms represent the mean +/- SEM from three independent DNA preparations; multiplex PCR analysis was repeated at least 3 times. **(C)** Real-time PCR of NFI-A binding to the G-CSFR promoter of Vector- and NFI-A-transduced K562 cells treated with or without Ara-C. Mean +/- SEM (n=3). **(D)** Real-time PCR of NFI-A binding to the G-CSFR promoter in Vector- or NFI-A-transduced HL-60 cells in the absence or presence of RA. Mean +/- SEM (n=3). Three independent DNA preparations were used for the above ChIP analyses. **(E)** Promoter assay showing NFI-A repressive activity on the G-CSFR promoter performed in K562 cells. Wild-type or mutant promoter constructs were transfected, and Firefly luciferase activity was normalized to Renilla luciferase activity for each transfection. The relative luciferase activity is represented as relative fold induction over the GR-Wt transfection. Data represent mean +/- SEM from 3 independent transfections. Each reading was repeated at least two times.

3.3 AIM III: To determine the role of TF NFI-A during both embryonic primitive and definitive hematopoiesis using the mouse as a model system.

In collaboration with Dr. Elisabetta Vivarelli we were able to study the expression level of NFI factors during hematopoietic ontogeny within the developing mouse embryo. Samples of adult peripheral blood, bone marrow and spleen together with total embryo, yolk sac (YS), aorta-gonad-mesonephros (AGM), dorsal aorta only, gonad-mesonephros (GM) only and liver were collected. The expression levels of NFI-A, B, C, and X were analyzed by semiquantitative PCR along with other lineage associated genes as follows. βh1 and βmaj encode embryonic and adult β-globin chains, respectively. TFs EKLF and GATA-1 are key to primitive and definitive erythropoiesis. TF AML1/RUNX1 is key to the development of definitive HSCs [29] and later is expressed in a cell type and maturation stage specific manner, being expressed in myeloid lineages, with a rapid downregulation during erythropoiesis, as well as being present in lymphoid cells [158]. *c-fms*, encoding the colony-stimulating factor-1 receptor (CSF-1R) regulates the survival, growth, and differentiation of monocytes [159], and was used as a marker for the monoctye/macrophage lineages. As seen in Figure 3-12, in respect to the other NFI family members, NFI-A shows the highest level of expression within the yolk sac (increasing from E8.0-9.0), is higher than the other factors in the AGM at E9.0, and dorsal aorta E10.0 and is also highly expressed within the liver and GM tissues. The expression of NFI-B in these tissues is similar to NFI-A but it's expressed at slightly lower levels. Within the peripheral blood, NFI-A shows a low expression, NFI-B is absent, NFI-C expression is low and NFI-X shows the highest level of expression. NFI-C and NFI-X are absent or at low levels within the other tissues except for high expression levels in AGM E11.0-12.0 and dorsal aorta E10.0 (Figure 3-12). βh1 is expressed starting at E8.0 and increases expression within the total embryo and yolk sac until E9.0, and upon later days in other tissues its expression is decreased, and is absent in adult peripheral blood, spleen and bone marrow. Instead, β-maj being the adult β-globin is expressed with increasing days post

coitus. It is expressed in the peripheral blood of the adult mice as a significant percentage of their reticulocytes complete maturation while circulating in the peripheral blood, which in turn have a higher resistance to lysis than erythrocytes [160] and in addition globin mRNAs are particularly stable [161]. GATA-1 and EKLF are expressed at high levels in yolk sac and liver. CSF-1R shows highest expression within the peripheral blood fraction, low expression at E9.0 within the yolk sac where myeloid progenitors have been noted to occur [12], and is expressed at E11.0-12.0 of the AGM. RUNX1 shows a high expression in the peripheral blood, bone marrow and spleen of the adult, and within the AGM at E11.0-E12.0 containing both myeloid progenitors and HSCs arising at E10.5-11.5 [16] (Figure 3-12).

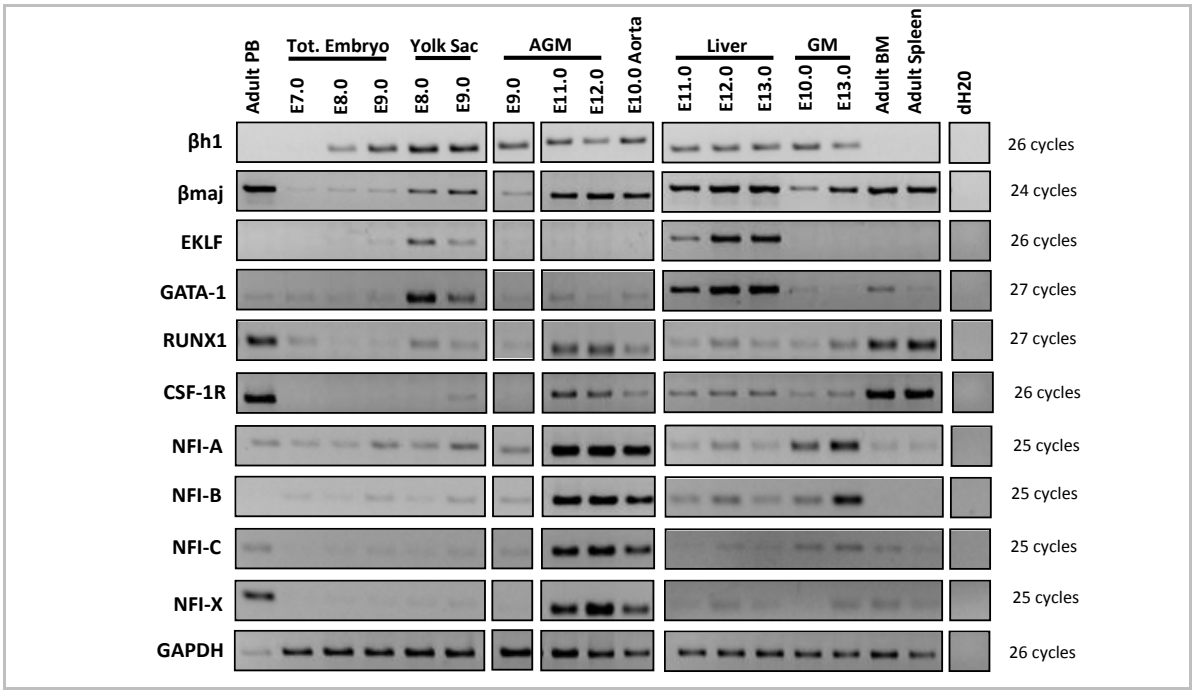

Figure 3-12 Semiquantitative PCR of NFI factors and other erythroid and myeloid associated genes in the embryo during hematopoietic ontogeny, as well as in adult peripheral blood (PB), bone marrow (BM), and spleen. GAPDH was used as a loading control. Number of PCR cycles is noted.

Based on the results of NFI-A mRNA expression we decided to look at NFI-A protein levels using a specific antibody within the embryo during hematopoietic development within the AGM region and yolk sac. As seen in Figure 3-13A, NFI-A is barely expressed in dorsal

aorta at E10.0, but is rapidly upregulated in dorsal aorta at E11.0-E12.0. NFI-A is also highly expressed in the GM region at E11.0-12.0. Within these samples RUNX1 is expressed at E10.0, and its expression remains relatively constant in the dorsal aorta and GM samples at E11.0-12.0. ε-globin is highly expressed in dorsal aorta and GM tissue samples at E10.0-12.0, probably due to the presence of primitive erythrocytes in circulation at this time as ε globin is expressed in primitive erythrocytes and is silenced during definitive erythropoiesis, where definitive erythrocytes are not plentiful in circulation until after E12.5 [162]. K562 ectopic expressing NFI-A and wild-type (Wt) cells show barely detectable levels of RUNX1, low ε-globin expression, and NFI-A is less expressed in K562 Wt cells than the embryonic dorsal aorta and GM tissues from E10.0-12.0 (Figure 3-13A).

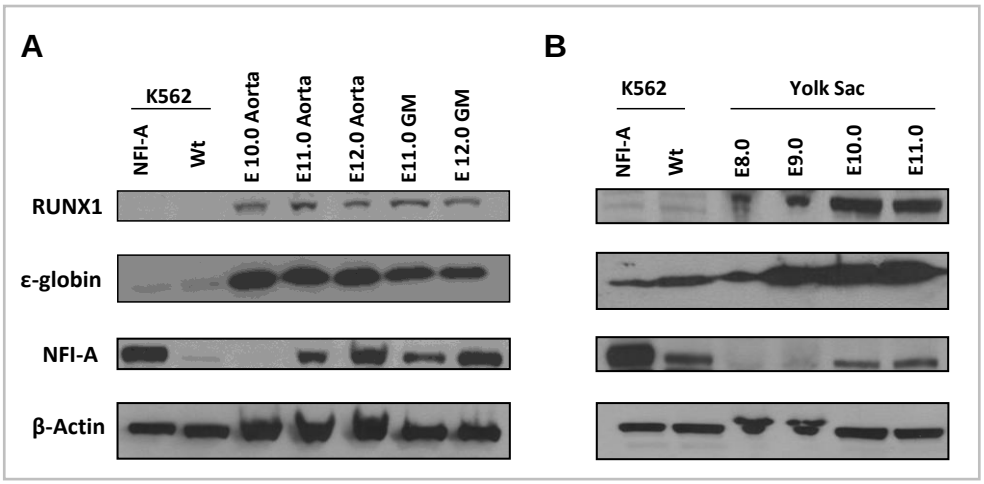

Figure 3-13 Western blot of NFI-A, ε-globin, and RUNX1 expression in K562 cells and embryonic samples. (A) Expression analysis in dorsal aorta and gonad-mesonephros (GM) samples from E10.0-E12.0. K562 wild-type (Wt) and NFI-A overexpressing samples were loaded as comparisons and control for NFI-A expression level. β-actin was used as a loading control. **(B)** Expression analysis in whole yolk sac samples from E8.0-E11.0. K562 Wt and NFI-A overexpressing samples were loaded as comparisons and control for NFI-A expression level. β-actin was used as a loading control.

In whole yolk sac samples taken from E8.0-E11.0, NFI-A is barely expressed at E8.0 but shows a time dependent upregulation with the highest expression at E11.0 (Figure 3-13B). RUNX1 is highly expressed at E8.0 and is upregulated with the highest expression at E10.0-11.0. ε-globin also shows increased expression from E8.0-E11.0 from the time that primitive

erythropoiesis starts to when primitive erythroblasts are prominent in the yolk sac and circulation after E9.0 (Figure 3-13B).

Interestingly NFI-A was upregulated in a time dependent manner in the yolk sac at both the mRNA and protein levels. Primitive erythropoiesis initiates in the yolk sac at E7.5 where primitive erythroblast progenitors (EryP-CFC) expand in numbers and are extinguished by E9.0 [12]. To explore the possibility of NFI-A having a role in primitive erythropoiesis, a cell culture system specifically for the development of primitive erythroblasts was established. Yolk sacs of E8.0 embryos were pooled, and single cell suspensions were plated within primitive colony media. After 6-7 days of culture colonies were scored: 94% of the colonies counted represented EryP-CFCs (Figure 3-14A), other colony types included primitive macrophage colonies (Mac-CFC) comprising 6% of the total CFCs and less than 1% represented definitive BFU-E colonies (Figure 3-14A). EryP-CFC colonies are small bright red compact colonies of a few hundred erythroblasts (Figure 3-14B), whose cell morphology can be seen in Figure 3-14B. Mac-CFC colony and cellular morphology are shown in Figure 3-14C.

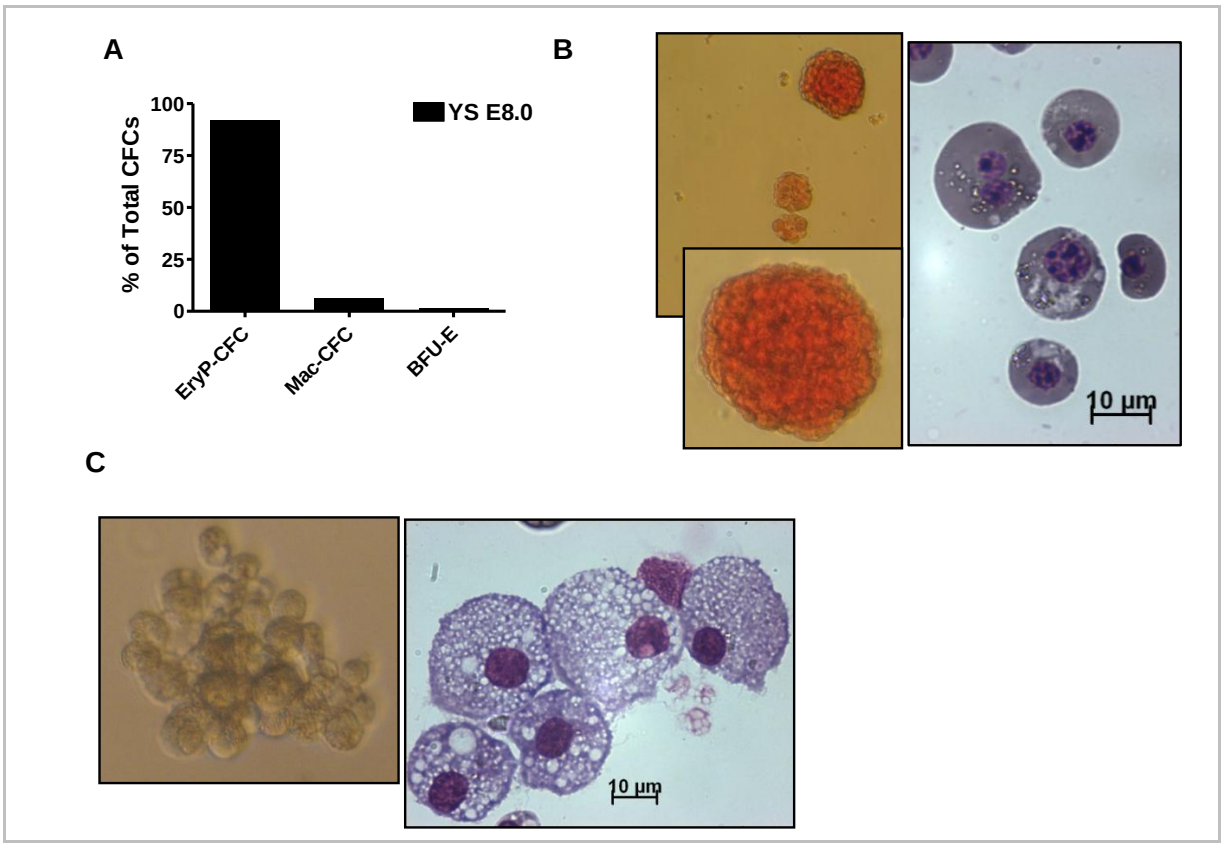

Figure 3-14 Yolk Sac (YS) E8.0 primitive colony assay. 1 x 10^5 yolk sac cells were plated in triplicate in primitive EryP-CFC methylcellulose media and colonies were scored after 7 days. **(A)** Percentage of primitive erythroblasts (EryP-CFC), primitive macrophage (Mac-CFC), and definitive erythroid (BFU-E) colonies out of the total colony forming cells (CFCs) present. **(B)** Representative EryP colony and cellular morphology (original magnification X 1000). **(C)** Representative Mac-CFC colony and cellular morphology (original magnification X 1000) (Mean +/- SD values from three independent experiments)

Individual EryP colonies were picked and pooled together, from which single cells were cytospun onto glass slides to examine NFI-A expression by indirect immunofluorescence. Using an antibody specific to NFI-A it was found that EryPs express NFI-A (Figure 3-15).

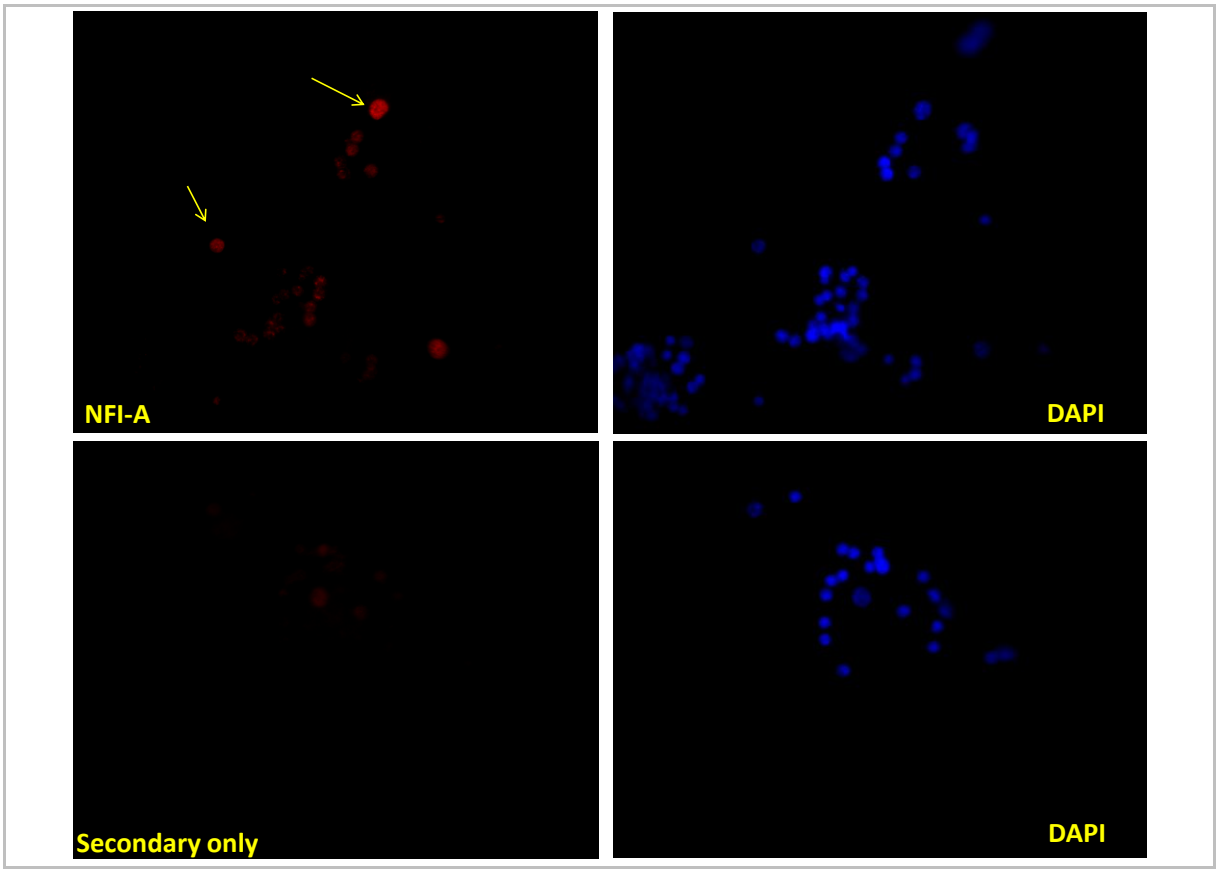

Figure 3-15 NFI-A detection in primitive erythroblasts. EryP colonies were picked and pooled together followed by cytospin onto glass slides. The upper left panel shows several bright red cells staining for nuclear localized NFI-A as detected by a NFI-A specific antibody. Nuclear localization is indicated by DAPI staining in the upper right panel, and the lower left panel contains staining by secondary antibody only as a control. The lower right panel shows the nuclear localization of the secondary only staining cells.

To confirm the results of indirect immunofluorescence RNA was also extracted from individual picked EryP colonies pooled together. Figure 3-16A shows that NFI-A expression increases at the mRNA level (via semiquantitative PCR analysis) in total embryo from E7.0-9.0, and in the yolk sac from E8.0-9.0. From two different experiments in picking and pooling EryP colonies together it can be seen that NFI-A is expressed at a higher level than total E9.0 yolk sac (Figure 3-16A). The embryonic globin βh1 is expressed starting at E8.0 in the total embryo and is present at E9.0 and throughout the yolk sac and EryP picked colonies. The adult βmaj chain is expressed in adult peripheral blood, the yolk sac E8.0-9.0, and is highly expressed in the EryP picked colonies (Figure 3-16A). Protein was extracted from pooled triplicate primitive colony assay plates (containing 94% EryPs and a small number of

primitive macrophage (6%) colonies) in order to obtain sufficient sample. Western blot analysis shows the time dependent increase of NFI-A within the yolk sac from E9.0-11.0, however, most striking is the large expression of NFI-A protein within the pooled plates, not fully appreciable by the western blot in Figure 3-16B due to the lower protein content of this sample. GATA-1 expression is found in the yolk sac E9.0-11.0, and is highly expressed in the pooled plates, and PU.1 is absent in the yolk sac E9.0-11.0 and expressed at a low level in the pooled plates that contain a small percentage of mature primitive macrophages (6%) (Figure 3-14A,C). Therefore, based on these expression studies we can conclude that NFI-A is highly expressed at the mRNA and protein level during primitive hematopoiesis, most likely within the EryPs as seen by indirect immunofluorescence, RNA analysis, and by western blot representing a pooled population of 94% EryPs, and 6% Mac-CFCs. Future studies with fluorescence-activated cell sorting (FACS) using specific markers for EryPs during their maturation [163] can be performed to determine the exact population of cells expressing NFI-A, and how NFI-A expression changes during their maturation.

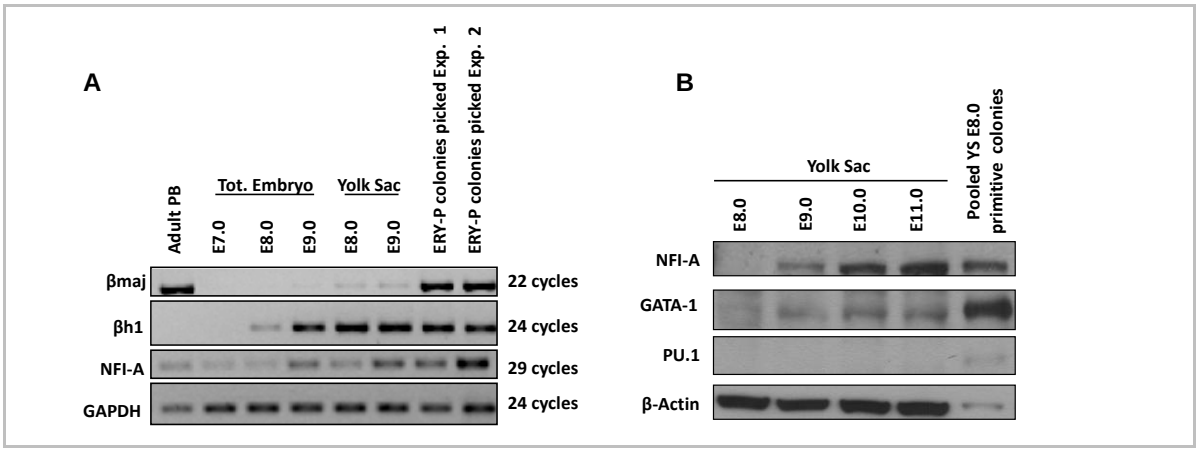

Figure 3-16 NFI-A mRNA and protein expression. (A) Semiquantitative mRNA expression analysis of β-maj, βh1 and NFI-A with GAPDH used as a loading control in peripheral blood (PB) from adult mice, total (tot.) embryo E7.0-9.0, yolk sac E8.0-9.0, and two separate experiments picking and pooling together individual EryP colonies. Number of PCR cycles is indicated. **(B)** Western blot for NFI-A, GATA-1 and PU.1 expression with β-actin used as a loading control in yolk sac E8.0-11.0 and in colonies pooled from the primitive colony assay.

The levels of NFI-A protein within yolk sac E8.0 EryP-CFCs can be exogenously manipulated by lentiviral overexpression of NFI-A, or by silencing. A lentiviral vector overexpressing mouse NFI-A and a siNFI-A specific to mouse NFI-A were designed and tested in mouse NIH 3T3 cells. As seen in Figure 3-17, these lentiviral vectors show a significant level of expression of NFI-A (A) and knockdown of NFI-A (B).

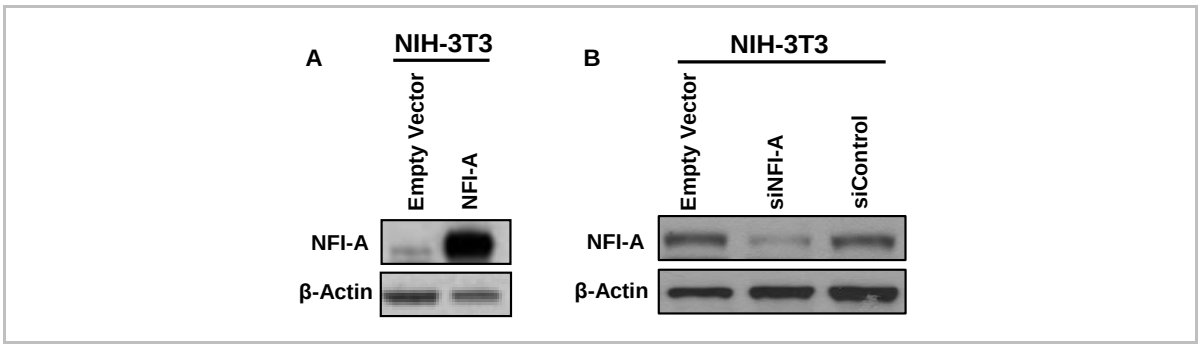

Figure 3-17 Immunoblot of NFI-A overexpression and silencing. (A) NFI-A overexpression in NIH 3T3 cells **(B)** siNFI-A designed against mouse NFI-A showing knockdown of NFI-A protein compared to empty Vector, and siControl cells infected with a lentiviral vector expressing a shRNA against luciferase.

Manipulation of NFI-A within the primitive erythroblast progenitors will allow us to determine if NFI-A is necessary for EryP colony formation and maturation.

The distribution of definitive progenitors types found in the yolk sac of normal wild-type mice at E9.0 was examined. Yolk sac from E9.0 embryos were obtained and single suspension cells were placed in pre-made clonogenic media for the detection of definitive hematopoietic colonies; burst forming units-erythroid (BFU-E), colony forming units-granulocyte macrophage (CFU-GM), CFU-macrophage (CFU-M), where each colony is derived from individual progenitors of the erythroid, granulocyte macrophage, and macrophage lineages respectively. This media also allows the detection of CFU-granulocyte erythroid macrophage megakaryocyte (CFU-GEMM) which is derived from a multipotent progenitor, and therefore cells within this colony can consist of the granulocyte, erythroid, macrophage and megakaryocyte lineages. As seen in Figure 3-18A, 50% of the cells from YS E9.0 are definitive erythroid progenitors (BFU-E), 11% are macrophage progenitors (CFU-

M), 12% are granulocyte macrophage progenitors (CFU-GM), and 23% are multipotent progenitors (CFU-GEMM). Figure 3-18B shows individual colony morphologies, and Figure 3-18C shows the cellular morphology of individual picked colonies. Of note, is the different colony and cellular morphology of the definitive erythroid cells derived from BFU-E colonies in comparison to the primitive erythroid cellular morphology in Figure 3-14B. Also, within the CFU-GM colonies there is a mixture of granulocyte types (Figure 3-18C).

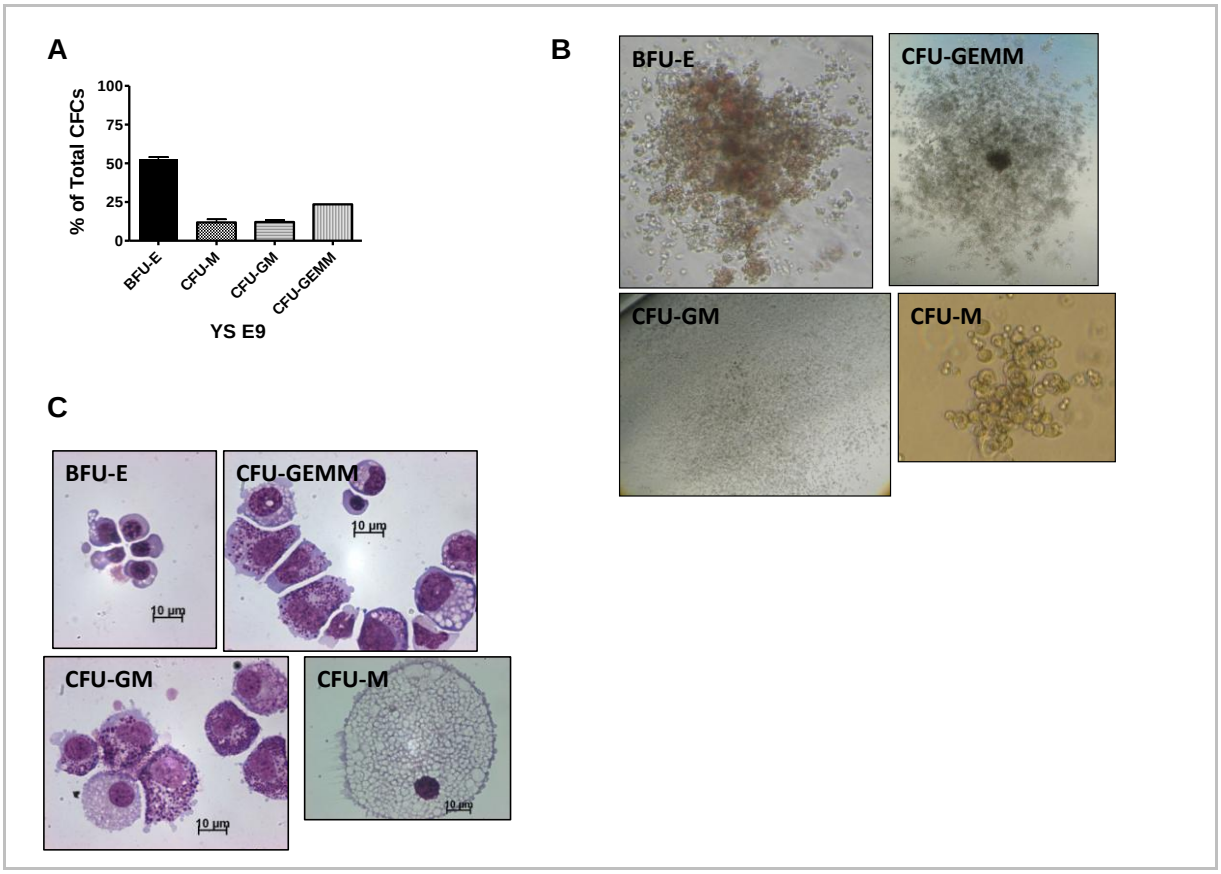

Figure 3-18 Definitive colony distribution and their respective morphology in yolk sac (YS) at E9.0. 12 x 10^3 cells from dissociated YS E9.0 were plated in triplicate in definitive colony clonogenic media, and colonies were scored after 8 days **(A)** Percentage of burst forming units-erythroid (BFU-E), colony forming units-macrophage (CFU-M), CFU-granulocyte macrophage (CFU-GM), CFU-granulocyte erythroid macrophage megakaryocyte (CFU-GEMM) out of total colony forming cells (CFCs) (Mean +/- SD values from two independent experiments) **(B)** Representative colony morphology and **(C)** cellular morphology of individual picked colonies (original magnification 1000X).

These data further confirm that the yolk sac at E9.0 contains many definitive progenitors, with the majority being definitive erythroid progenitors in line with previous findings [12]. The distribution of definitive colonies has also been examined in AGM E11.0 and E12.0 (Figure

3-19A) tissues as well as liver E11.0, and E14.0 (Figure 3-19B). Within the AGM at E11.0 there is a majority of multipotent progenitors (CFU-GEMM) as well as granulocyte macrophage progenitors (CFU-GM), whereas at E12.0, there is the presence of a majority of CFU-GM progenitors and less multipotent progenitors (Figure 3-19A). In the liver at E11.0 the majority of progenitors are erythroid (BFU-E), whereas later at E14.0 the majority of the progenitors present are myeloid (CFU-M and CFU-GM) (Figure 3-19B). These results are also in line with previous findings [36], and establish for us the CFCs distribution profiles for normal wild-type mice, while we are in the process of breeding mice obtained from Dr. Richard Gronostajski, to repeat these definitive colony assays in tissues of NFI-A$^{-/-}$ mice and their littermate controls.

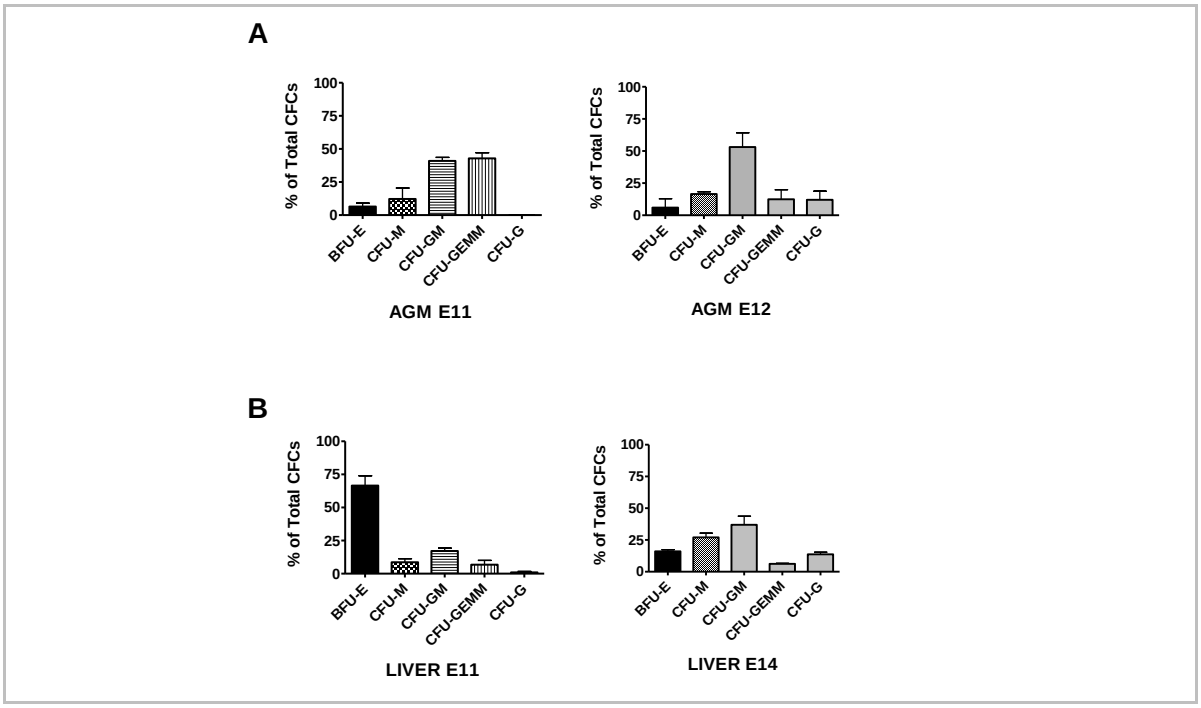

Figure 3-19 Definitive colony distribution in AGM E11.0-12.0 and Liver E11.0 and E14.0 tissues. (A) 20 x 10^3 AGM dissociated cells were plated in triplicate in definitive clonogenic media and colonies were scored after 8 days (Mean +/- SD values from triplicate platings). (A) Percentage of burst-forming units-erythroid (BFU-E), colony forming units-macrophage (CFU-M), CFU-granulocyte macrophage (CFU-GM), CFU-granulocyte erythroid macrophage megakaryocyte (CFU-GEMM) and CFU-granulocyte (CFU-G) from AGM E11.0 (left) and AGM E12.0 (right) out of total colony forming cells (CFCs) present. **(B)** 12 x 10^3 liver E11.0, and 30 x 10^3 liver E14.0 dissociated cells were plated in triplicate within definitive clonogenic media and colonies were scored after 8 days (Mean +/- SD values from triplicate platings). Percentages of BFU-E, CFU-M, CFU-GM, CFU-GEMM, and CFU-G out of total CFCs present in liver E11.0 (left) and liver E14.0 (right) plated cells.

Recently, we were able to obtain leg bones and spleens from rare NFI-A knockout mice and their littermate controls at 9 days after birth from Dr. Richard Gronostajski. Leg bones are currently being decalcified for paraffin embedding followed by sectioning and staining to examine the cellularity of the bone marrow compartment. Gross examination of NFI-$A^{-/-}$ spleens shows that they are smaller in size compared to their littermate controls and that the spleens are less red in colour showing hypocellularity in the erythroid red pulp component (Figure 3-20). Spleens are currently being paraffin embedded and sectioned to look at cellular morphology.

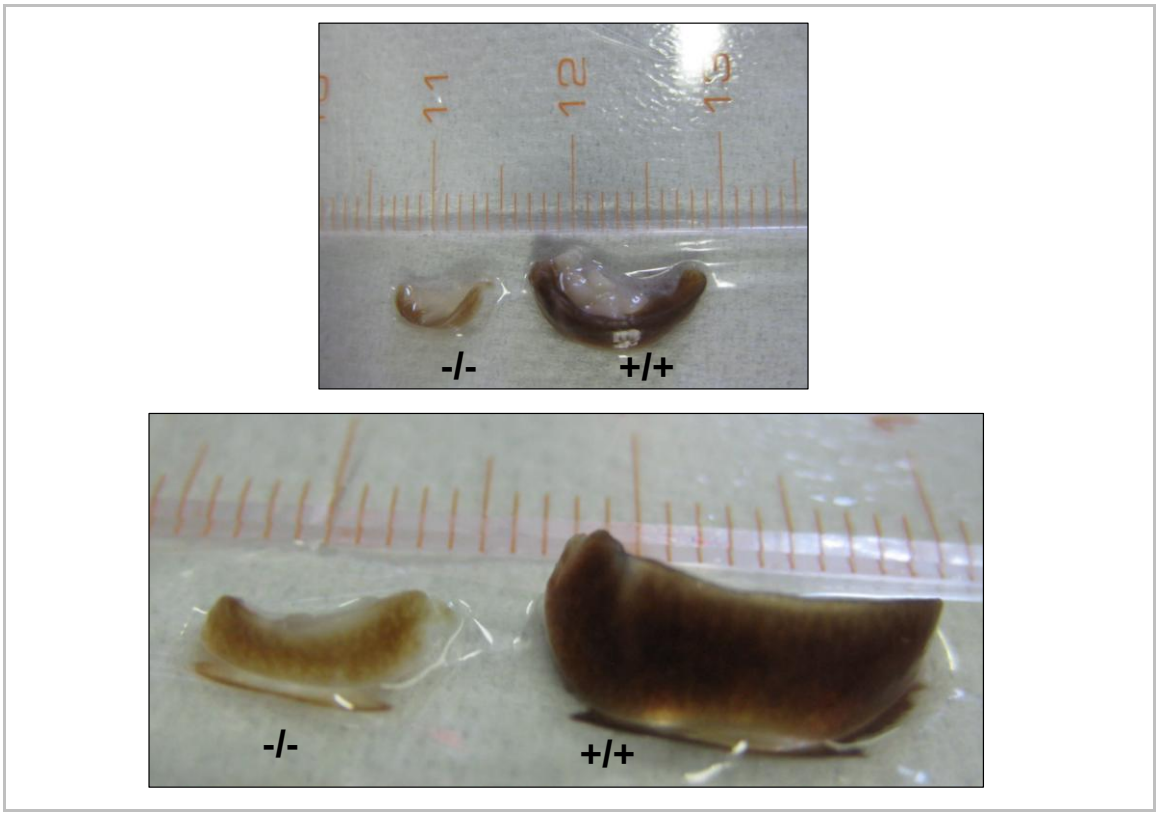

Figure 3-20 Photograph of gross spleen morphology of NFI-A wt (+/+) and knockout (-/-) mice.

Chapter Four: DISCUSSION & FUTURE DIRECTIONS

Previous results from our lab identified two new factors governing RA induced differentiation of leukemic APL blasts; miR-223 and the TF NFI-A [126]. In undifferentiated APL blasts and NB4 leukemic cells, miR-223 levels are low due to its repression by NFI-A which binds a CCAAT box within the proximal miR-223 promoter region. Upon RA treatment, a second TF C/EBPα that is necessary for granulocytic differentiation [93] binds to this CCAAT box, displacing NFI-A, and stimulates the transcription of miR-223. miR-223 expression levels rise and it targets the 3'UTR of NFI-A mRNA silencing NFI-A protein levels within these cells so that NFI-A can no longer compete with C/EBPα to repress miR-223 expression [126]. This newly identified minicircuitry effectively demonstrates the importance of the quantity and timing of TF expression within hematopoietic cells at discrete stages of differentiation and indicates miRs as important players of this process by acting as fine tuners of developmental gene expression. It also implicates new therapeutic targets for the treatment of leukemia.

Due to the suggestion of miR-223 being an important regulator of normal granulocytic development, we set out to examine the expression of miR-223 within different leukemia subtypes. Interestingly, it was found that within the FAB M2 subtype harboring the AML1/ETO fusion protein caused by the t;(8:21) genetic lesion, the miR-223 levels were low. This was also true of the SKNO-1 AML-M2 cell line that harbors the constitutively expressed AML1/ETO fusion protein. The AML1/ETO fusion protein is associated with about 40% of the M2 AML cases with karyotypic abnormalities [164] and represents the most frequent genetic lesion in leukemia (18-20%) [165]. AML1/ETO can heterodimerize with CBFβ (the TF AML1/RUNX1 heterodimerization partner) more efficiently than AML1 itself, and bind to cognate AML1 binding sequences to block wild-type AML1 binding. Repression of AML1

target genes occurs via AML1/ETO interaction with histone deacetylases (HDACs), and DNA methyltransferases (DNMTs). AML1/ETO also has the ability to bind to and interfere with key transcription factors such as C/EBPα and PU.1 that act as transcriptional activators and with PLZF which acts as a transcriptional repressor [166]. Therefore, the AML1/ETO fusion protein has multifaceted actions which make it a potent oncogenic fusion protein. Some transcriptional targets identified for AML1/ETO include *bcl-2* [167], *c-fms* [168], *GM-CSF* [169], and *RARβ* [145]. Our recent results indicate that miR-223 is another target of the AML1/ETO oncogenic fusion. AML1/ETO is able to recruit HDACs and DNMTs to the cognate AML1 binding site on the miR-223 proximal promoter region to repress its transcription, contributing to the myeloid block of differentiation. Of note, the overexpression of miR-223 within cell lines harboring the AML1/ETO fusion protein (SKNO-1 of the AML M2 FAB classification) or within a cell line lacking a genetic lesion (HL-60-AML M2) was able to induce granulocytic differentiation. AML patient blasts (M3 and M4-M5 subtypes) infected with miR-223 were also able to undergo granulocytic differentiation. This is the first evidence linking heterochromatic gene silencing of a miR to the differentiation block of leukemia induced by an oncogenic fusion protein and implicates that miR-223 expression levels are critical for the development of the granulocytic differentiation program and that titrated miR-223 expression can reprogram myeloid differentiation in different leukemia subtypes independently from the presence of a specific genetic lesion.

We next decided to investigate a possible role for NFI-A during normal human hematopoiesis of the erythroid and granulocytic lineages. To carry out our investigation we used as a model system unilineage erythroid (E) and granulocytic (G) cultures of human HPCs: these assays recapitulate the *in vivo* differentiation/maturation of these hematopoietic series, hence allowing analysis of lineage-specific cells at discrete sequential stages of erythropoiesis and granulopoiesis[151, 170]. We discovered NFI-A expression to be low in

undifferentiated $CD34^+$ HPCs followed by an inverse lineage specific pattern of NFI-A expression during E vs. G differentiation. NFI-A was found to be sharply upmodulated at the transcriptional and protein levels during E differentiation while during G differentiation NFI-A transcription was shut off and its protein levels rapidly decreased to non-expressed levels by day 7 of granulocytic differentiation. This pattern of expression is like other TFs important for lineage specification such as GATA-1[171], PU.1[172] and C/EBPα[173] which are expressed at low levels being "primed" in undifferentiated HSCs/HPCs and then are rapidly upregulated in their specific lineage. These important TFs act to initiate lineage specific gene programs and at the same time antagonize the expression of non-lineage associated genes either by direct transcriptional inhibition or by direct protein interaction and inhibition of TFs needed for induction of differentiation of opposing lineages; the paradigmatic example being GATA-1 and PU.1.

Using lentiviral shRNA technology we were able to demonstrate that NFI-A is necessary for erythroid differentiation as in its absence no erythroid cells were formed in unilineage E culture; instead only myeloid cells were formed. The formation of myeloid cells is presumably due to the presence of small amounts of IL-3 and GM-CSF in the E unilineage culture media. Both IL-3 and GM-CSF display a pro-survival activity on granulo-monocytic cells [174, 175], and GM-CSF stimulates M-CSF release in monocytes [176], giving rise to a positive autocrine feedback loop.

NFI-A is not only necessary for erythroid development but it is also capable of driving E differentiation. NFI-A overexpression via lentiviral infection of HPCs showed that its overexpression was found to compensate for low to minimal EPO stimulus. During normal erythropoiesis, Epo binds to the EpoR and activates several signaling cascades including the PI3K/AKT, STAT5-Bcl_{xL}, and Ras/MAPK pathways ultimately resulting in anti-apoptotic effects and proliferation coupled with E differentiation/maturation [177]. *In vivo* when *EpoR* is

inactivated yolk sac hematopoiesis is significantly reduced leading to severe anemia and definitive erythropoiesis is completely impaired resulting in embryonic lethality by E13.0-E15.0 [178]. *In vitro* Epo binding to the EpoR contributes to the commitment of multipotent CFU-GEMM to the erythroid lineage and the differentiation of BFU-E to CFU-E. At later stages EpoR is crucial to the survival of CFU-E progenitors and their terminal differentiation [178, 179]. Erythroid progenitors lacking a functional EpoR do not mature into erythrocytes and show phenotypic abnormalities [178, 180]. In suboptimal E culture, due to a low or minimal Epo stimulus, NFI-A overexpression was able to restore E differentiation/maturation: this suggests that NFI-A may directly target key molecules involved the E gene program independently of EpoR signaling. Further studies will need to be performed to determine if NFI-A acts downstream of EpoR signaling, is independent of EpoR signaling or is downstream of a parallel pathway important for erythropoiesis. GATA-1 is an example of a critical TF for erythropoiesis that is activated downstream of Epo signaling [181].

NFI-A overexpression in E culture resulted in a significant increase of the β-globin content in erythroblasts. In the erythroleukemic K562 cells, incapable of synthesizing β-globin even upon Ara-C induced E differentiation [154] , ectopic expression of NFI-A induced a marked expression of β-globin. These results indicate a tight correlation between NFI-A levels and β-globin expression. Identifying new players involved in the transcriptional regulation of β-globin is potentially of clinical significance, since mutations in the gene or promoter *cis*-elements are relevant in β-thalassemias. We observed that NFI-A specifically binds the β-globin proximal promoter, primarily at position -73 to -78, and activates transcription. This NFI-A binding site overlaps with the CCAAT- element, which also binds to other factors and is one of three elements required for maximal transcription of the β-globin promoter [182]. Interestingly, a recently described case of β^{++}-thalassemia (mild β-thalassemia intermedia) was linked to a mutation of -73 (A to T) within the conserved CCAAT box [183].

NFI-A occupancy on the β-globin promoter was seen to increase with E differentiation in HPCs, and in Ara-C treated K562 cells. This is due not only to increasing concentrations of NFI-A (during E differentiation of HPCs) but is also due to chromatin status, interacting factors bound at nearby *cis*-acting elements and the number and/or affinity of NFI-A binding motif features, as what has been demonstrated for GATA-1. GATA-1 target genes are differentially sensitive to the GATA-1 level/activity, and this target sensitivity involves not only the parameters that determine chromatin occupancy but also those regulating chromatin-bound factors [184]. Further studies will need to be carried out to determine the exact mechanism of NFI-A action at the β-globin promoter, i.e. interacting factors at neighbouring *cis*-elements, protein modifications, and interaction with chromatin modifying enzymes or components of the basal transcriptional machinery. Interestingly LMO2 was recently discovered as a target of miR-223 and miR-223 levels are downregulated during E differentiation. miR-223 ectopic expression within $CD34^+$ HPCs placed in unilineage E differentiation showed an impairment in their differentiation capacity [185]. The overexpression of miR-223 presumably was unable to dampen the large transcriptional increase of NFI-A during erythropoiesis, therefore not showing a complete block in erythropoiesis as was shown in our study in the absence of NFI-A.

It is known that unbalanced synthesis of globins and heme modifies the activity of heme-regulated inhibitor kinase, affecting proliferation and differentiation of erythroid precursors, where defective globin synthesis (as that observed in thalassemia) leads to the apoptosis of erythroid progenitors [186-188]. Therefore, factors such as NFI-A affecting globin chain synthesis directly affect the erythropoietic differentiation program. Recently, to explore the molecular networks downstream of NFI-A, we performed a transcriptome-wide analysis in $CD34^+$ progenitors transduced with NFI-A or the empty Vector. We are currently validating the results of the microarray within K562 NFI-A overexpressing vs. empty Vector

cells as well as in $CD34^+$ transduced cells. Preliminary data indicate that NFI-A upregulates not only β-globin but also many important erythroid associated genes, therefore NFI-A acts to upregulate the erythroid gene program. Targets include α-globin and key heme synthesis enzymes (further implicating NFI-A as an important regulator of correct hemoglobin chain synthesis), as well as important erythrocyte membrane structural proteins (data not shown in results section). The targets currently being analyzed are very similar to previous gene expression profiles obtained for two other important TFs for erythropoiesis, EKLF and GATA-1: the erythroid gene profile for EKLF null cells was performed using EKLF $^{-/-}$ vs. Wt fetal livers [76], for GATA-1 the profile obtained was in G1E-ER4 (GATA-1 erythroid subclone ER4) cells, an immortalized GATA-1 null cell line derived from gene-targeted mouse embryonic stem cells where upon estradiol treatment GATA-1 is expressed and these cells undergo terminal erythroid differentiation [189].

NFI-A transduced HPCs as well as HL-60 AML M2 leukemic cells showed a block in granulocytic differentiation. The G-CSFR was identified as a target of NFI-A, which plays a crucial role in the production and function of granulocytes [190]. Knockdown of NFI-A in E culture led to activation of G-CSFR, whereas NFI-A transduction in G culture blocked the receptor expression. In fact, the absence of NFI-A was found to be permissive for granulopoiesis channelling HPCs preferentially towards granulocytic differentiation, due in part to the increase in G-CSFR expression. We found that NFI-A binds to a *cis*-element located between nucleotides -318 and -334 in the G-CSFR promoter and represses its transcription in reporter and functional assays. So far, only a few transcriptional regulators of this receptor have been discovered; some (e.g., PU.1 and C/EBPα) have been extensively characterized [90, 191], while the contribution of others (e.g., AP-1 and AP-2, GF-1) still needs to be clarified [192]. It is noteworthy that the G-CSFR is also expressed in human monocytes and directly modulates inflammatory cytokine secretion [193]. In acute promyelocytic leukemias

bearing leukemogenic fusion proteins G-CSFR function is disrupted: [194] NFI-A knockdown may provide an attractive therapeutic approach, possibly in combination with RA+G-CSF differentiation therapy [194].

The results obtained in E+G liquid phase and clonogenic culture of HPCs indicate that NFI-A up- or downmodulation governs the erythro-granulocytic lineage branchpoint, directing precursor cells into the E or G fate respectively. NFI-A accumulation during initial erythroid differentiation results in progressive activation of β-globin transcription (and as we are now discovering other essential erythroid genes), coupled with repression of G-CSFR, thus channelling HPCs and early precursors into the E lineage and shutting off their granulocytic potential. Conversely, NFI-A suppression in early granulopoiesis activates G-CSFR transcription and impedes erythroid gene expression including β-globin transcription, thereby directing HPCs and early precursors into the granulocytic pathway.

Our results indicating that NFI-A levels are important in governing normal human adult definitive granulo- erythropoiesis prompted us to examine the expression of NFI-A within the embryo during hematopoietic ontogeny during both primitive and definitive hematopoiesis. Our preliminary results indicate that NFI-A is expressed in hematopoietic tissues including the yolk sac, AGM, and liver. We were able to establish a culture system allowing the examination of primitive erythroblasts from early yolk sac (E8.0) and found that NFI-A is highly expressed; implicating it in having a possible role in primitive hematopoiesis. Lentiviral vectors to overexpress or silence NFI-A within mouse tissues were recently designed and tested where NFI-A silencing will be performed in yolk sac E8.0 tissues to determine if NFI-A is necessary for primitive erythropoiesis. Normal distribution of definitive hematopoietic colonies from yolk sac E9.0 indicate that at this time there is a majority of erythroid BFU-E progenitors, lower levels of CFU-GEMM and lowest are myeloid progenitors, in line with previous findings [12]. Within the AGM E11.0 tissue there is a high

proportion of multipotent progenitors, as well as myeloid progenitors, and at E12.0 instead the majority of the progenitors are solely myeloid in potential. Within the Liver at E11.0 there is a predominance of erythroid BFU-E progenitors. The BFU-E progenitors found within the liver at this time presumably are derived from the yolk sac as definitive BFU-E progenitors start to be produced here by E8.25 [9]. These BFU-E progenitors expand in numbers and differentiate to release large numbers of definitive erythrocytes at E12.5 onwards [9]. Knowing the normal distribution of CFCs within wild-type mice hematopoietic tissues is an important starting point for further studies using lentiviral technology to exogenously manipulate NFI-A levels within these hematopoietic tissues or as a basis for starting with NFI-A knockout mouse studies.

NFI-$A^{-/-}$ embryos and littermate controls are required to fully examine the function of NFI-A during embryonic hematopoiesis. Knockout of NFI-A causes death of 95% of the mice at post-natal day 1 due to severe neurological defects including hydrocephalus, and agenesis of the corpus callosum [136], however embryonic hematopoiesis may still be studied in these animals. Currently, we are breeding NFI-$A^{-/+}$ animals recently obtained from Dr. Richard Gronostajski. When NFI-$A^{-/-}$ and Wt littermate control embryos are available, examination of NFI-$A^{-/-}$ yolk sac E8.0 primitive erythroblasts will verify any results obtained from the knockdown of NFI-A using lentiviral vectors and if any observed defects can be rescued by NFI-A overexpression. Yolk sac E9.0, AGM E10.5-E12.0 and liver E11.0-14.0 tissues from NFI-$A^{-/-}$ embryos can be plated in clonogenic media along with Wt littermate controls to compare percentages of CFCs of the embryonic definitive erythroid and myeloid series within these tissues at exact stages of development. As clonogenic assays do not allow one to monitor terminal differentiation of cells step by step or in a highly quantitative manner, flow cytometry analysis of isolated cells from NFI-$A^{-/-}$ and Wt littermate controls can be performed to understand the precise differentiation stage affected by NFI-A. Cells can be isolated from

early yolk sac E8.0-9.0 as well as from the liver E11.0-15.0 (the organ of definitive hematopoiesis at this time) and a panel of lineage specific markers can be used to determine exact populations and stages of differentiation of cells within these tissues. For example, we would expect based on our results from human HPCs in unilineage culture differentiation systems that there would most likely be a defect during definitive erythropoiesis, indicating that NFI-A$^{-/-}$ animals are possibly anaemic. A flow cytometry method was established by Zhang, *et al*. to assess spleen and bone marrow erythroblast differentiation in adult mice, and in fetal liver cells at E14.5 [195]. Liver E14.5 samples can be obtained for flow cytometry analysis with the erythroid specific TER119 and the CD71 (transferrin receptor) antibodies to determine changes in erythroid populations between Wt and NFI-A$^{-/-}$ animals, as it is known that E14.5 fetal liver erythroblasts can be separated into 5 distinct populations using these antibodies [195]. Also a simple examination of the ratio of primitive: definitive erythrocytes can be performed at E13.0-14.0 in Wt and NFI-A$^{-/-}$ fetal blood to indicate if there is a defect in definitive or primitive erythroid differentiation/maturation.

Using the NFI-A$^{-/-}$ animals will also facilitate examination of the expression levels of the other NFI factors when there is an absence of NFI-A. This is a very important point to consider, that perhaps one of the other members of the NFI family can partly compensate for the complete absence of NFI-A *in vivo* in these mice.

Very recently leg bone and spleen samples from rare surviving NFI-A$^{-/-}$ mice at post-natal day 9 were obtained from Dr. Richard Gronostajski. NFI-A$^{-/-}$ mice have smaller spleens, and when the cellularity of the spleen is examined by gross morphological examination there appears to be less red blood cells present in the red pulp component. The red pulp is composed of a 3D meshwork of splenic cords and venous sinuses. Splenic cords are comprised of reticular fibers, reticular cells, and associated macrophages who are highly phagocytic clearing damaged red blood cells. Within the spaces between the cords are blood

cells including erythrocytes, granulocytes and circulating mononuclear cells [196]. After E16.0 in the mouse, the spleen is an extramedullary hematopoietic organ and definitive erythropoiesis does occur here [178]. These samples are currently being processed for morphological analysis by hematoxylin and eosin staining. Sections will also be used for histochemical analysis using benzidine stain specific for differentiated erythroblasts and myeloperoxidase staining specific for granulocytic cells. Immunohistochemical studies using specific antibodies for erythroid and myeloid progenitors can also be performed. Leg samples are currently being decalcified for sectioning to examine the bone marrow cellularity of Wt vs. knockout animals.

In summary, this work has uncovered NFI-A as a novel factor whose levels are important for directing human $CD34^+$ HPCs to the erythroid or granulocytic fates. Preliminary results implicate NFI-A possibly having a role during early embryonic primitive erythropoiesis, and future studies using NFI-$A^{-/-}$ animals in combination with lentiviral vectors will allow a deep analysis of NFI-A function during embryonic primitive and definitive hematopoiesis. TFs are important intrinsic regulators as part of a complex network participating in positive and negative cross-regulations at the transcriptional and post-transcriptional level [197]. Future experiments will need to be performed to understand how NFI-A interacts with these other TF circuitries during hematopoietic lineage specification and differentiation. Dysregulation of key TFs leads to haematological disorders of both the myeloid and erythroid compartments, and our data indicating the necessity of proper levels of NFI-A during hematopoietic differentiation of erythroid and granulocytic compartments indicates that NFI-A could be involved in the pathogenesis of haematological diseases further underlying its importance in hematopoietic development.

REFERENCES

1. Dzierzak, E. & Speck, N.A. Of lineage and legacy: the development of mammalian hematopoietic stem cells. *Nature immunology* **9**, 129-136 (2008).
2. Tavian, M. & Peault, B. Embryonic development of the human hematopoietic system. *Int J Dev Biol* **49**, 243-250 (2005).
3. Tavian, M. & Peault, B. The changing cellular environments of hematopoiesis in human development in utero. *Exp Hematol* **33**, 1062-1069 (2005).
4. Tavian, M. & Peault, B. Analysis of hematopoietic development during human embryonic ontogenesis. *Methods Mol Med* **105**, 413-424 (2005).
5. Xiong, J.W. Molecular and developmental biology of the hemangioblast. *Dev Dyn* **237**, 1218-1231 (2008).
6. Ferkowicz, M.J. & Yoder, M.C. Blood island formation: longstanding observations and modern interpretations. *Exp Hematol* **33**, 1041-1047 (2005).
7. Ueno, H. & Weissman, I.L. Clonal analysis of mouse development reveals a polyclonal origin for yolk sac blood islands. *Dev Cell* **11**, 519-533 (2006).
8. Chasis, J.A. & Mohandas, N. Erythroblastic islands: niches for erythropoiesis. *Blood* **112**, 470-478 (2008).
9. Palis, J. Ontogeny of erythropoiesis. *Current opinion in hematology* **15**, 155-161 (2008).
10. Palis, J. & Yoder, M.C. Yolk-sac hematopoiesis: the first blood cells of mouse and man. *Exp Hematol* **29**, 927-936 (2001).
11. Klimchenko, O. *et al.* A common bipotent progenitor generates the erythroid and megakaryocyte lineages in embryonic stem cell-derived primitive hematopoiesis. *Blood* **114**, 1506-1517 (2009).
12. Palis, J., Robertson, S., Kennedy, M., Wall, C. & Keller, G. Development of erythroid and myeloid progenitors in the yolk sac and embryo proper of the mouse. *Development (Cambridge, England)* **126**, 5073-5084 (1999).
13. McGrath, K.E. & Palis, J. Hematopoiesis in the yolk sac: more than meets the eye. *Exp Hematol* **33**, 1021-1028 (2005).
14. Yoder, M.C. *et al.* Characterization of definitive lymphohematopoietic stem cells in the day 9 murine yolk sac. *Immunity* **7**, 335-344 (1997).
15. Samokhvalov, I.M., Samokhvalova, N.I. & Nishikawa, S. Cell tracing shows the contribution of the yolk sac to adult haematopoiesis. *Nature* **446**, 1056-1061 (2007).
16. Medvinsky, A. & Dzierzak, E. Definitive hematopoiesis is autonomously initiated by the AGM region. *Cell* **86**, 897-906 (1996).
17. Muller, A.M., Medvinsky, A., Strouboulis, J., Grosveld, F. & Dzierzak, E. Development of hematopoietic stem cell activity in the mouse embryo. *Immunity* **1**, 291-301 (1994).
18. de Bruijn, M.F., Speck, N.A., Peeters, M.C. & Dzierzak, E. Definitive hematopoietic stem cells first develop within the major arterial regions of the mouse embryo. *Embo J* **19**, 2465-2474 (2000).
19. Eilken, H.M., Nishikawa, S. & Schroeder, T. Continuous single-cell imaging of blood generation from haemogenic endothelium. *Nature* **457**, 896-900 (2009).
20. Gekas, C., Dieterlen-Lievre, F., Orkin, S.H. & Mikkola, H.K. The placenta is a niche for hematopoietic stem cells. *Dev Cell* **8**, 365-375 (2005).
21. Ottersbach, K. & Dzierzak, E. The murine placenta contains hematopoietic stem cells within the vascular labyrinth region. *Dev Cell* **8**, 377-387 (2005).

22. Orkin, S.H. & Zon, L.I. Hematopoiesis: an evolving paradigm for stem cell biology. *Cell* **132**, 631-644 (2008).
23. Faloon, P. *et al.* Basic fibroblast growth factor positively regulates hematopoietic development. *Development (Cambridge, England)* **127**, 1931-1941 (2000).
24. Shalaby, F. *et al.* Failure of blood-island formation and vasculogenesis in Flk-1-deficient mice. *Nature* **376**, 62-66 (1995).
25. Winnier, G., Blessing, M., Labosky, P.A. & Hogan, B.L. Bone morphogenetic protein-4 is required for mesoderm formation and patterning in the mouse. *Genes & development* **9**, 2105-2116 (1995).
26. Wang, Q. *et al.* Disruption of the Cbfa2 gene causes necrosis and hemorrhaging in the central nervous system and blocks definitive hematopoiesis. *Proceedings of the National Academy of Sciences of the United States of America* **93**, 3444-3449 (1996).
27. Cai, Z. *et al.* Haploinsufficiency of AML1 affects the temporal and spatial generation of hematopoietic stem cells in the mouse embryo. *Immunity* **13**, 423-431 (2000).
28. North, T.E. *et al.* Runx1 expression marks long-term repopulating hematopoietic stem cells in the midgestation mouse embryo. *Immunity* **16**, 661-672 (2002).
29. Chen, M.J., Yokomizo, T., Zeigler, B.M., Dzierzak, E. & Speck, N.A. Runx1 is required for the endothelial to haematopoietic cell transition but not thereafter. *Nature* **457**, 887-891 (2009).
30. Tsai, F.Y. *et al.* An early haematopoietic defect in mice lacking the transcription factor GATA-2. *Nature* **371**, 221-226 (1994).
31. Ling, K.W. *et al.* GATA-2 plays two functionally distinct roles during the ontogeny of hematopoietic stem cells. *J Exp Med* **200**, 871-882 (2004).
32. Robb, L. *et al.* Absence of yolk sac hematopoiesis from mice with a targeted disruption of the scl gene. *Proceedings of the National Academy of Sciences of the United States of America* **92**, 7075-7079 (1995).
33. Yamada, Y. *et al.* The T cell leukemia LIM protein Lmo2 is necessary for adult mouse hematopoiesis. *Proceedings of the National Academy of Sciences of the United States of America* **95**, 3890-3895 (1998).
34. Houssaint, E. Differentiation of the mouse hepatic primordium. II. Extrinsic origin of the haemopoietic cell line. *Cell Differ* **10**, 243-252 (1981).
35. Johnson, G.R. & Moore, M.A. Role of stem cell migration in initiation of mouse foetal liver haemopoiesis. *Nature* **258**, 726-728 (1975).
36. Mikkola, H.K. & Orkin, S.H. The journey of developing hematopoietic stem cells. *Development (Cambridge, England)* **133**, 3733-3744 (2006).
37. Morrison, S.J., Hemmati, H.D., Wandycz, A.M. & Weissman, I.L. The purification and characterization of fetal liver hematopoietic stem cells. *Proceedings of the National Academy of Sciences of the United States of America* **92**, 10302-10306 (1995).
38. Lansdorp, P.M., Dragowska, W. & Mayani, H. Ontogeny-related changes in proliferative potential of human hematopoietic cells. *J Exp Med* **178**, 787-791 (1993).
39. Jordan, C.T., McKearn, J.P. & Lemischka, I.R. Cellular and developmental properties of fetal hematopoietic stem cells. *Cell* **61**, 953-963 (1990).
40. Traver, D. *et al.* Fetal liver myelopoiesis occurs through distinct, prospectively isolatable progenitor subsets. *Blood* **98**, 627-635 (2001).
41. Nicolini, F.E. *et al.* Unique differentiation programs of human fetal liver stem cells shown both in vitro and in vivo in NOD/SCID mice. *Blood* **94**, 2686-2695 (1999).
42. Christensen, J.L., Wright, D.E., Wagers, A.J. & Weissman, I.L. Circulation and chemotaxis of fetal hematopoietic stem cells. *PLoS Biol* **2**, E75 (2004).

43. Kiel, M.J. & Morrison, S.J. Uncertainty in the niches that maintain haematopoietic stem cells. *Nat Rev Immunol* **8**, 290-301 (2008).
44. Sugiyama, T., Kohara, H., Noda, M. & Nagasawa, T. Maintenance of the hematopoietic stem cell pool by CXCL12-CXCR4 chemokine signaling in bone marrow stromal cell niches. *Immunity* **25**, 977-988 (2006).
45. Kiel, M.J. & Morrison, S.J. Maintaining hematopoietic stem cells in the vascular niche. *Immunity* **25**, 862-864 (2006).
46. Yoshihara, H. *et al.* Thrombopoietin/MPL signaling regulates hematopoietic stem cell quiescence and interaction with the osteoblastic niche. *Cell Stem Cell* **1**, 685-697 (2007).
47. Arai, F. *et al.* Tie2/angiopoietin-1 signaling regulates hematopoietic stem cell quiescence in the bone marrow niche. *Cell* **118**, 149-161 (2004).
48. Weber, J.M. & Calvi, L.M. Notch signaling and the bone marrow hematopoietic stem cell niche. *Bone* (2009).
49. Kiel, M.J., Acar, M., Radice, G.L. & Morrison, S.J. Hematopoietic stem cells do not depend on N-cadherin to regulate their maintenance. *Cell Stem Cell* **4**, 170-179 (2009).
50. Akala, O.O. & Clarke, M.F. Hematopoietic stem cell self-renewal. *Curr Opin Genet Dev* **16**, 496-501 (2006).
51. Taichman, R.S. & Emerson, S.G. Human osteoblasts support hematopoiesis through the production of granulocyte colony-stimulating factor. *J Exp Med* **179**, 1677-1682 (1994).
52. Zhu, J. *et al.* Osteoblasts support B-lymphocyte commitment and differentiation from hematopoietic stem cells. *Blood* **109**, 3706-3712 (2007).
53. Rieger, M.A., Hoppe, P.S., Smejkal, B.M., Eitelhuber, A.C. & Schroeder, T. Hematopoietic cytokines can instruct lineage choice. *Science (New York, N.Y* **325**, 217-218 (2009).
54. Hock, H. *et al.* Tel/Etv6 is an essential and selective regulator of adult hematopoietic stem cell survival. *Genes & development* **18**, 2336-2341 (2004).
55. Hock, H. *et al.* Gfi-1 restricts proliferation and preserves functional integrity of haematopoietic stem cells. *Nature* **431**, 1002-1007 (2004).
56. Zeng, H., Yucel, R., Kosan, C., Klein-Hitpass, L. & Moroy, T. Transcription factor Gfi1 regulates self-renewal and engraftment of hematopoietic stem cells. *Embo J* **23**, 4116-4125 (2004).
57. Park, I.K. *et al.* Bmi-1 is required for maintenance of adult self-renewing haematopoietic stem cells. *Nature* **423**, 302-305 (2003).
58. Iwama, A. *et al.* Enhanced self-renewal of hematopoietic stem cells mediated by the polycomb gene product Bmi-1. *Immunity* **21**, 843-851 (2004).
59. Iwasaki, H. & Akashi, K. Myeloid lineage commitment from the hematopoietic stem cell. *Immunity* **26**, 726-740 (2007).
60. Cross, M.A. & Enver, T. The lineage commitment of haemopoietic progenitor cells. *Curr Opin Genet Dev* **7**, 609-613 (1997).
61. Miyamoto, T. *et al.* Myeloid or lymphoid promiscuity as a critical step in hematopoietic lineage commitment. *Dev Cell* **3**, 137-147 (2002).
62. Rekhtman, N., Radparvar, F., Evans, T. & Skoultchi, A.I. Direct interaction of hematopoietic transcription factors PU.1 and GATA-1: functional antagonism in erythroid cells. *Genes & development* **13**, 1398-1411 (1999).
63. Nerlov, C., Querfurth, E., Kulessa, H. & Graf, T. GATA-1 interacts with the myeloid PU.1 transcription factor and represses PU.1-dependent transcription. *Blood* **95**, 2543-2551 (2000).

64. Kim, S.I. & Bresnick, E.H. Transcriptional control of erythropoiesis: emerging mechanisms and principles. *Oncogene* **26**, 6777-6794 (2007).
65. Fujiwara, Y., Browne, C.P., Cunniff, K., Goff, S.C. & Orkin, S.H. Arrested development of embryonic red cell precursors in mouse embryos lacking transcription factor GATA-1. *Proceedings of the National Academy of Sciences of the United States of America* **93**, 12355-12358 (1996).
66. Weiss, M.J., Keller, G. & Orkin, S.H. Novel insights into erythroid development revealed through in vitro differentiation of GATA-1 embryonic stem cells. *Genes & development* **8**, 1184-1197 (1994).
67. Heyworth, C., Pearson, S., May, G. & Enver, T. Transcription factor-mediated lineage switching reveals plasticity in primary committed progenitor cells. *Embo J* **21**, 3770-3781 (2002).
68. Iwasaki, H. *et al.* GATA-1 converts lymphoid and myelomonocytic progenitors into the megakaryocyte/erythrocyte lineages. *Immunity* **19**, 451-462 (2003).
69. Tsiftsoglou, A.S., Vizirianakis, I.S. & Strouboulis, J. Erythropoiesis: model systems, molecular regulators, and developmental programs. *IUBMB Life* **61**, 800-830 (2009).
70. Drissen, R. *et al.* The erythroid phenotype of EKLF-null mice: defects in hemoglobin metabolism and membrane stability. *Molecular and cellular biology* **25**, 5205-5214 (2005).
71. Gregory, R.C. *et al.* Functional interaction of GATA1 with erythroid Kruppel-like factor and Sp1 at defined erythroid promoters. *Blood* **87**, 1793-1801 (1996).
72. Merika, M. & Orkin, S.H. Functional synergy and physical interactions of the erythroid transcription factor GATA-1 with the Kruppel family proteins Sp1 and EKLF. *Molecular and cellular biology* **15**, 2437-2447 (1995).
73. Orkin, S.H. *et al.* Linkage of beta-thalassaemia mutations and beta-globin gene polymorphisms with DNA polymorphisms in human beta-globin gene cluster. *Nature* **296**, 627-631 (1982).
74. Nuez, B., Michalovich, D., Bygrave, A., Ploemacher, R. & Grosveld, F. Defective haematopoiesis in fetal liver resulting from inactivation of the EKLF gene. *Nature* **375**, 316-318 (1995).
75. Perkins, A.C., Sharpe, A.H. & Orkin, S.H. Lethal beta-thalassaemia in mice lacking the erythroid CACCC-transcription factor EKLF. *Nature* **375**, 318-322 (1995).
76. Hodge, D. *et al.* A global role for EKLF in definitive and primitive erythropoiesis. *Blood* **107**, 3359-3370 (2006).
77. Pilon, A.M. *et al.* Failure of terminal erythroid differentiation in EKLF-deficient mice is associated with cell cycle perturbation and reduced expression of E2F2. *Molecular and cellular biology* **28**, 7394-7401 (2008).
78. Mikkola, H.K. *et al.* Haematopoietic stem cells retain long-term repopulating activity and multipotency in the absence of stem-cell leukaemia SCL/tal-1 gene. *Nature* **421**, 547-551 (2003).
79. Goardon, N. *et al.* ETO2 coordinates cellular proliferation and differentiation during erythropoiesis. *Embo J* **25**, 357-366 (2006).
80. Schuh, A.H. *et al.* ETO-2 associates with SCL in erythroid cells and megakaryocytes and provides repressor functions in erythropoiesis. *Molecular and cellular biology* **25**, 10235-10250 (2005).
81. Wadman, I. *et al.* Specific in vivo association between the bHLH and LIM proteins implicated in human T cell leukemia. *Embo J* **13**, 4831-4839 (1994).
82. Wadman, I.A. *et al.* The LIM-only protein Lmo2 is a bridging molecule assembling an erythroid, DNA-binding complex which includes the TAL1, E47, GATA-1 and Ldb1/NLI proteins. *Embo J* **16**, 3145-3157 (1997).

83. Warren, A.J. *et al.* The oncogenic cysteine-rich LIM domain protein rbtn2 is essential for erythroid development. *Cell* **78**, 45-57 (1994).
84. Skalnik, D.G. Transcriptional mechanisms regulating myeloid-specific genes. *Gene* **284**, 1-21 (2002).
85. Scott, E.W., Simon, M.C., Anastasi, J. & Singh, H. Requirement of transcription factor PU.1 in the development of multiple hematopoietic lineages. *Science (New York, N.Y* **265**, 1573-1577 (1994).
86. McKercher, S.R. *et al.* Targeted disruption of the PU.1 gene results in multiple hematopoietic abnormalities. *Embo J* **15**, 5647-5658 (1996).
87. DeKoter, R.P. & Singh, H. Regulation of B lymphocyte and macrophage development by graded expression of PU.1. *Science (New York, N.Y* **288**, 1439-1441 (2000).
88. Pahl, H.L. *et al.* The proto-oncogene PU.1 regulates expression of the myeloid-specific CD11b promoter. *The Journal of biological chemistry* **268**, 5014-5020 (1993).
89. Zhang, D.E., Hetherington, C.J., Chen, H.M. & Tenen, D.G. The macrophage transcription factor PU.1 directs tissue-specific expression of the macrophage colony-stimulating factor receptor. *Molecular and cellular biology* **14**, 373-381 (1994).
90. Smith, L.T., Hohaus, S., Gonzalez, D.A., Dziennis, S.E. & Tenen, D.G. PU.1 (Spi-1) and C/EBP alpha regulate the granulocyte colony-stimulating factor receptor promoter in myeloid cells. *Blood* **88**, 1234-1247 (1996).
91. Hohaus, S. *et al.* PU.1 (Spi-1) and C/EBP alpha regulate expression of the granulocyte-macrophage colony-stimulating factor receptor alpha gene. *Molecular and cellular biology* **15**, 5830-5845 (1995).
92. Scott, L.M., Civin, C.I., Rorth, P. & Friedman, A.D. A novel temporal expression pattern of three C/EBP family members in differentiating myelomonocytic cells. *Blood* **80**, 1725-1735 (1992).
93. Zhang, D.E. *et al.* Absence of granulocyte colony-stimulating factor signaling and neutrophil development in CCAAT enhancer binding protein alpha-deficient mice. *Proceedings of the National Academy of Sciences of the United States of America* **94**, 569-574 (1997).
94. Rangatia, J. *et al.* Downregulation of c-Jun expression by transcription factor C/EBPalpha is critical for granulocytic lineage commitment. *Molecular and cellular biology* **22**, 8681-8694 (2002).
95. Dahl, R. *et al.* Regulation of macrophage and neutrophil cell fates by the PU.1:C/EBPalpha ratio and granulocyte colony-stimulating factor. *Nature immunology* **4**, 1029-1036 (2003).
96. Bennett, J.M. *et al.* Proposals for the classification of the acute leukaemias. French-American-British (FAB) co-operative group. *British journal of haematology* **33**, 451-458 (1976).
97. Cozzio, A. *et al.* Similar MLL-associated leukemias arising from self-renewing stem cells and short-lived myeloid progenitors. *Genes & development* **17**, 3029-3035 (2003).
98. Krivtsov, A.V. *et al.* Transformation from committed progenitor to leukaemia stem cell initiated by MLL-AF9. *Nature* **442**, 818-822 (2006).
99. Huntly, B.J. *et al.* MOZ-TIF2, but not BCR-ABL, confers properties of leukemic stem cells to committed murine hematopoietic progenitors. *Cancer Cell* **6**, 587-596 (2004).
100. Lapidot, T. *et al.* A cell initiating human acute myeloid leukaemia after transplantation into SCID mice. *Nature* **367**, 645-648 (1994).
101. Jordan, C.T., Guzman, M.L. & Noble, M. Cancer stem cells. *The New England journal of medicine* **355**, 1253-1261 (2006).

102. Tenen, D.G. Disruption of differentiation in human cancer: AML shows the way. *Nat Rev Cancer* **3**, 89-101 (2003).
103. Gilliland, D.G., Jordan, C.T. & Felix, C.A. The molecular basis of leukemia. *Hematology Am Soc Hematol Educ Program*, 80-97 (2004).
104. Speck, N.A. & Gilliland, D.G. Core-binding factors in haematopoiesis and leukaemia. *Nat Rev Cancer* **2**, 502-513 (2002).
105. Renneville, A. *et al.* Cooperating gene mutations in acute myeloid leukemia: a review of the literature. *Leukemia* **22**, 915-931 (2008).
106. Mueller, B.U. *et al.* ATRA resolves the differentiation block in t(15;17) acute myeloid leukemia by restoring PU.1 expression. *Blood* **107**, 3330-3338 (2006).
107. Walter, M.J. *et al.* Reduced PU.1 expression causes myeloid progenitor expansion and increased leukemia penetrance in mice expressing PML-RARalpha. *Proceedings of the National Academy of Sciences of the United States of America* **102**, 12513-12518 (2005).
108. Melnick, A. & Licht, J.D. Deconstructing a disease: RARalpha, its fusion partners, and their roles in the pathogenesis of acute promyelocytic leukemia. *Blood* **93**, 3167-3215 (1999).
109. Lo Coco, F. *et al.* Progress in differentiation induction as a treatment for acute promyelocytic leukemia and beyond. *Cancer research* **62**, 5618-5621 (2002).
110. Truong, B.T. *et al.* CCAAT/Enhancer binding proteins repress the leukemic phenotype of acute myeloid leukemia. *Blood* **101**, 1141-1148 (2003).
111. Guibal, F.C. *et al.* Identification of a myeloid committed progenitor as the cancer initiating cell in acute promyelocytic leukemia. *Blood* (2009).
112. Leroy, H. *et al.* CEBPA point mutations in hematological malignancies. *Leukemia* **19**, 329-334 (2005).
113. Pabst, T. *et al.* Dominant-negative mutations of CEBPA, encoding CCAAT/enhancer binding protein-alpha (C/EBPalpha), in acute myeloid leukemia. *Nat Genet* **27**, 263-270 (2001).
114. Pabst, T. *et al.* AML1-ETO downregulates the granulocytic differentiation factor C/EBPalpha in t(8;21) myeloid leukemia. *Nature medicine* **7**, 444-451 (2001).
115. Wouters, B.J. *et al.* Distinct gene expression profiles of acute myeloid/T-lymphoid leukemia with silenced CEBPA and mutations in NOTCH1. *Blood* **110**, 3706-3714 (2007).
116. Winter, J., Jung, S., Keller, S., Gregory, R.I. & Diederichs, S. Many roads to maturity: microRNA biogenesis pathways and their regulation. *Nat Cell Biol* **11**, 228-234 (2009).
117. Calin, G.A. *et al.* Frequent deletions and down-regulation of micro- RNA genes miR15 and miR16 at 13q14 in chronic lymphocytic leukemia. *Proceedings of the National Academy of Sciences of the United States of America* **99**, 15524-15529 (2002).
118. Poy, M.N. *et al.* A pancreatic islet-specific microRNA regulates insulin secretion. *Nature* **432**, 226-230 (2004).
119. van Rooij, E. *et al.* A signature pattern of stress-responsive microRNAs that can evoke cardiac hypertrophy and heart failure. *Proceedings of the National Academy of Sciences of the United States of America* **103**, 18255-18260 (2006).
120. Calin, G.A. & Croce, C.M. MicroRNA-cancer connection: the beginning of a new tale. *Cancer research* **66**, 7390-7394 (2006).
121. Garzon, R., Fabbri, M., Cimmino, A., Calin, G.A. & Croce, C.M. MicroRNA expression and function in cancer. *Trends Mol Med* **12**, 580-587 (2006).

122. Garzon, R. *et al.* MicroRNA signatures associated with cytogenetics and prognosis in acute myeloid leukemia. *Blood* **111**, 3183-3189 (2008).
123. Garzon, R. *et al.* Distinctive microRNA signature of acute myeloid leukemia bearing cytoplasmic mutated nucleophosmin. *Proceedings of the National Academy of Sciences of the United States of America* **105**, 3945-3950 (2008).
124. Baltimore, D., Boldin, M.P., O'Connell, R.M., Rao, D.S. & Taganov, K.D. MicroRNAs: new regulators of immune cell development and function. *Nature immunology* **9**, 839-845 (2008).
125. Georgantas, R.W., 3rd *et al.* CD34+ hematopoietic stem-progenitor cell microRNA expression and function: a circuit diagram of differentiation control. *Proceedings of the National Academy of Sciences of the United States of America* **104**, 2750-2755 (2007).
126. Fazi, F. *et al.* A minicircuitry comprised of microRNA-223 and transcription factors NFI-A and C/EBPalpha regulates human granulopoiesis. *Cell* **123**, 819-831 (2005).
127. Chen, C.Z., Li, L., Lodish, H.F. & Bartel, D.P. MicroRNAs modulate hematopoietic lineage differentiation. *Science (New York, N.Y* **303**, 83-86 (2004).
128. Rosa, A. *et al.* The interplay between the master transcription factor PU.1 and miR-424 regulates human monocyte/macrophage differentiation. *Proc Natl Acad Sci U S A* **104**, 19849-19854 (2007).
129. Gronostajski, R.M. Roles of the NFI/CTF gene family in transcription and development. *Gene* **249**, 31-45 (2000).
130. Roulet, E. *et al.* Experimental analysis and computer prediction of CTF/NFI transcription factor DNA binding sites. *J Mol Biol* **297**, 833-848 (2000).
131. Bedford, F.K., Julius, D. & Ingraham, H.A. Neuronal expression of the 5HT3 serotonin receptor gene requires nuclear factor 1 complexes. *J Neurosci* **18**, 6186-6194 (1998).
132. Spitz, F. *et al.* A combination of MEF3 and NFI proteins activates transcription in a subset of fast-twitch muscles. *Molecular and cellular biology* **17**, 656-666 (1997).
133. Bachurski, C.J., Kelly, S.E., Glasser, S.W. & Currier, T.A. Nuclear factor I family members regulate the transcription of surfactant protein-C. *The Journal of biological chemistry* **272**, 32759-32766 (1997).
134. Jackson, D.A. *et al.* Modulation of liver-specific transcription by interactions between hepatocyte nuclear factor 3 and nuclear factor 1 binding DNA in close apposition. *Molecular and cellular biology* **13**, 2401-2410 (1993).
135. Leahy, P., Crawford, D.R., Grossman, G., Gronostajski, R.M. & Hanson, R.W. CREB binding protein coordinates the function of multiple transcription factors including nuclear factor I to regulate phosphoenolpyruvate carboxykinase (GTP) gene transcription. *The Journal of biological chemistry* **274**, 8813-8822 (1999).
136. das Neves, L. *et al.* Disruption of the murine nuclear factor I-A gene (Nfia) results in perinatal lethality, hydrocephalus, and agenesis of the corpus callosum. *Proceedings of the National Academy of Sciences of the United States of America* **96**, 11946-11951 (1999).
137. Grunder, A. *et al.* Nuclear factor I-B (Nfib) deficient mice have severe lung hypoplasia. *Mech Dev* **112**, 69-77 (2002).
138. Driller, K. *et al.* Nuclear factor I X deficiency causes brain malformation and severe skeletal defects. *Molecular and cellular biology* **27**, 3855-3867 (2007).
139. Chaudhry, A.Z., Lyons, G.E. & Gronostajski, R.M. Expression patterns of the four nuclear factor I genes during mouse embryogenesis indicate a potential role in development. *Dev Dyn* **208**, 313-325 (1997).

140. Kulkarni, S. & Gronostajski, R.M. Altered expression of the developmentally regulated NFI gene family during phorbol ester-induced differentiation of human leukemic cells. *Cell Growth Differ* **7**, 501-510 (1996).
141. Downs, K.M. & Davies, T. Staging of gastrulating mouse embryos by morphological landmarks in the dissecting microscope. *Development (Cambridge, England)* **118**, 1255-1266 (1993).
142. Lowry, O.H., Rosebrough, N.J., Farr, A.L. & Randall, R.J. Protein measurement with the Folin phenol reagent. *The Journal of biological chemistry* **193**, 265-275 (1951).
143. Ballarino, M., Morlando, M., Pagano, F., Fatica, A. & Bozzoni, I. The cotranscriptional assembly of snoRNPs controls the biosynthesis of H/ACA snoRNAs in Saccharomyces cerevisiae. *Molecular and cellular biology* **25**, 5396-5403 (2005).
144. Moffat, J. *et al.* A lentiviral RNAi library for human and mouse genes applied to an arrayed viral high-content screen. *Cell* **124**, 1283-1298 (2006).
145. Fazi, F. *et al.* Heterochromatic gene repression of the retinoic acid pathway in acute myeloid leukemia. *Blood* **109**, 4432-4440 (2007).
146. Liu, S. *et al.* Interplay of RUNX1/MTG8 and DNA methyltransferase 1 in acute myeloid leukemia. *Cancer research* **65**, 1277-1284 (2005).
147. Birnie, G.D. The HL60 cell line: a model system for studying human myeloid cell differentiation. *The British journal of cancer* **9**, 41-45 (1988).
148. Lozzio, C.B. & Lozzio, B.B. Human chronic myelogenous leukemia cell-line with positive Philadelphia chromosome. *Blood* **45**, 321-334 (1975).
149. Luisi-DeLuca, C., Mitchell, T., Spriggs, D. & Kufe, D.W. Induction of terminal differentiation in human K562 erythroleukemia cells by arabinofuranosylcytosine. *The Journal of clinical investigation* **74**, 821-827 (1984).
150. Tetteroo, P.A., Massaro, F., Mulder, A., Schreuder-van Gelder, R. & von dem Borne, A.E. Megakaryoblastic differentiation of proerythroblastic K562 cell-line cells. *Leukemia research* **8**, 197-206 (1984).
151. Felli, N. *et al.* MicroRNAs 221 and 222 inhibit normal erythropoiesis and erythroleukemic cell growth via kit receptor down-modulation. *Proceedings of the National Academy of Sciences of the United States of America* **102**, 18081-18086 (2005).
152. De Maria, R. *et al.* Negative regulation of erythropoiesis by caspase-mediated cleavage of GATA-1. *Nature* **401**, 489-493 (1999).
153. Jones, K.A., Kadonaga, J.T., Rosenfeld, P.J., Kelly, T.J. & Tjian, R. A cellular DNA-binding protein that activates eukaryotic transcription and DNA replication. *Cell* **48**, 79-89 (1987).
154. Watanabe, T. *et al.* Effects of 1-beta-D-arabinofuranosylcytosine and phorbol ester on differentiation of human K562 erythroleukemia cells. *Molecular pharmacology* **27**, 683-688 (1985).
155. Marinescu, V.D., Kohane, I.S. & Riva, A. The MAPPER database: a multi-genome catalog of putative transcription factor binding sites. *Nucleic Acids Res* **33**, D91-97 (2005).
156. Grabe, N. AliBaba2: context specific identification of transcription factor binding sites. *In Silico Biol* **2**, S1-15 (2002).
157. Cartharius, K. *et al.* MatInspector and beyond: promoter analysis based on transcription factor binding sites. *Bioinformatics* **21**, 2933-2942 (2005).
158. Lorsbach, R.B. *et al.* Role of RUNX1 in adult hematopoiesis: analysis of RUNX1-IRES-GFP knock-in mice reveals differential lineage expression. *Blood* **103**, 2522-2529 (2004).

159. Yue, X. *et al.* Transcriptional control of the expression of the c-fms gene encoding the receptor for macrophage colony-stimulating factor (CSF-1). *Immunobiology* **195**, 461-476 (1996).
160. Koury, M.J., Koury, S.T., Kopsombut, P. & Bondurant, M.C. In vitro maturation of nascent reticulocytes to erythrocytes. *Blood* **105**, 2168-2174 (2005).
161. Weiss, I.M. & Liebhaber, S.A. Erythroid cell-specific determinants of alpha-globin mRNA stability. *Molecular and cellular biology* **14**, 8123-8132 (1994).
162. Harju, S., McQueen, K.J. & Peterson, K.R. Chromatin structure and control of beta-like globin gene switching. *Experimental biology and medicine (Maywood, N.J* **227**, 683-700 (2002).
163. Fraser, S.T., Isern, J. & Baron, M.H. Maturation and enucleation of primitive erythroblasts during mouse embryogenesis is accompanied by changes in cell-surface antigen expression. *Blood* **109**, 343-352 (2007).
164. Bitter, M.A. *et al.* Associations between morphology, karyotype, and clinical features in myeloid leukemias. *Human pathology* **18**, 211-225 (1987).
165. Look, A.T. Oncogenic transcription factors in the human acute leukemias. *Science (New York, N.Y* **278**, 1059-1064 (1997).
166. Licht, J.D. AML1 and the AML1-ETO fusion protein in the pathogenesis of t(8;21) AML. *Oncogene* **20**, 5660-5679 (2001).
167. Klampfer, L., Zhang, J., Zelenetz, A.O., Uchida, H. & Nimer, S.D. The AML1/ETO fusion protein activates transcription of BCL-2. *Proceedings of the National Academy of Sciences of the United States of America* **93**, 14059-14064 (1996).
168. Rhoades, K.L. *et al.* Synergistic up-regulation of the myeloid-specific promoter for the macrophage colony-stimulating factor receptor by AML1 and the t(8;21) fusion protein may contribute to leukemogenesis. *Proceedings of the National Academy of Sciences of the United States of America* **93**, 11895-11900 (1996).
169. Frank, R. *et al.* The AML1/ETO fusion protein blocks transactivation of the GM-CSF promoter by AML1B. *Oncogene* **11**, 2667-2674 (1995).
170. Ziegler, B. *et al.* Unilineage hematopoietic differentiation in bulk and single cell culture. *Stem cells (Dayton, Ohio)* **16 Suppl 1**, 51-73 (1998).
171. Pan, X. *et al.* Graded levels of GATA-1 expression modulate survival, proliferation, and differentiation of erythroid progenitors. *J Biol Chem* **280**, 22385-22394 (2005).
172. Laslo, P. *et al.* Multilineage transcriptional priming and determination of alternate hematopoietic cell fates. *Cell* **126**, 755-766 (2006).
173. Radomska, H.S. *et al.* CCAAT/enhancer binding protein alpha is a regulatory switch sufficient for induction of granulocytic development from bipotential myeloid progenitors. *Molecular and cellular biology* **18**, 4301-4314 (1998).
174. Barreda, D.R., Hanington, P.C. & Belosevic, M. Regulation of myeloid development and function by colony stimulating factors. *Dev Comp Immunol* **28**, 509-554 (2004).
175. Fleetwood, A.J., Cook, A.D. & Hamilton, J.A. Functions of granulocyte-macrophage colony-stimulating factor. *Crit Rev Immunol* **25**, 405-428 (2005).
176. Horiguchi, J., Warren, M.K. & Kufe, D. Expression of the macrophage-specific colony-stimulating factor in human monocytes treated with granulocyte-macrophage colony-stimulating factor. *Blood* **69**, 1259-1261 (1987).
177. Socolovsky, M. Molecular insights into stress erythropoiesis. *Curr Opin Hematol* **14**, 215-224 (2007).
178. Wu, H., Liu, X., Jaenisch, R. & Lodish, H.F. Generation of committed erythroid BFU-E and CFU-E progenitors does not require erythropoietin or the erythropoietin receptor. *Cell* **83**, 59-67 (1995).

179. Lin, C.S., Lim, S.K., D'Agati, V. & Costantini, F. Differential effects of an erythropoietin receptor gene disruption on primitive and definitive erythropoiesis. *Genes & development* **10**, 154-164 (1996).
180. Ghaffari, S. *et al.* Erythropoiesis in the absence of janus-kinase 2: BCR-ABL induces red cell formation in JAK2(-/-) hematopoietic progenitors. *Blood* **98**, 2948-2957 (2001).
181. Zhao, W., Kitidis, C., Fleming, M.D., Lodish, H.F. & Ghaffari, S. Erythropoietin stimulates phosphorylation and activation of GATA-1 via the PI3-kinase/AKT signaling pathway. *Blood* **107**, 907-915 (2006).
182. Gordon, C.T., Fox, V.J., Najdovska, S. & Perkins, A.C. C/EBPdelta and C/EBPgamma bind the CCAAT-box in the human beta-globin promoter and modulate the activity of the CACC-box binding protein, EKLF. *Biochim Biophys Acta* **1729**, 74-80 (2005).
183. Chen, X.W., Mo, Q.H., Li, Q., Zeng, R. & Xu, X.M. A novel mutation of -73(A-->T) in the CCAAT box of the beta-globin gene identified in a patient with the mild beta-thalassemia intermedia. *Ann Hematol* **86**, 653-657 (2007).
184. Johnson, K.D., Kim, S.I. & Bresnick, E.H. Differential sensitivities of transcription factor target genes underlie cell type-specific gene expression profiles. *Proc Natl Acad Sci U S A* **103**, 15939-15944 (2006).
185. Felli, N. *et al.* MicroRNA 223-dependent expression of LMO2 regulates normal erythropoiesis. *Haematologica* **94**, 479-486 (2009).
186. Centis, F. *et al.* The importance of erythroid expansion in determining the extent of apoptosis in erythroid precursors in patients with beta-thalassemia major. *Blood* **96**, 3624-3629 (2000).
187. Schrier, S.L. Pathophysiology of thalassemia. *Current opinion in hematology* **9**, 123-126 (2002).
188. Rivella, S. Ineffective erythropoiesis and thalassemias. *Current opinion in hematology* **16**, 187-194 (2009).
189. Welch, J.J. *et al.* Global regulation of erythroid gene expression by transcription factor GATA-1. *Blood* **104**, 3136-3147 (2004).
190. Ward, A.C. The role of the granulocyte colony-stimulating factor receptor (G-CSF-R) in disease. *Front Biosci* **12**, 608-618 (2007).
191. Friedman, A.D. C/EBPalpha and the G-CSF receptor gene--partners in granulopoiesis? *Blood* **98**, 2291-2292 (2001).
192. Seto, Y., Fukunaga, R. & Nagata, S. Chromosomal gene organization of the human granulocyte colony-stimulating factor receptor. *J Immunol* **148**, 259-266 (1992).
193. Saito, M. *et al.* Granulocyte colony-stimulating factor directly affects human monocytes and modulates cytokine secretion. *Experimental hematology* **30**, 1115-1123 (2002).
194. de Figueiredo, L.L., de Abreu e Lima, R.S. & Rego, E.M. Granulocyte colony-stimulating factor and leukemogenesis. *Mediators Inflamm* **13**, 145-150 (2004).
195. Zhang, J., Socolovsky, M., Gross, A.W. & Lodish, H.F. Role of Ras signaling in erythroid differentiation of mouse fetal liver cells: functional analysis by a flow cytometry-based novel culture system. *Blood* **102**, 3938-3946 (2003).
196. Cesta, M.F. Normal structure, function, and histology of the spleen. *Toxicologic pathology* **34**, 455-465 (2006).
197. Graf, T. Differentiation plasticity of hematopoietic cells. *Blood* **99**, 3089-3101 (2002).

APPENDIX I

The following PDFs can be found attached after this cover page:

Fazi F., Racanicchi S., Zardo G., Starnes L.M., Mancini M., Travaglini L., Diverio D., Ammatuna E., Cimino G., Lo-Coco F., Grignani F., Nervi C. "Epigenetic silencing of the myelopoiesis-regulator microRNA-223 by the AML1/ETO oncoprotein". Cancer Cell. 2007 Nov;12(5):457-66.

*Starnes L.M. *Sorrentino A., Pelosi E., Ballarino M., Morsilli O., Biffoni M., Santoro S., Felli N., Castelli G., De Marchis M.L., Mastroberardino G., Gabbianelli M., Fatica A., Bozzoni I., Nervi C., Peschle C. "NFI-A directs the fate of hematopoietic progenitors to the erythroid or granulocytic lineage and controls β-globin and G-CSF receptor expression". Blood. 2009 Aug;114(9):1753-63.(* Equal contribution)

Cancer Cell
Article

Epigenetic Silencing of the Myelopoiesis Regulator microRNA-223 by the AML1/ETO Oncoprotein

Francesco Fazi,[1,3] Serena Racanicchi,[4] Giuseppe Zardo,[2,3] Linda M. Starnes,[1,3] Marco Mancini,[2] Lorena Travaglini,[1,3] Daniela Diverio,[2] Emanuele Ammatuna,[5] Giuseppe Cimino,[2] Francesco Lo-Coco,[5] Francesco Grignani,[4] and Clara Nervi[1,3,*]
[1]Department of Histology and Medical Embryology
[2]Department of Cellular Biotechnologies and Hematology
University La Sapienza, Rome, 00161, Italy
[3]San Raffaele Biomedical Park Foundation, Rome, 00128, Italy
[4]Department of Clinical and Experimental Medicine, General Pathology, University of Perugia, 06100, Italy
[5]Department of Biopathology, University Tor Vergata, Rome, 00133, Italy
*Correspondence: clara.nervi@uniroma1.it
DOI 10.1016/j.ccr.2007.09.020

SUMMARY

Hematopoietic transcription factors are involved in chromosomal translocations, which generate fusion proteins contributing to leukemia pathogenesis. Analysis of patient's primary leukemia blasts revealed that those carrying the t(8;21) generating AML1/ETO, the most common acute myeloid leukemia-associated fusion protein, display low levels of a microRNA-223 (miR-223), a regulator of myelopoiesis. Here, we show that *miR-223* is a direct transcriptional target of AML1/ETO. By recruiting chromatin remodeling enzymes at an AML1-binding site on the *pre-miR-223* gene, AML1/ETO induces heterochromatic silencing of *miR-223*. Ectopic miR-223 expression, RNAi against AML1/ETO, or demethylating treatment enhances miR-223 levels and restores cell differentiation. Here, we identify an additional action for a leukemia fusion protein linking the epigenetic silencing of a microRNA locus to the differentiation block of leukemia.

INTRODUCTION

Hematopoietic stem cell self-renewal and differentiation along different lineages is defined by a dynamic interplay between lineage-specific transcriptional and posttranscriptional regulators, including microRNAs (miRNAs), whose key role in hematopoiesis is recently emerging (Tenen, 2003; Chen and Lodish, 2005). Epigenetic mechanisms such as DNA methylation and posttranslational modifications of nucleosomal histone proteins contribute to the correct modulation of gene expression and to the maintenance of tissue- and cell-type-specific functions (Jaenisch and Bird, 2003; Grewal and Moazed, 2003; Klose and Bird, 2006; Mikkelsen et al., 2007). Deregulation of epigenetic mechanisms cooperates with genetic alterations to the establishment and progression of cancer (Jones and Baylin, 2007; Tenen, 2003).

MiRNAs are a new class of evolutionary conserved small RNAs affecting gene expression at the posttranscriptional level by blocking translation or degrading target messenger RNAs (mRNAs) (Bartell, 2004; Ambros, 2004; Chen et al., 2004). Their expression is highly regulated according to the cell's developmental lineage and shows restricted expression profiles in adult tissues, including in the

SIGNIFICANCE

AML1/ETO is the fusion product of the t(8;21), the most frequent chromosomal translocation in acute myeloid leukemia. We show that the expression of AML1/ETO triggers heterochromatic silencing of genomic regions generating a microRNA, the miR-223, whose activity is linked to the differentiation fate of myeloid precursors. Overall, our study identifies miR-223 as an additional pathogenic target for a leukemia fusion protein and provides evidence that links the epigenetic silencing of a microRNA locus to the differentiation block of myeloid precursors. Suppression of a *miRNA* gene expands the oncogenic activity of the fusion protein, since miRNA represses the expression of multiple target proteins. Thus, repression of *miRNA* expression may represent a key event in the differentiation block underlying leukemogenesis.

hematopoietic cell system (Chen et al., 2004; Cheng et al., 2005; Zhao et al., 2005; Bartell, 2004; Chen et al., 2006; Fazi et al., 2005). MiRNAs have been found to participate in regulatory circuits that control development of skeletal and cardiac muscle and lineage-differentiation fate of hematopoietic cells (Fazi et al., 2005; Zhao et al., 2005; Chen et al., 2006). However, little information is currently available on factors that modulate *miRNA* transcription and expression at the basal or tissue-specific level (Kim and Nam, 2006).

Developmental programs of normal hematopoiesis are altered in acute myeloid leukemias (AMLs), which represents the clonal expansion of hematopoietic precursors blocked at different stages of erythroid, granulocytic, monocytic, or megakaryocytic differentiation (Tenen, 2003). Hematopoietic transcription factors and miRNAs have been found mutated or consistently altered by chromosomal translocations associated to leukemias; their role in the pathogenesis of these malignancies has been proposed (Chen, 2005; Hammond, 2006; Calin and Croce, 2006; Saito et al., 2006; Tenen, 2003).

Our previous findings showed a crucial role for the transcriptional activation of miR-223 expression in human myelopoiesis (Fazi et al., 2005). Here, we investigated whether deregulated miR-223 expression could be associated with the differentiation block underlying the pathogenesis of distinct leukemia subtypes.

RESULTS AND DISCUSSION

MiR-223 Expression Is Downregulated in AML1/ETO-Positive Primary Blasts and Cell Lines

The expression levels of miR-223 were quantified in human hematopoietic cells isolated from healthy donors and from diagnostic samples of 31 leukemia patients whose morphological and genetic features are shown in Table 1. Figure 1A shows that miR-223 is expressed at high levels in total nucleated cells from peripheral blood (PB) and bone marrow (BM) from healthy donors, respectively, consisting of mature granulocytes (~50%–70%) and committed/mature myeloid precursors. MiR-223 was detected at the lowest levels of expression in immature CD34+-hematopoietic stem/progenitor cells isolated from either normal PB, BM, or cord blood (CB) in leukemias related to the erythroblastic (M6) or lymphoid lineages and in the 6 AMLs presenting the most immature myeloid phenotype (M0 and M1, by FAB classification) (Bennett et al., 1985). Intermediate levels of miR-223 were measurable in primary samples expressing the more mature AML phenotypes (acute-promyelocytic (M3), -myelomonocytic (M4), and -monoblastic (M5) leukemias), and in chronic myeloid leukemia in blast crisis (CML-BC) (Figure 1A). Overall, these results confirmed the induction of miR-223 during myeloid differentiation (Fazi et al., 2005) and related its expression levels to the stage of maturation block underlying myeloid leukemia subtypes. However, among the myeloblastic AML-M2 subtype, miR-223 is expressed at high levels in 3/8 de novo cases and at low levels in 4/4 cases harboring the

Table 1. Morphological and Genetic Features of Primary Leukemia Samples

Patient No.	Morphology by FAB	Karyotype
1	AML/M0	46,XY,der(12)t(12;?)(q23;?)/46,XY
2	AML/M0	Complex aberrations[a]
3	MDS-AML/M1	46,XY,del(7)(q31)
4	AML/M1	47,XX,+11
5	MDS-AML/M1	not available
6	MDS-AML/M1	46,XY,t(3;7;10)(q27;p?;p?),del(7)q31
7	AML/M2	not available
8	AML/M2	47,XX,add(12)(q23),+mar
9	AML/M2	46,XX
10	AML/M2	not available
11	AML/M2	46,XX,t(8;21)(q22;q22)/47,idem,+15
12	AML/M2	46,XY,t(8;21)(q22;q22)
13	AML/M2	46,XX,t(8;21)(q22;q22)
14	AML/M2	46,XY,t(8;21)(q22;q22)
15	AML/M3	46,XY,t(15;17)(q22;q21)
16	AML/M3	46,XY,t(15;17)(q22;q21)
17	AML/M3	46,XY,t(11;17)(q23;q21)
18	AML/M3	46,XY,t(15;17)(q22;q21)
19	AML/M4eo	46,XY
20	AML/M4	46,XY,t(4;16)(q25;q22)
21	AML/M4	not available
22	AML/M4	not available
23	AML/M4-M5	not available
24	AML/M5	not available
25	AML/M5a	45,XY,del(7),−16
26	AML/M6	46,XY
27	AML/M6	not available
28	CML blast crisis	45,XX,−7,t(9;22)(q34;q11)
29	leukemic mantle cell lymphoma	46,XY
30	ALL	46,XY,del(12)(p13;pter)/46,XY
31	ALL	46,XX

Leukemias were classified according to FAB classification (Bennett et al., 1985). MDS, myelodisplastic phase preceding AML; ALL, acute lymphocytic leukemia. Cases with no detectable aberrations by conventional karyotyping were also negative for the fusion genes PML/RARα, CBFβ/MYH11, DEK/CAN, BCR/ABL, and MLL rearrangements.

[a] 45,X,inv(Y)(p11q11),−3,del(5)(q15q35),−7,der(12),−14,del(15)(q24q26),der(17),−18,−20,+4 mar.

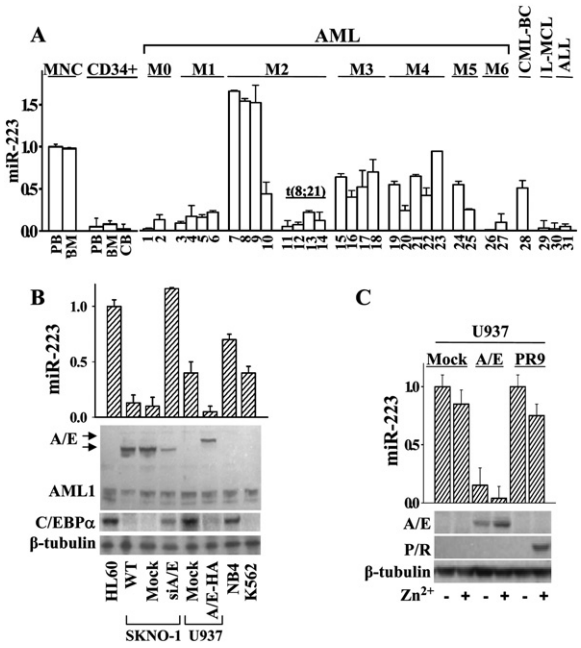

Figure 1. MiR-223 Levels in Human Hematopoietic Cells and in Leukemias

(A) Relative qRT-PCR quantization of miR-223 level in mononucleated cells (MNC) and CD34+ hematopoietic progenitors isolated from healthy donors PB, BM, CB, and from 31 leukemia patients classified by FAB (Bennett et al., 1985), which relies on blasts morphologic and cytochemical characteristics (Table 1). L-MCL and ALL are PB blasts from a leukemic mantle cell lymphoma and two acute lymphocytic leukemia patients, respectively.

(B and C) Upper panels: Relative quantization of miR-223 expression levels in the indicated leukemia cell lines. SKNO-1 wild-type cells (WT), SKNO-1 cells infected with a lentiviral empty vector (Mock), and SKNO-1 cells infected with a lentiviral vector expressing siRNAs against the fusion region of the AML1/ETO mRNA (siA/E). U937 cells stably transfected with an empty vector (Mock), HA-tagged AML1/ETO (A/E-HA), or the PML/RARα (PR9) cDNAs. The results represent the average of three independent evaluations ± SD. Lower panels: Immunoblot analysis for the detection of AML1 and AML1/ETO (A/E) with an anti-AML1 antibody. The increased molecular weight of the AML1/ETO product in A/E-HA cells in respect to SKNO-1 cells is due to the HA-tagged domain of the vector. The PML/RARα and C/EBPα protein were detected with the anti-RARα and anti-C/EBPα antibodies, respectively. The level of β-tubulin visualized the equal amount of protein loading. ZnSO4 treatment (100 μM) was used to increase the expression of AML1/ETO and PML/RARα products in U937 cells.

chromosomal translocation t(8;21) generating the AML1/ETO fusion product (Figure 1A).

In analogy to primary AML blasts, miR-223 was expressed at the highest levels in the AML-M2 HL60 cell line (Dalton et al., 1988), while low levels of miR-223 were measurable in the t(8;21)-AML-M2 cell line SKNO-1 constitutively expressing the AML1/ETO oncoprotein (Fazi et al., 2007) (Figure 1B). The NB4, U937, or K562 cell lines derived from patients respectively presenting AML-M3, AML-M5, or a CML-BC expressed miR-223 levels that were lower than HL60 but significantly higher than in SKNO-1 cells (Figure 1B).

We next infected SKNO-1 cells with a siRNA lentiviral construct knocking down the AML1/ETO product (SKNO-1 siA/E cells). This strongly increased the endogenous levels of miR-223 in respect to those measurable in SKNO-1-wild-type (WT) or -Mock cells (Figure 1B). Moreover, we ectopically expressed an HA tagged AML1/ETO cDNA in U937 cells (U937-A/E-HA) in a stable or zinc-inducible manner. In these cells, the expression levels of miR-223 were strongly reduced relative to U937-Mock cells (Figures 1B and 1C). No effect on miR-223 expression was exerted by the expression in U937 cells of PML/RARα, the AML-M3-associated fusion oncoprotein (Figure 1C). These results suggested that the AML1/ETO fusion product specifically triggers the transcriptional silencing of miR-223.

AML1/ETO Oncoprotein Localizes at an AML1-Binding Site on the *pre-miR-223* Gene Affecting Its Transcriptional Regulation

AML1/ETO is the fusion product of the t(8;21) translocation, the most common karyotypic abnormality of AML, which is detected in about 15% of total cases and in up to 40% of the FAB AML-M2 subtype. Expression of AML1/ETO in hematopoietic stem/precursor cells dramatically expands myeloid progenitors in vitro causing preleukemic myeloproliferative disorder in vivo. AML1/ETO maintains the ability of AML1 to bind the consensus sequence TGT/cGGT on target gene promoters and acts as a dominant-negative repressor of AML1 target genes, including *c-fms*, *GM-CSF*, *p14^{ARF}*, and the *retinoic acid receptor β* among others (Linggi et al., 2002; Frank et al., 1995; Zhang et al., 1994; Fazi et al., 2007; Nimer and Moore, 2004; Hess and Hug, 2004).

A bioinformatic search showed the presence of a putative AML1 binding site at the 5′ end of the predicted "core-promoter" sequence on the *pre-miR-223* upstream region (Zhou et al., 2007). By chromatin immunoprecipitation (ChIP) assay we investigated the in vivo localization of the AML1/ETO protein constitutively present in SKNO-1 cells or ectopically expressed in U937 cells at the AML1-binding site on the *miR-223* gene. We found that DNA sequences containing the AML1-binding site are immunoprecipitated by an α-AML1 antibody (Figures 2A and 2B, oligo1). Since these myeloid cell lines express the wild-type AML1, the AML1/ETO occupancy of this chromatin region was indicated by the detection of ETO immunocomplexes in SKNO-1 and U937-A/E-HA cells, but not in U937-Mock cells (Figures 1B and 2B). ChIP analysis performed with an α-HA antibody to distinguish the AML1/ETO-HA fusion protein, expressed by U937-A/E-HA cells from the endogenous AML1 or ETO products, confirmed the presence of AML1/ETO at this AML1 target site. The specificity of these interactions was indicated by their absence if distal sequences on *miR-223* gene lacking the AML1-binding sites were amplified in the same samples (Figures 2A and 2B oligo2). These findings suggested that the AML1 site on the *pre-miR-223* "core-promoter" sequence is a molecular target for the AML1/ETO oncoprotein in vivo.

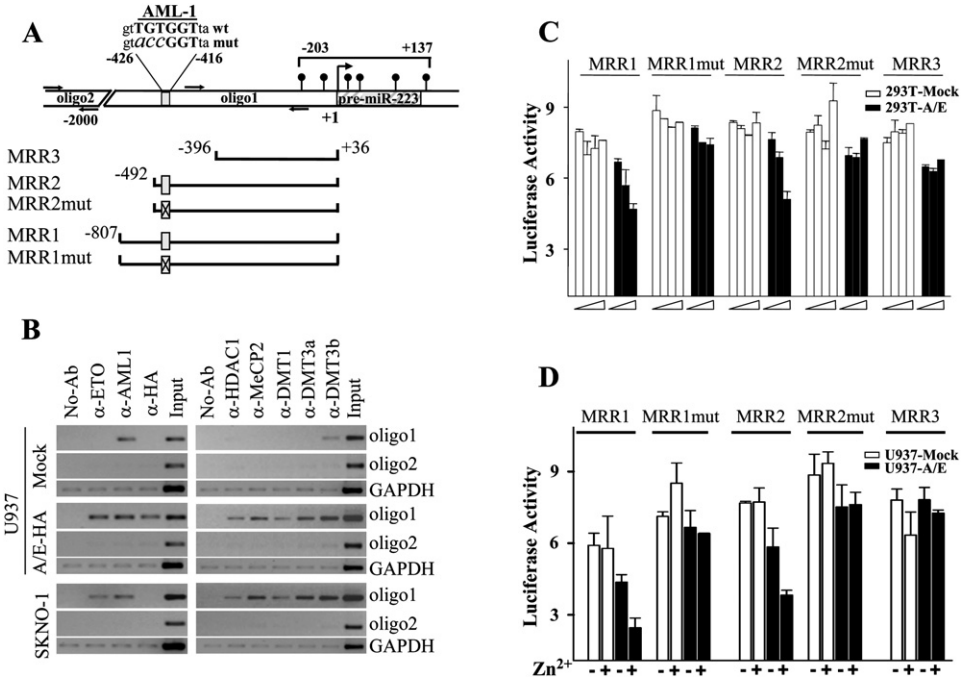

Figure 2. The AML1/ETO Oncoprotein Acts on the AML1 DNA-Binding Site on the *pre-miR-223* Upstream Sequence

(A) Schematic representation of the AML1 site (nt −426 to −416) and of the distribution of the CpG dinucleotides (black circles) (nt −203 to +137) along the *miR-223* gene. Numbers are the nucleotides relative to the 5′ end of the *pre-miR-223* (+1). Arrows indicate the location of the primers used in ChiP assay.

(B) Chromatin was immunoprecipitated using the indicated antibodies or in absence of antibody (no-Ab). PCR was performed by using oligo1 primers designed to amplify DNA sequences surrounding the AML1-binding site and the CpGs on *pre-miR-223* gene. Oligo2 primers (A) were designed for the amplification of a distal region on *miR-223* gene lacking the AML1 site to evaluate the specificity of protein binding. Input shows the amplification from sonicated chromatin. Amplification of GAPDH DNA was a control for nonspecific precipitated sequences.

(C) Human 293T cells were transiently cotransfected for 48 hr with luciferase reporter vectors containing the sequence of the *miR-223* regulatory regions (MRRs showed in [A]), and increasing amounts (10, 50, and 100 ng) of pcDNA3 vectors containing (293T-A/E) or not (293T-Mock) HA-tagged-AML1/ETO cDNAs.

(D) MMR luciferase reporter vectors were transiently transfected for 48 hr into U937 cells expressing a HA-tagged-AML1/ETO in a stable or zinc-inducible manner (U937-A/E) or an empty vector (U937-Mock) cells. ZnSO4 treatment (100 μM) was used to increase the expression of AML1/ETO. The data are expressed as activity relative to that of the empty pGL2-LUC vector alone. A cotransfected Renilla Luciferase vector pRL-SV40 was used as an internal control for normalization of the luciferase activity in each sample. The results shown are the average of three independent evaluations ± SD.

We therefore addressed the transcriptional regulatory functions of AML1/ETO product on miR-223 expression. Luciferase reporter constructs containing different portions of the *pre-miR-223* regulatory region (MRR) surrounding the AML-1 site (schematically represented in Figure 2A) were cotransfected with increasing amounts of expression plasmids encoding for the AML1/ETO product (A/E) or for the empty vector (Mock) into 293T cells. The same MRR reporter vectors were also transfected into U937-Mock and U937-A/E cells, which have a stable expression of the AML1/ETO protein that can be further induced by zinc. In both 293T and U937 cells, the expression of AML1/ETO caused a dose-dependent decrease in the activity of the MRR1 and MRR2 constructs, both presenting the putative AML1 site on *pre-miR-223*, but not of the MRR3 lacking this binding site.

Notably, the luciferase activity of the MRR1 mut and the MRR2 mut vectors, both mutated in the AML1-binding site was not modified by AML1/ETO presence (Figures 2C and 2D), thus showing the contribution of this site to the AML1/ETO- dependent silencing of *miR-223*.

AML1/ETO Triggers the Heterochromatic Silencing of *miR-223* Genomic Regions

The oncogenic properties of AML1/ETO are linked to its ability to form oligomeric complexes with increased affinity for histone deacetylase (HDAC) and DNA methyltransferases (DNMTs) rendering AML1/ETO a potent transcriptional repressor (Liu et al., 2005, 2006; Fazi et al., 2007). DNMTs methylate the cytosine within CpG dinucleotides (CpGs), frequently gathered in clusters (“CpG islands”) (Jaenisch and Bird, 2003; Jones and Baylin, 2007). Methylated CpGs recruit DNA-methyl CpG-binding proteins (MeCPs and MBDs). Often, DNMTs, MeCPs, and MBDs are associated with other chromatin remodeling activities including HDACs (Jaenisch and Bird, 2003; Jones and Baylin, 2007; Klose and Bird, 2006). However, it has been shown that genomic underrepresented and randomly

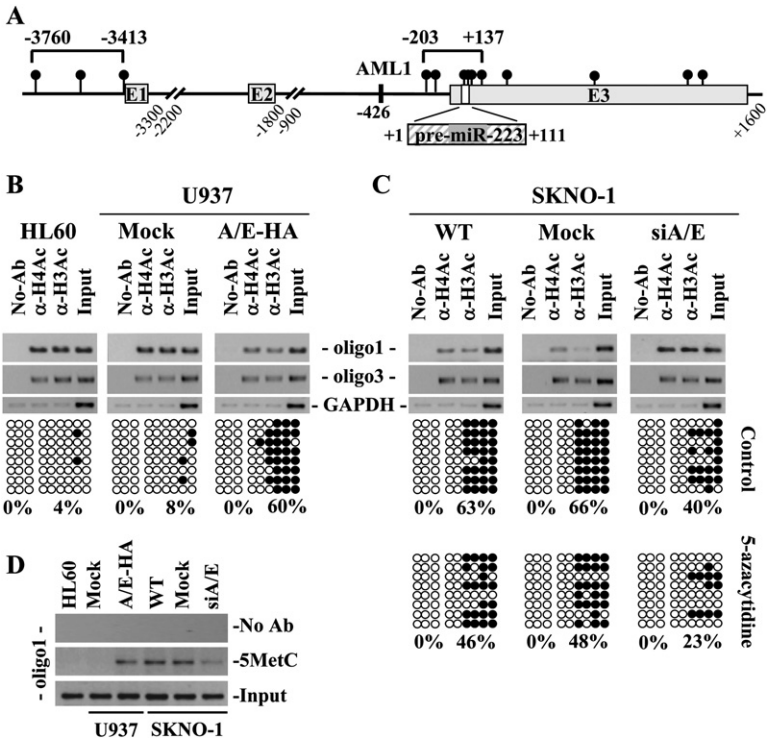

Figure 3. Epigenetic Status of *miR-223* Gene in AML1/ETO-Positive Cells

(A) Schematic representation of the genomic structure of human *miR-223* gene as reported by the UCSC Genome Browser website (http://genome.ucsc.edu/). The location of the exon sequences (E), the AML1-binding site, and the CpG dinucleotides (indicted as black circles along nt −203 to +137 and nt −3760 to −3413) on the miR-223 gene are numbered relative to the 5′ end of the *pre-miR-223* (nt +1 to +111).

(B and C) Upper panels: ChIp assays performed in the indicated cell lines using antibodies specific for the acetyl-H4 and acetyl-H3 forms or (D) for the 5-methylcytosine (5MetC). PCR amplifications were performed using oligo1, designed to amplify DNA sequences surrounding the AML1-binding site and the nearby CpGs (described in Figures 2A and 2B), and oligo 3 designed to amplify the 5′ end upstream region of *miR-223* gene (nt −3514 to −3300). Lower panels: Genomic bisulfite sequencing assay was performed to detect the methylation status of the three CpG dinucleotides dispersed along nt −3760 to −3413 (plotted as circles on the left side of each methylation subpanel) and the six CpG dinucleotides clusterized along nt −203 to +137 of *miR-223* gene sequence (circles on the right side of each methylation subpanel). Black circles and empty circles represent methylated and unmethylated CpG dinucleotides, respectively. Cells were also treated or not with 1 μM 5-azacytidine for 40 hr. For each sample, the percentages of global methylation level of these regions on the *miR-223* gene are indicated.

distributed CpG dinucleotides can act as hotspots for aberrant methylation and gene silencing (Santoro et al., 2002).

ChIP analysis revealed the presence of DNMT1, DNMT3a, DNMT3b, MeCP2, and HDAC1 at the *pre-miR-223* chromatin regions occupied by AML1/ETO in U937-A/E-HA and SKNO-1 cells, whereas only a faint DNMT3 reactivity was detectable at this site in U937-Mock cells (Figure 2B). We therefore investigated if the aberrant recruitment of HDAC1, DNMTs, and MeCP2 activities by AML1/ETO modifies nucleosomal histone tails and DNA methylation status on the *pre-miR-223* upstream sequence (Figure 3A). We performed ChIP analysis using antibodies recognizing the acetylated forms of histone H3 and H4 and PCR amplification of *pre-miR-223* upstream regions adjacent the AML1 site. At this chromatin region, H3 and H4 histones are hyperacetylated in HL60 and U937-Mock cells, while decreased acetylation levels are measurable in both U937-A/E and SKNO-1 cells (Figures 3B and 3C). The reduced histone acetylation in AML1/ETO-expressing samples suggested a hindered transcription at these chromatin sites on the *pre-miR-223* gene (Klose and Bird, 2006). Moreover, ChiP assay performed with an α-5′-methylcytosine antibody to immunoprecipitate sonicated naked DNA showed that cytosines on the DNA region near the AML1 site on *pre-miR-223* gene are methylated in both SKNO-1 and A/E-HA cells, but not in Mock or HL60 cells (Figure 3D). Notably, along a 340 bp sequence (nt −203 to +137) containing *pre-miR-223*, six CpG dinucleotides are all assembled in the upstream, body, and downstream regions of the *pre-miR-223* sequence at a distance of one or two nucleosomes from the AML1 site, while only four sparse CpGs were present within about 1500 bp downstream from this region, as schematically represented in Figure 2A. Interestingly, genomic bisulfite sequencing showed a higher frequency of methylated CpG dinucleotides encompassing the endogenous *pre-miR-223* gene sequences in U937-A/E-HA (60%) and in SKNO-1 cells (63%) as compared to Mock (8%) or HL60 (4%) cells, confirming the basal hypermethylated status of these CpGs in AML1/ETO-positive cells (Figures 3B and 3C). Notably, in U937-siA/E cells in which the knockdown of AML1/ETO reactivated miR-223 expression (Figure 1B, 4A), histone H3 and H4 were hyperacetylated and the CpGs methylation level was decreased (40%) at these sites on *pre-miR-223* gene (Figure 3C).

While this paper was in preparation, Fukao et al. (2007) identified a conserved promoter region located at about 3400 bp relative to the 5′ end of the *pre-miR-223* (Figure 3A). The sequence analysis of this region revealed the presence of three dispersed CpG dinucleotides (Figure 3A). Bisulfite genomic sequencing demonstrated that these CpGs are constitutively unmethylated in human myeloid cell lines and that their methylation status is not changed either in the presence or in the absence of the AML1/ETO fusion protein (Figures 3B and 3C). Accordingly, ChIP analysis showed that the histones H3 and H4 acetylation status at this chromatin site did not change in relation to AML1/ETO expression (Figures 3B and 3C).

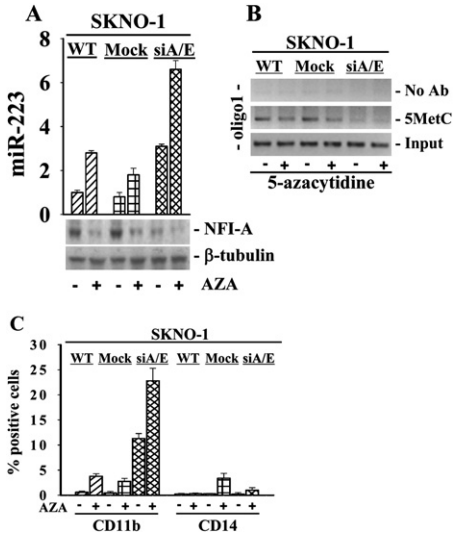

Figure 4. Enhancement of microRNA-223 Levels by siAML1/ETO and 5-azacytidine Treatment Restores Myeloid Differentiation of SKNO-1 Cells

(A) SKNO-1 cells (WT, Mock, and si-A/E), were treated or not with 1 μM 5-azacytidine (AZA) for 40 hr. MiR-223 relative expression levels were evaluated by qRT-PCR. Immunoblot analysis was performed using an anti-NFI-A antibody. The immunodetection of β-tubulin was used as loading control.

(B) ChIP assay performed with the anti-5-methylcytosine (5MetC) antibody and the oligo1 or primers.

(C) Effect of 40 hr treatment with 5-azacytidine on the percentage of cells positively stained for CD11b and CD14 surface markers as measured by FACS analysis. The results represent the average of three independent evaluations ± SD.

Of note, the DNA sequence of this upstream regulatory region (Fukao et al., 2007) also lacked a putative AML1-binding site as revealed by bioinformatic searches performed with the MatInspector Professional and the Transfac softwares. Thus, the chromatin remodeling complex aberrantly formed by AML1/ETO and the hypermethylation of the small CpG-cluster present in a close vicinity to the *miR-223* "core promoter region" containing the AML1-binding site appear to be a key mechanism for transcriptional gene silencing of *miR-223*. Whether methylation at this site could be associated to the tissue-specificity of *miR-223* gene is an interesting question arising from the recent work from Zhang et al., (2006), which requires a more in depth investigation in the human hematopoietic system.

Demethylating Treatment, RNAi against AML1/ETO, or Ectopic miR-223 Expression Enhances miR-223 Level and Restores Blasts Differentiation

We next treated the AML1/ETO-positive SKNO-1 cells with the DNMT inhibitor 5-azacytidine. This demethylating drug (1) increased by about 2- to 3-fold miR-223 expression (Figure 4A), (2) decreased both the ability of the α-5′-methylcytosine antibody to immunoprecipitate naked DNA at chromatin sites surrounding the AML1 site on *pre-miR-223* gene (Figure 4B) and the methylation status

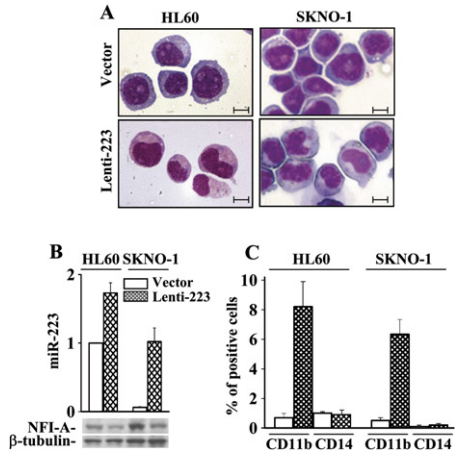

Figure 5. Ectopic miR-223 Expression Reprograms Myeloid Differentiation in SKNO-1 and HL60 Myeloid Leukemia Cells

HL60 and SKNO-1 cells were infected with a lentiviral vector expressing miR-223 (Lenti-223, hatched bars) or with the empty lentiviral vector (Vector, white bars).

(A) Changes in morphology by light-field microscopy of Wright-Giemsa stained cells (Scale bars, 5 μm).

(B) Relative miR-223 expression levels as evaluated by qRT-PCR. Immunoblot analysis was performed using an anti-NFI-A antibody. The immunodetection of β-tubulin was used as loading control.

(C) Percentage of cells positively stained for CD11b and CD14 myeloid surface markers as measured by FACS analysis. The results represent the average of three independent evaluations ± SD.

of endogenous *pre-miR-223* CpGs (from 63% to 46% of 5-methylcytosine) (Figure 3C), (3) decreased the accumulation of the NFI-A protein, a recognized target of miR-223 action (Fazi et al., 2005), thus indicating that the demethylating action of 5-azacytidine is able to restore a functional endogenous mature miR-223 (Figure 4A), and (4) induced granulocytic maturation of the cells as indicated by the increased expression levels of the myeloid differentiation marker CD11b, but not of the monocytic marker CD14 (Figure 4C). Interestingly, in si-A/E cells miR-223 re-expression reduced the protein levels of its target NFI-A and increased the percentage of cells expressing the myeloid differentiation marker CD11b (Figures 4A and 4C). Treatment of siA/E cells with 5-azacytidine affected either methylation or phenotypic changes with respect to those measurable in untreated cells (Figures 4B, 4C, and 3C), further linking AML1/ETO expression, heterochromatic transcriptional silencing of *miR-223* to the differentiation block present in t(8;21) AML blasts.

In agreement with this evidence, stable ectopic expression of miR-223 in SKNO-1 cells obtained by infection with the lenti-223 vector reduced the accumulation of the NFI-A product and induced granulocytic maturation as measured by morphology (showing chromatin condensation with nuclear segmentation, decreased nuclear/cytoplasmic ratio, decreased cytosolic basophilia, appearance of paranuclear Golgi region, and appearance of specific granules), expression of myeloid surface differentiation marker CD11b (Figure 5) and by NBT reduction assay (data not shown).

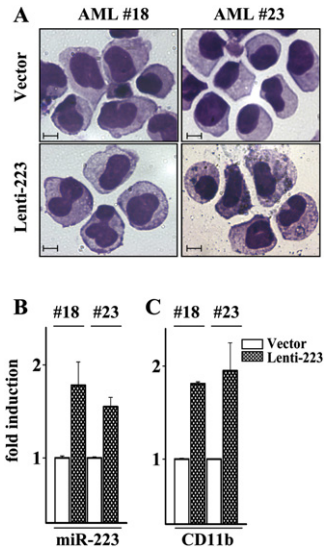

Figure 6. Ectopic miR-223 Expression Reprograms Myeloid Differentiation in Primary Blasts from Acute Myeloid Leukemia Patients

Fresh primary blasts were isolated from the peripheral blood of two newly diagnosed AML patients (18 and 23 of Table 1), showing an initial percentage of circulating blasts greater than 95%. Blasts were infected (Lenti-223, hatched bars) with the lentiviral vector expressing miR-223 or with the empty lentiviral vector (Vector, white bars). Afterwards, cells were cultured for a week and collected for morphological, immunophenotypic, and miR-223 expression level evaluation. (A) Changes in morphology by light-field microscopy of Wright-Giemsa stained cells (scale bars, 5 μm). (B) The values indicate the miR-223 expression level in primary AML blasts ectopically expressing the Lenti-223 versus that measured in the same blasts infected with the empty vector as evaluated by qRT-PCR. (C) Ratio of the CD11b myeloid differentiation antigen expression levels in Lenti-223 primary AML blasts versus that measured in empty vector infected blasts by quantitative FACS analysis The results represent the average of two independent evaluations ± SD.

The AML1/ETO knocking down by siRNAs appears to have a stronger effect in restoring SKNO-1 cell differentiation than ectoptic miR-223 expression, as indicated by the percentage of CD11b-positive cells (Figure 4C and 5C). This may suggest that the silencing of miR-223 expression by AML1/ETO only accounts for part of the differentiation block caused by AML1/ETO. Supporting this hypothesis, the expression of the CCAAT/enhancer binding protein alpha (C/EBPα) product in SKNO-1 siA/E cells is restored (Figure 1B). C/EBPα is a key transcriptional regulator of granulocytic differentiation of myeloid precursor (Radomska et al., 1998), which is indirectly silenced by AML1/ETO via protein-protein interaction blocking the positive autoregulatory regulation of *C/EBPα* own promoter (Pabst et al., 2001).

We recently described the transcriptional activation of *C/EBPα* and posttranscriptional regulation of NFI-A by miR-223 as essential for granulocytic differentiation response of acute promyelocytic leukemia blasts to the differentiating agent retinoic acid (Fazi et al., 2005). In the same study, we also reported granulocytic differentiation in miR-223-transduced acute promyelocytic leukemia patient-derived NB4 cells carrying the t(15:17) chromosomal translocation and expressing the PML/RARα fusion product (Fazi et al., 2005). Here, we show that, when engineered with the lenti-223 to overexpress the miR-223, the human myeloblastic HL60 cell line, which do not carry oncogenic fusion products, also entered a granulocytic pathway of differentiation (Figure 5).

Moreover, the infection of fresh primary blasts isolated from the peripheral blood of two consecutive newly diagnosed acute myeloid leukemia patients (18 and 23 of Table 1) with a lentiviral vector expressing miR-223, increased the expression level of miRNA-223 of about 1.6- to 1.8-fold after a week of culture. This induction resulted in primary blast granulocytic differentiation as shown by morphology and by the increased expression (about 2-fold) of the immunophenotypic myeloid differentiation marker CD11b, but not of CD14 (Figure 6 and data not shown). This indicates that the levels of miR-223 expression are critical for the development of the granulocytic differentiation program and that titrated miR-223 expression can reprogram myeloid differentiation in different leukemia subtypes independently from the presence of a specific genetic lesion.

Cancer is a genetic and epigenetic disease (Jones and Baylin, 2007; Zardo et al., 2002). Compelling evidence indicates a role for genetic alteration in the initiation and progression of tumors. The deregulation of epigenetic mechanisms of gene expression, such as hypermethylation of promoter and coding sequences, is also a key oncogenic mechanism for the inactivation of tumor suppressors in a wide range of tumor types. Heterochromatic gene silencing can represent an alternative oncogenic mechanism to gene mutation or deletion for the transcriptional repression of tumor suppressor genes (Zardo et al., 2002; Baylin and Ohm, 2006; Jones and Baylin, 2007). Tumor suppressor or oncogenic activities have been recently proposed for miRNAs (Chen, 2005; Hammond, 2006; Calin and Croce, 2006; Saito et al., 2006).

Here, we show that the heterochromatic silent state of genomic regions generating a miRNA, the *miR-223* gene, whose activity is linked to the differentiation fate of myeloid precursors is triggered by the expression of AML1/ETO, the oncogenic fusion product of the most frequent chromosomal translocation in AML. AML1/ETO targets the *miR-223* due to its interaction with the AML1 site at the *pre-miR-223* upstream region where it recruits HDAC and DNMT activities that deacetylate histone proteins and methylate CpGs. Newly methylated CpGs act as docking sites for the DNA-methyl CpG-binding protein MeCP2. Through changes in chromatin conformation, the AML1/ETO-associated complex resets the *miR-223* gene to a repressed ground state contributing to the differentiation block of myeloid precursors (Figure 7). Of note, that either ectopic miR-223 expression, downregulation of AML1/ETO protein levels, or the use of demethylating agents reactivate miR-223 expression and restore myeloid differentiation in t(8;21)-AML blasts. Preliminary immunophenotypic data obtained on primary blasts from

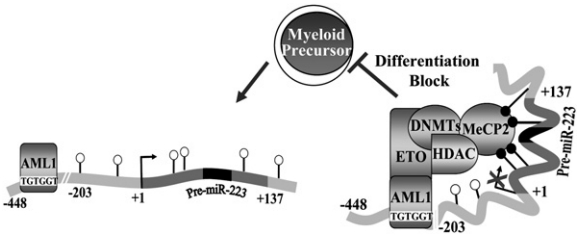

Figure 7. Schematic Model for the Heterochromatic Silencing of miR-223 Gene by AML1/ETO

In myeloid precursors, the occupancy of the AML1-binding site (TGTGGT) on the *pre-miR-223* promoter by AML1 is associated with a chromatin status permissive for transcription. The AML1/ETO oncoprotein targets this binding site, where it aberrantly recruits HDAC, DNMT and MeCP2 activities that deacetylate histone proteins and methylate CpGs. This produces a chromatin packaging nonpermissive for *miR-223* transcription, which contributes to the differentiation block of AML1/ETO+ myeloid precursors. White and black circles indicate the unmethylated and methylated CpG dinucleotides, respectively. Dark gray marks the *pre-miR-223* region, while that encoding the miR-223 mature form is marked in black. Numbers are the nucleotides relative to the 5′ end of the *pre-miR-223* (+1).

a single AML1/ETO-positive patient (row 14 of Table 1) also supported the ability of either the AML1/ETO knockdown by siRNAs or the ectopic miR-223 expression to reprogram primary leukemia cells into a granulocytic pathway of differentiation (data not shown).

This evidence establishes an important relationship between aberrant heterochromatic silencing of a tissue and developmental stage-specific miRNA transcription and differentiation block of leukemia. Suppression of a miRNA gene also carries the potential to greatly expand the fusion protein oncogenic activity since miRNA represses the expression of multiple target proteins.

The relevance of the *miR-223* silencing is also highlighted by the consequences of its ectopic expression that alone is sufficient to reprogram the myeloid differentiation program in distinct myeloid leukemia subtypes. This suggests deregulated miRNA production as a common pathway required for the differentiation block underlying myeloid leukemia pathogenesis and reveals miRNAs as additional molecular targets for therapeutic intervention in cancer.

EXPERIMENTAL PROCEDURES

Clinical Samples

The study was approved by the local internal review boards and ethic committees. Written informed consent was obtained from each subject. Normal mononuclear cells and CD34+ cells were isolated from the BM, PB, or CB of healthy donors as reported (Fazi et al., 2007). Leukemia blasts were obtained from the BM and/or PB of 31 leukemia patients. Cases were classified according to the FAB classification and showed an initial percentage of circulating blasts greater than 60% (Bennett et al., 1985). Blasts isolation and molecular analysis to detect the AML-associated fusion genes were performed as described (Fazi et al., 2007).

Cell Lines and Cell Cultures

HL60, NB4, K562, U937, U937-A/E-HA clone 9, U937-PR9, SKNO-1, and SKNO-1-siA/E-RNA cell lines were maintained in RPMI 1640 medium supplemented with 50 μg/ml streptomycin, 50 IU penicillin, and 10% FCS as described (Drexler et al., 1999; Grignani et al., 1993; Fazi et al., 2005, 2007). Primary AML blasts were cultured in IMDM medium supplemented with 50 μg/ml streptomycin, 50 IU penicillin, and 20% FCS. The lentiviral vector Lenti-223 was used for the ectopic induction of the miR223 into myeloid cell lines (SKNO-1 and HL60) and primary blasts to generate the Lenti-223 cells (Fazi et al., 2005). Cells were infected and purified by fluorescence activated cell sorting as reported (Fazi et al., 2005). Treatment with 5-azacytidine (Sigma-Aldrich, Milan, Italy) was performed at a concentration of 1 μM for 40 hr. Human embryonic kidney 293T cells were cultured in DMEM medium supplemented with 50 μg/ml streptomycin, 50 IU penicillin, and 10% FCS.

RNA Extraction and Analysis

Total RNA was extracted from cells using the TRIzol RNA isolation system (Invitrogen). The relative quantity of miR-223 was measured on 200 ng of total RNA by qRT-PCR using the *mir*-Vana Detection Kit (Ambion, Applied Biosystem, Milan) in the ABI PRISM 7000 Sequence Detection System (Applied Biosystem), and it was determined by the comparative C_T method using snRNA U6 levels for normalization as recommended by the manufacturer's instructions.

Immunoblot Assays

Immunoblot assays were performed on total cell lysates (50 μg) using the rabbit polyclonal antibodies anti-AML1/RHD (Oncogene Science), anti-RARα (Santa Cruz Biotechnology, Santa Cruz, CA), anti-NFI-A (Abcam, Cambidge, UK), or the anti-C/EBPα (Santa Cruz Biotechnology). The anti-β-tubulin mouse monoclonal IgG (Sigma-Aldrich) was used to normalize the amount of the samples analyzed. The immunoreactivity was determined by the ECL method (Amersham Biosciences).

Transactivation Assays

DNA fragments from nt −807 (MRR1) or nt −492 (MRR2) or nt −396 (MRR3) to nt +36 relative to the *pre-miR-223* were PCR amplified from human genomic DNA using the forward primers 5′-GGGCACTTTAATAGCTGCCA-3′ or 5′-GGTTGCCTAACTAGCTAATG-3′ or 5′-GAATTGAGAAGAGGGAGCAA-3′, respectively, coupled with the reverse primer 5′-TCAAATACACGGAGCGTGG-3′. All the PCR fragments were inserted in the pGL2-LUC reporter vector (Promega). The MRR1, MRR2, and MRR3 constructs were used to generate the MRR1-, MRR2-, and MRR3-mut plasmids in which the 5′-TGTGGT-3′ direct motif of the AML1 site was mutated to 5′-*ACC*GGT-3′. To generate the mutations the QuikChange Site-Directed Mutagenesis Kit (Stratagene) was used according to manufacturer instructions. Human embryonic kidney 293T cells (2×10^5) were plated in 12-well plates and transiently cotransfected by the Lipofectamine Reagent method (Invitrogen) with 10, 50, or 100 ng of the pcDNA3 vectors containing or not the HA-tagged-AML1/ETO cDNAs (Fazi et al., 2007), 300 ng of the LUC reporter constructs described above. U937-Mock and U937-A/E cells were pretreated or not with 100 μM ZnSO4 (16 hr) and then plated (5×10^5/well) in 24-well plates. Cells were transiently transfected by the FuGENE reagent (Roche, Mannheim, Germany) with 1.5 μg of the LUC reporter constructs described above. A cotransfected pRL-SV40 Renilla Luciferase reporter vector (Promega) was used as an internal control for normalization of luciferase activity in each sample. Cells were harvested 48 hr posttransfection and assayed with Dual Luciferase Assay (Promega) according to the manufacturer's instructions.

Chromatin Immunoprecipitation Assay

The addition to cultured cells (2×10^6) of formaldehyde (1% final concentration) for 10 min at 37°C was used to crosslink the proteins to DNA. After sonication, the chromatin was immunoprecipitated overnight with 5 μl of the following antibodies recognizing AML1/RHD, ETO (Ab-1) (Oncogene Science), HA monoclonal (Babco, Richmond, CA), DNMT1 (New England BioLabs, Ipswich, MA), DNMT3a and DNMT3b (Abcam), HDAC1 (Santa Cruz Biotechnology), MeCP2,

acetyl-histone-H4, and acetyl-histone-H3 (Upstate Biotechnology, Lake Placid, NY). ChIP using the Cytosine (5-Methyl) (Abcam) antibody was performed on naked and sonicated DNA extracted from the same cell samples. A genomic *pre-miR-223* upstream gene region close to the putative AML1-binding site indicated by the MatInspector Professional (http://www.genomatix.de) and the TransFac software packages (http://www.gene-regulation.com/pub/programs.html), was amplified with the following primer sequences designed by the Primer Express software (Applied Biosystem): oligo1 (nt −400 to −186) forward 5′-GGGAGAATTGAGAAGAGGGA-3′ and oligo1 reverse 5′-GATAAG CAGGTAAAGCCCGA-3′. The other pre-miR-223 upstream regions were amplified with the following primer sequences: oligo2 (nt −2467 to −2272) forward 5′-TCTGGGATTTTTAGGCATGG-3′ and oligo2-reverse 5′-AAGAGCGTCATCAAGCCACT-3′; oligo3 (nt −3514 to −3300) forward 5′-GCATCCAGATTTCCGTTGGCTAAC-3′ and oligo3-reverse 5′-GGCAAATGGATACCATACCTGTCA-3′. PCR for GAPDH was performed using the conditions and primers already described (Fazi et al., 2005).

Cell Differentiation

Cell differentiation was evaluated by light microscopy morphological examination of Wright-Giemsa-stained cytospins; nitroblue tetrazolium (NBT) dye reduction assay (at least 500 morphologically intact cells per experimental condition were counted and corrected for viability, measured by trypan blue exclusion method); direct immunofluorescence staining of cells using an allophycocyanin (APC)-conjugated mouse anti-human CD11b antibody; and a peridinin chlorophyll protein (PerCP)-conjugated mouse anti-human CD14 antibody (Becton Dickinson, San Jose, CA) as described (Fazi et al., 2005, 2007). A minimum of 50,000 events were collected for each sample by a FACScan flow cytometer (Becton Dickinson) using CellFit software (Becton Dickinson) for data acquisition and analysis.

Bisulfite Modification and Genomic Sequencing

The methylation status of the CpG dinucleotides within two regions (nt −203 to +137 and nt −3760 to −3413), relative to the 5′ end of the *pre-miR-223* gene, was analyzed. Bisulfite sequencing assay was performed on 2.5 μg of bisulfite-treated genomic DNA from HL60, U937 (Mock, A/E-HA), and SKNO-1 (WT, Mock, and siA/E) cell lines. After bisulfite conversion performed as previously described (Zardo et al., 2002), the fragments of interest were amplified using the following specific primer pairs: oligo1 forward 5′-AGTTTTTAGT TGAGTATTGGGTG-3′; oligo1 reverse 5′-CTTATATCCAACTAACAAT CCATTC-3′; oligo2 forward 5′-AATTTGTTTTGTGATATTGAGTATTT TT-3′; oligo2 reverse 5′-TACAAAAACCAAATAAAATTAAACTTTC-3′. PCR products were gel purified and cloned into the TOPO TA Cloning/pCR2.1 TOPO kit (Invitrogen). We subjected individual bacterial colonies to PCR using vector-specific primers (sequences available upon request), and the products were sequenced for the analyses of DNA methylation.

ACKNOWLEDGMENTS

This work was supported by grants from the Italian Association for Cancer Research (AIRC and AIRC-ROC); University of Roma "La Sapienza," Ministero dell'Istruzione dell'Università e della Ricerca (PRIN), and Ministero della Salute. We thank Drs. Pier Giuseppe Pelicci and Irene Bozzoni for expertise and reagents, Drs. Silvia Di Cesare and Fabrizio Padula for cell sorting and FACS analysis, Drs. Alberto Ciolfi and Laura Vian for experimental support and discussion. We also thank Sue Ellen Vignetti, M. Rita Mosini, and Sonia Buffolino for technical assistance.

Received: March 15, 2007
Revised: August 8, 2007
Accepted: September 20, 2007
Published: November 12, 2007

REFERENCES

Ambros, V. (2004). The function of animal miRNAs. Nature *431*, 350–355.

Bartell, D.P. (2004). MicroRNAs: Genomics, biogenesis, mechanism and function. Cell *116*, 281–297.

Baylin, S.B., and Ohm, J.E. (2006). Epigenetic gene silencing in cancer - a mechanism for early oncogenic pathway addiction? Nat. Rev. Cancer *6*, 107–116.

Bennett, J.M., Catovsky, D., Daniel, M.T., Flandrin, G., Galton, D.A., Gralnick, H.R., and Sultan, C. (1985). Proposed revised criteria for the classification of acute myeloid leukemia. A report of the French-American-British Cooperative Group. Ann. Intern. Med. *103*, 620–625.

Calin, G.A., and Croce, C.M. (2006). MicroRNA signatures in human cancers. Nat. Rev. Cancer *6*, 857–866.

Chen, C.-Z., Li, L., Lodish, H.F., and Bartell, D.P. (2004). MicroRNAs Modulate Hematopoietic Lineage Differentiation. Science *303*, 83–86.

Chen, C.Z. (2005). MicroRNAs as oncogenes and tumor suppressors. N. Engl. J. Med. *353*, 1768–1771.

Chen, C.Z., and Lodish, H.F. (2005). MicroRNAs as regulators of mammalian hematopoiesis. Semin. Immunol. *17*, 155–165.

Chen, J.F., Mandel, E.M., Thomson, J.M., Wu, Q., Callis, T.E., Hammond, S.M., Conlon, F.L., and Wang, D.Z. (2006). The role of microRNA-1 and microRNA-133 in skeletal muscle proliferation and differentiation. Nat. Genet. *38*, 228–233.

Cheng, L.C., Tavazoie, M., and Doetsch, F. (2005). Stem Cells From Epigenetics to microRNAs. Neuron *46*, 363–367.

Dalton, W.T., Jr., Ahearn, M.J., McCredie, K.B., Freireich, E.J., Stass, S.A., and Trujillo, J.M. (1988). HL-60 cell line was derived from a patient with FAB-M2 and not FAB-M3. Blood *71*, 242–247.

Drexler, H.G., Macleod, R.A., and Uphoff, C.C. (1999). Leukemia cell lines: In vitro models for the study of Philadelphia chromosome-positive leukemia. Leuk. Res. *23*, 207–215.

Fazi, F., Rosa, A., Fatica, A., Gelmetti, V., De Marchis, M.L., Nervi, C., and Bozzoni, I. (2005). A Minicircuitry Comprised of MicroRNA-223 and Transcription Factors NFI-A and C/EBPalpha Regulates Human Granulopoiesis. Cell *123*, 819–831.

Fazi, F., Zardo, G., Gelmetti, V., Travaglini, L., Ciolfi, A., Di Croce, L., Rosa, A., Bozzoni, I., Grignani, F., Lo-Coco, F., et al. (2007). Heterochromatic gene repression of the retinoic acid pathway in acute myeloid leukemia. Blood *109*, 4432–4440.

Frank, R., Zhang, J., Uchida, H., Meyers, S., Hiebert, S.W., and Nimer, S.D. (1995). The AML1/ETO fusion protein blocks transactivation of the GM-CSF promoter by AML1B. Oncogene *11*, 2667–2674.

Fukao, T., Fukuda, Y., Kiga, K., Sharif, J., Hino, K., Enomoto, Y., Kawamura, A., Nakamura, K., Takeuchi, T., and Tanabe, M. (2007). An evolutionarily conserved mechanism for microRNA-223 expression revealed by microRNA gene profiling. Cell *129*, 617–631.

Grewal, S.I., and Moazed, D. (2003). Heterochromatin and epigenetic control of gene expression. Science *301*, 798–802.

Grignani, F., Ferrucci, P.F., Testa, U., Talamo, G., Fagioli, M., Alcalay, M., Mencarelli, A., Peschle, C., Nicoletti, I., and Pelicci, P.G. (1993). The acute promyelocytic leukaemia specific PML/RARα fusion protein inhibits differentiation and promotes survival of myeloid precursor cells. Cell *74*, 423–429.

Hammond, S.M. (2006). MicroRNAs as oncogenes. Curr. Opin. Genet. Dev. *16*, 4–9.

Hess, J.L., and Hug, B.A. (2004). Fusion-protein truncation provides new insights into leukemogenesis. Proc. Natl. Acad. Sci. USA *101*, 16985–16986.

Jaenisch, R., and Bird, A. (2003). Epigenetic regulation of gene expression: How the genome integrates intrinsic and environmental signals. Nat. Genet. Suppl. *33*, 245–254.

Jones, P.A., and Baylin, S.B. (2007). The Epigenomics of Cancer. Cell *128*, 683–692.

Kim, V.N., and Nam, J.W. (2006). Genomics of microRNA. Trends Genet. *22*, 165–173.

Klose, R.J., and Bird, A.P. (2006). Genomic DNA methylation: The mark and its mediators. Trends Biochem. Sci. *31*, 89–97.

Linggi, B., Muller-Tidow, C., van de Locht, L., Hu, M., Nip, J., Serve, H., Berdel, W.E., van der Reijden, B., Quelle, D.E., Rowley, J.D., et al. (2002). The t(8;21) fusion protein, AML1 ETO, specifically represses the transcription of the p14(ARF) tumor suppressor in acute myeloid leukemia. Nat. Med. *8*, 743–750.

Liu, S., Shen, T., Huynh, L., Klisovic, M.I., Rush, L.J., Ford, J.L., Yu, J., Becknell, B., Li, Y., Liu, C., et al. (2005). Interplay of RUNX1/MTG8 and DNA methyltransferase 1 in acute myeloid leukemia. Cancer Res. *65*, 1277–1284.

Liu, Y., Cheney, M.D., Gaudet, J.J., Chruszcz, M., Lukasik, S.M., Sugiyama, D., Lary, J., Cole, J., Dauter, Z., Minor, W., et al. (2006). The tetramer structure of the Nervy homology two domain, NHR2, is critical for AML1/ETO's activity. Cancer Cell *9*, 249–260.

Mikkelsen, T.S., Ku, M., Jaffe, D.B., Issac, B., Lieberman, E., Giannoukos, G., Alvarez, P., Brockman, W., Kim, T.K., Koche, R.P., et al. (2007). Genome-wide maps of chromatin state in pluripotent and lineage-committed cells. Nature *448*, 553–560.

Nimer, S.D., and Moore, M.A. (2004). Effects of the leukemia-associated AML1-ETO protein on hematopoietic stem and progenitor cells. Oncogene *23*, 4249–4254.

Pabst, T., Mueller, B.U., Harakawa, N., Schoch, C., Haferlach, T., Behre, G., Hiddemann, W., Zhang, D.E., and Tenen, D.G. (2001). AML1-ETO downregulates the granulocytic differentiation factor C/EBPalpha in t(8;21) myeloid leukemia. Nat. Med. *7*, 444–451.

Radomska, H.S., Huettner, C.S., Zhang, P., Cheng, T., Scadden, D.T., and Tenen, D.G. (1998). CCAAT/enhancer binding protein alpha is a regulatory switch sufficient for induction of granulocytic development from bipotential myeloid progenitors. Mol. Cell. Biol. *18*, 4301–4314.

Saito, Y., Liang, G., Egger, G., Friedman, J.M., Chuang, J.C., Coetzee, G.A., and Jones, P.A. (2006). Specific activation of microRNA-127 with downregulation of the proto-oncogene BCL6 by chromatin-modifying drugs in human cancer cells. Cancer Cell *9*, 435–443.

Santoro, R., Li, J., and Grummt, I. (2002). The nucleolar remodeling complex NoRC mediates heterochromatin formation and silencing of ribosomal gene transcription. Nat. Genet. *32*, 393–396.

Tenen, D.G. (2003). Disruption of differentiation in human cancer: AML shows the way. Nat. Rev. Cancer *3*, 89–101.

Zardo, G., Tiirikainen, M.I., Hong, C., Misra, A., Feuerstein, B.G., Volik, S., Collins, C.C., Lamborn, K.R., Bollen, A., Pinkel, D., et al. (2002). Integrated genomic and epigenomic analyses pinpoint biallelic gene inactivation in tumors. Nat. Genet. *32*, 453–458.

Zhang, D.E., Fujioka, K., Hetherington, C.J., Shapiro, L.H., Chen, H.M., Look, A.T., and Tenen, D.G. (1994). Identification of a region which directs the monocytic activity of the colony-stimulating factor 1 (macrophage colony-stimulating factor) receptor promoter and binds PEBP2/CBF (AML1). Mol. Cell. Biol. *14*, 8085–8095.

Zhang, X., Yazaki, J., Sundaresan, A., Cokus, S., Chan, S.W., Chen, H., Henderson, I.R., Shinn, P., Pellegrini, M., Jacobsen, S.E., and Ecker, J.R. (2006). Genome-wide high-resolution mapping and functional analysis of DNA methylation in arabidopsis. Cell *126*, 1189–1201.

Zhao, Y., Samal, E., and Srivastava, D. (2005). Serum response factor regulates a muscle-specific microRNA that targets Hand2 during cardiogenesis. Nature *436*, 214–220.

Zhou, X., Ruan, J., Wang, G., and Zhang, W. (2007). Characterization and Identification of MicroRNA Core Promoters in Four Model Species. PLoS Comput. Biol. *3*, e37. 10.1371/journal.pcbi.0030037.

blood

2009 114: 1753-1763
Prepublished online Jun 19, 2009;
doi:10.1182/blood-2008-12-196196

NFI-A directs the fate of hematopoietic progenitors to the erythroid or granulocytic lineage and controls ²-globin and G-CSF receptor expression

Linda Marie Starnes, Antonio Sorrentino, Elvira Pelosi, Monica Ballarino, Ornella Morsilli, Mauro Biffoni, Simona Santoro, Nadia Felli, Germana Castelli, Maria Laura De Marchis, Gianfranco Mastroberardino, Marco Gabbianelli, Alessandro Fatica, Irene Bozzoni, Clara Nervi and Cesare Peschle

Blood (print ISSN 0006-4971, online ISSN 1528-0020), is published semimonthly by the American Society of Hematology, 1900 M St, NW, Suite 200, Washington DC 20036.

NFI-A directs the fate of hematopoietic progenitors to the erythroid or granulocytic lineage and controls β-globin and G-CSF receptor expression

*Linda Marie Starnes,[1,2] *Antonio Sorrentino,[3] Elvira Pelosi,[3] Monica Ballarino,[4] Ornella Morsilli,[3] Mauro Biffoni,[3] Simona Santoro,[3] Nadia Felli,[3] Germana Castelli,[3] Maria Laura De Marchis,[4] Gianfranco Mastroberardino,[5] Marco Gabbianelli,[3] Alessandro Fatica,[4] Irene Bozzoni,[4] Clara Nervi,[1,2] and Cesare Peschle[6]

[1]Department of Histology and Medical Embryology, University "La Sapienza," Rome; [2]San Raffaele Biomedical Park Foundation, Rome; [3]Department of Hematology, Oncology and Molecular Medicine, Istituto Superiore di Sanità, Rome; Departments of [4]Genetics and Molecular Biology and Istituto di Biologia e Patologia Molecolari (IBPM) and [5]Medicine, University "La Sapienza," Rome; and [6]Istituto di Ricovero e Cura a Carattere Scientifico (IRCCS) MultiMedica, Milan, Italy

It is generally conceded that selective combinations of transcription factors determine hematopoietic lineage commitment and differentiation. Here we show that in normal human hematopoiesis the transcription factor nuclear factor I-A (NFI-A) exhibits a marked lineage-specific expression pattern: it is upmodulated in the erythroid (E) lineage while fully suppressed in the granulopoietic (G) series. In unilineage E culture of hematopoietic progenitor cells (HPCs), NFI-A overexpression or knockdown accelerates or blocks erythropoiesis, respectively: notably, NFI-A overexpression restores E differentiation in the presence of low or minimal erythropoietin stimulus. Conversely, NFI-A ectopic expression in unilineage G culture induces a sharp inhibition of granulopoiesis. Finally, in bilineage E + G culture, NFI-A overexpression or suppression drives HPCs into the E or G differentiation pathways, respectively. These NFI-A actions are mediated, at least in part, by a dual and opposite transcriptional action: direct binding and activation or repression of the promoters of the *β-globin* and *G-CSF* receptor gene, respectively. Altogether, these results indicate that, in early hematopoiesis, the NFI-A expression level acts as a novel factor channeling HPCs into either the E or G lineage. (Blood. 2009;114:1753-1763)

Introduction

Hematopoietic stem cells (HSCs), endowed with extensive self-renewal potential and multilineage differentiation capacity, sustain the hematopoietic system throughout life.[1] HSCs generate undifferentiated hematopoietic progenitor cells (HPCs), which gradually lose their self-renewal ability. Multipotent common myeloid progenitors, the functional equivalent of colony-forming units of mixed type (CFU-mix) or CFU-GEMM, undergo progressive restriction of their lineage commitment, eventually separating into 2 major bipotent progenitor types: megakaryocyte-erythroid progenitor and granulocyte-monocyte progenitor. These progenitor types are responsible for producing unilineage progenitors for the erythroid (E), megakaryocytic (Mk), granulocytic (G), and monocytic (M) lineage, respectively, termed burst-forming unit (BFU-E) and CFU-E, BFU-Mk and CFU-Mk, CFU-G, and CFU-M. The unilineage HPCs, in turn, generate differentiated precursors, which eventually mature into terminal circulating blood cells.

Multiple hematopoietic genes, particularly transcription factors (TFs) and growth factor receptors, are promiscuously coexpressed in HSCs and HPCs, a phenomenon referred to as lineage priming.[2] Their coexistence grants differentiation flexibility and allows lineage fate commitment at the multipotent stage. Key lineage-restricted factors are characterized by a low level of expression in the undifferentiated state but become dominant in their specific lineages, whose development is thereby promoted while alternative cell fates are antagonized.[3]

Whereas GATA-1 and PU.1 represent a paradigm of lineage programming TFs driving the fate of HSCs/HPCs,[4-6] growing evidence indicates that other TFs play a pivotal role in the complex scenario of lineage specification.[7,8] In this regard, the TF Nuclear Factor I-A (NFI-A) acts as a transcriptional activator or repressor in a cell type and promoter-specific context.[9,10] NFI-A belongs to the NFI TF family consisting of 4 different genes that contain a highly conserved N-terminal DNA-binding/dimerization domain and a divergent C-terminal transactivation/repression domain, which confers unique functions to each member. NFI-A has a major role in brain development and shows a unique pattern of expression in the developing mouse beginning early on in the heart and brain with a broader tissue expression pattern as development progresses.[11] Recent studies showed that NFI-A is a relevant target of the myeloid regulator miR-223 in promyelocytic leukemia cells[12] and suppresses monocytic differentiation of HPCs,[13] whereas nothing is known on its role in normal erythro-granulopoiesis.

Two lineage-associated genes, *β-globin* and *G-CSFR*, are key determinants for the erythroid and granulocytic pathways, respectively. The human β-globin locus consists of 5 genes, including the embryonic ϵ, the fetal Gγ, Aγ, the adult δ, and β, which are sequentially activated during ontogeny: the transcriptional control of hemoglobin from embryonic to adult life is only partially understood[14,15] and involves complex DNA-protein and protein-protein interactions at *cis*-elements located in both proximal promoter regions and distal regulatory sequences.[16] Granulocyte

Submitted December 22, 2008; accepted May 14, 2009. March 31, 2009. Prepublished online as *Blood* First Edition paper, June 19, 2009; DOI 10.1182/blood-2008-12-196196.

*L.M.S. and A.S. contributed equally to this study.

The online version of this article contains a data supplement.

The publication costs of this article were defrayed in part by page charge payment. Therefore, and solely to indicate this fact, this article is hereby marked "advertisement" in accordance with 18 USC section 1734.

colony-stimulating factor (G-CSF), the main cytokine stimulator of the G pathway, binds to the G-CSF receptor (G-CSFR) to mediate activation of neutrophils and differentiation of their progenitors/precursors in the bone marrow.[17-19] In this study, we describe a central role of NFI-A in the human erythro-granulopoietic lineage decision and differentiation. In HPCs, NFI-A upmodulation favors the development of the E lineage and represses the G pathway, in part by direct transcriptional activation of β-globin and repression of G-CSFR.

Methods

Cell culture

Cord blood (CB) was obtained from healthy, full-term pregnancies according to institutional guidelines and with the approval of the University of Rome "La Sapienza." Informed consent was obtained in accordance with the Declaration of Helsinki. Human growth factors were purchased from PeproTech, human erythropoietin (Epo) was provided by Amgen.

$CD34^+$ collection, isolation, and unilineage cultures were performed as previously described.[20] In unilineage cultures, serum-free medium was supplemented with: Epo (3 U/mL), interleukin-3 (IL-3; 0.01 U/mL) and GM-CSF (0.001 ng/mL) for erythroid (E) and IL-3 (1 U/mL), GM-CSF (0.1 ng/mL), and G-CSF (500 U/mL) for granulocytic (G).

In bilineage E + G culture, serum-free medium was supplemented with IL-3 (1 U/mL), GM-CSF (0.1 ng/mL), Epo (0.6 U/mL), and G-CSF (500 U/mL).

Viable cells were counted every 2 to 3 days using Trypan Blue Staining (Sigma-Aldrich) and passaged at 2×10^5 cells/mL.

In clonogenic assay, 10^2 $CD34^+$ cells were plated in duplicate in serum-free medium containing 0.9% methylcellulose MethoCult H4100 (StemCell Technologies). The following cytokines were used: for BFU-E assay, IL-3 (0.01 U/mL), GM-CSF (0.001 ng/mL), and Epo (3 U/mL). For CFU-G assay, IL-3 (1 U/mL), GM-CSF (0.1 ng/mL), and G-CSF (500 U/mL). For BFU-E/CFU-G assay, IL-3 (1 U/mL), GM-CSF (0.1 ng/mL), Epo (0.6 U/mL), and G-CSF (500 U/mL; supplemental data, available on the *Blood* website; see the Supplemental Materials link at the top of the online article).

Morphologic analysis

Cells were harvested from day 3 to days 21 to 24, smeared on glass slides by cytospin centrifugation, stained with standard May-Grünwald-Giemsa, and observed by conventional light field microscopy, to evaluate morphology and cell differentiation through the erythroid and granulocytic pathways. Proerythroblasts, basophilic, polychromatophilic, and orthochromatic cells in the erythroid series, myeloblasts, promyelocytes, myelocytes, and mature cells (meta/band) in the granulocytic series were identified, and their percentage value was obtained. At least 500 cells were counted per slide.

Slides were viewed with a Nikon Eclipse E1000 microscope (Nikon) using Plan Fluor lenses at 20×/0.75 PH and 40×/1.30 PH oil with DPX mounting medium (Laboratory Supplies). Colonies were viewed using a Plan Fluor lense at 10×/0.30 PH. Images were acquired using Nikon digital camera model DXM1200 and were processed with Nikon ACT-1 software Version 2.63.

RNA analysis

Total RNA was isolated by Trizol (Invitrogen) following the manufacturer's instructions. First-strand cDNA was synthesized with SuperScript II (Invitrogen) using equivalent amounts of total RNA for each sample and oligo (dT) (Invitrogen) primers. mRNA quantification by real-time polymerase chain reaction (PCR) was performed using the ABI PRISM 7700 Sequence Detection System (Applied Biosystems) and inventoried TaqMan gene expression assays (Applied Biosystems) with ΔC_t values normalized using endogenous GAPDH as control.

ChIP assay

Formaldehyde was added to cultured cells (2×10^6) at a final concentration of 1% for 10 minutes at 37°C to cross-link DNA and protein complexes. Chromatin was sheared by sonication and immunoprecipitated with 3 μg of anti-NFI-A (Abcam). Genomic regions of approximately 200 bp containing the NFI-A consensus site were amplified by multiplex PCR[21] in the presence of [α-^{32}P] dATP using the primers listed in supplemental Table 1. PCR signals were quantified using Typhoon Trio Phosphoimager (Amersham Biosciences) and ImageQuant software (Molecular Dynamics). The relative occupancy of NFI-A present on the promoter (Prom) specific regions is normalized to the input (I) signal, following the algorithm: $[(IP\text{-}BO)/I]_{PROM}/[(IP\text{-}BO)/I]_{UR.}$ IP represents chromatin immunoprecipitated by the NFI-A antibody. BO (beads only) represents nonspecific signal in absence of antibody. The coamplification of tubulin (mentioned as unrelated genomic region [UR]) within the same multiplex reaction serves as an internal control for background nonspecific chromatin. PCRs were performed within the linear range of amplification (supplemental data).

Lentiviral production and infection

Infectious particles were produced as previously described.[22] Cells were infected by the spin-inoculation method. $CD34^+$ cells were infected at day 1 of culture. At 48 hours after infection, the cells were monitored for GFP expression by flow cytometry using FACScan instrument (BD Biosciences), showing an average transduction efficiency ranging from 15% to 20% (for the HA-NFI-A construct) to 30% to 40% (for vector and siNFI-A). At this time, GFP^+ cells were sorted using the FACSaria instrument (BD Biosciences) and placed in liquid phase culture or clonogenic medium (supplemental data).

Flow cytometry

Phycoerythrin (PE)-conjugated antihuman Glycophorin-A (GPA), CD34, CD15, CD14, CD11b, and CD114 antibodies were purchased from BD Biosciences Pharmingen. G-CSFR total protein expression was assessed by immunostaining using a PE-conjugated anti-CD114 antibody in cells fixed and permeabilized with 100 μL of Cytofix/Cytoperm (BD Biosciences Pharmingen). Immunophenotype and 7-amino-actinomycin D (Calbiochem) cell viability staining (final concentration of 5 μg/mL), performed according to the manufacturer's instructions were analyzed by flow cytometry using FACScan instrument (BD Biosciences).

Assay of globin-chain content

High performance liquid chromatography (HPLC) separation of globin chains was performed according to the previously published method[15] (supplemental data).

Plasmids, constructs, luciferase assay

The lentiviral vector encoding HA-NFI-A was previously described.[13] The siNFI-A vector was generated by cloning the siNFI-A sense 5′-AACCAGAGGTCAAGCAGAA-3′ into the pRRLcPPT.hPGK.EGFP.WPRE lentiviral vector (named vector; supplemental data). Supplemental data contain information on luciferase assay, and supplemental Table 1 contains information on PCR primers.

Immunoblotting

Total protein was extracted using CelLytic M Lysis Reagent (Sigma-Aldrich) following the manufacturer's protocol, supplemented with Protease Inhibitor Cocktail (Sigma-Aldrich). Total cell extracts were fractionated by 10% sodium dodecyl sulfate-polyacrylamide gel electrophoresis followed by electroblotting. Blots were probed with the primary and secondary antibodies listed in Supplemental data. Immunoreactivity was measured using the enhanced chemiluminescence method (Amersham Biosciences).

Statistical analysis

Comparison between multiple groups was made by one-way analysis of variance and the Tukey post test to analyze significance. Two-tailed *t* test analysis for

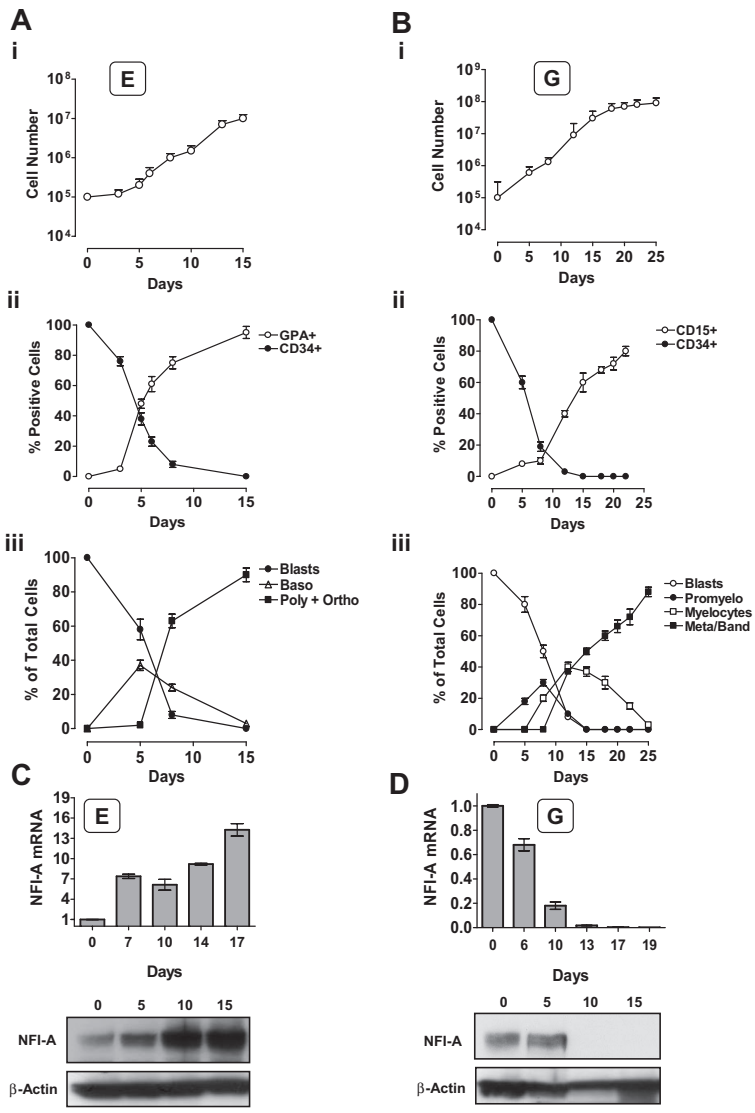

Figure 1. Unilineage erythroid (E) and granulocytic (G) culture of HPCs: NFI-A expression pattern during E and G differentiation/maturation. (A) Unilineage E culture of CB CD34$^+$ HPCs. (i) Growth curve, (ii) CD34 and GPA surface marker expression, and (iii) percentage of blasts, proerythroblasts (Blasts), basophilic (Baso), polychromatophilic (Poly), and orthochromatic (Ortho) erythroblasts (mean ± SEM values; n = 7). (B) Unilineage G culture of CB CD34$^+$ HPCs. (i) Growth curve, (ii) CD34 and CD15 surface marker expression, and (iii) percentage of blasts, promyelocytes (Promyelo), myelocytes, mature metamyelocytes, and band cells (Meta/band). Mean ± SEM values (n = 8). (C) NFI-A increases in E culture. (Top) Real-time PCR evaluation of NFI-A mRNA. Normalized mean ± SEM values (n = 3). (Bottom) Immunoblot of NFI-A protein. β-Actin was used as loading control. (D) NFI-A decrease in G culture. (Top) Real-time PCR evaluation of NFI-A mRNA. Normalized mean ± SEM values (n = 3). (Bottom) Immunoblot of NFI-A protein.

significance was used to compare individual data to control values. Differences were considered significant at *P* values less than .05 or less than .01.

Results

NFI-A expression is upmodulated during erythropoiesis and shut off during granulopoiesis

Human CB CD34$^+$ HPCs were induced into unilineage erythroid (E; Figure 1Ai-iii) or granulocytic (G; Figure 1Bi-iii) proliferation and differentiation/maturation in serum-free suspension cultures. The unilineage cultures recapitulate the in vivo differentiation/maturation of HPCs[20,23-25]; therefore, these assays allow analysis of sequential, discrete stages of differentiation/maturation through a single lineage.

In the E culture, NFI-A was sharply upmodulated at both the RNA and protein levels (Figure 1C), in parallel with the increase of Glycophorin-A$^+$ (GPA) cells and erythroblast differentiation/maturation (Figure 1Aii-iii). Conversely, in G culture, we observed a drastic decrease of NFI-A, reaching undetectable RNA and protein levels starting from days 10 to 13 (Figure 1D): this correlated with the increasing number of CD15$^+$ cells and G differentiation/maturation at morphology level (Figure 1Bii-iii).

In line with these findings, NFI-A was expressed at a higher level in the erythroleukemic K562 cell line than the myeloblastic leukemia HL-60 cell line; moreover, NFI-A levels decreased in HL-60 cells undergoing G differentiation after treatment with retinoic acid (RA; supplemental Figure 1A).

NFI-A up-regulation is required for erythroid differentiation of HPCs

The dichotomy of NFI-A expression patterns in the E versus G lineage suggested that this TF may exert opposite functional actions in these cell differentiation pathways.

To verify this hypothesis, we first monitored the effects of NFI-A knockdown in HPCs seeded in E culture using a lentiviral construct encoding an shRNA-targeting NFI-A mRNA (named siNFI-A). To exclude possible off-target effects, siNFI-A was compared with a previously published shRNA against NFI-A[12] (here named siNFI-A-2): both the constructs specifically knocked down NFI-A, and siNFI-A showed the maximum silencing efficiency (supplemental Figure 1B) without triggering an off-target interferon response (supplemental Figure 1C). In E culture, HPCs stably expressing siNFI-A showed an impaired growth capacity: by day 8, the majority of the cells were nonviable (Figure 2A-B), with no significant changes in the cell cycle

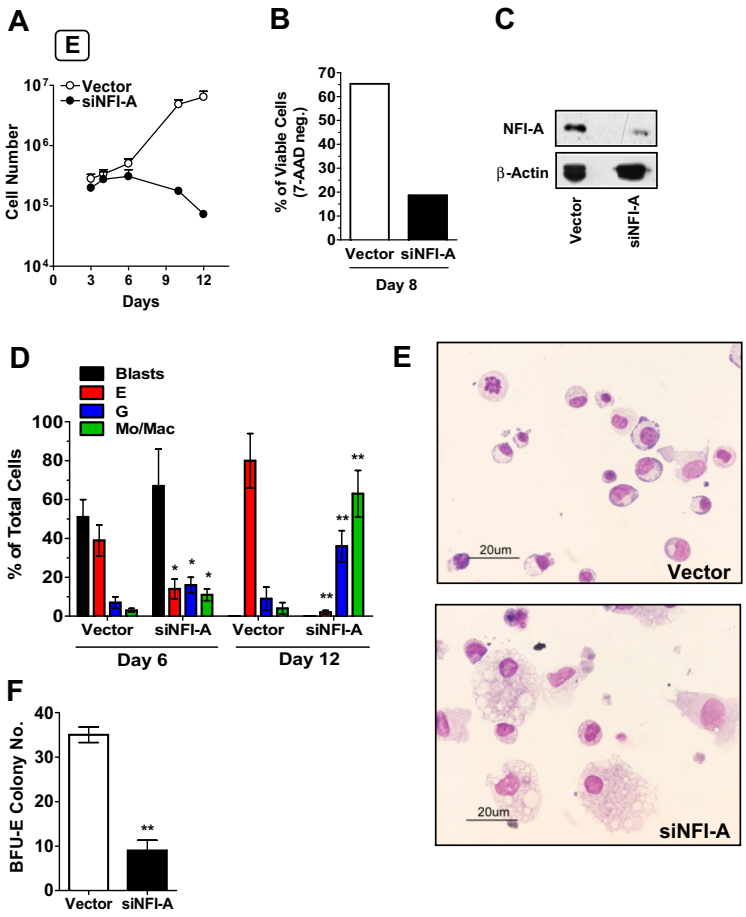

Figure 2. NFI-A knockdown impairs erythroid (E) differentiation of HPCs. (A) Growth curve of HPCs in unilineage E culture infected with control vector or siNFI-A (mean ± SEM values of 3 independent experiments). (B) The histogram shows the percentage of viable (or 7-amino-actinomycin D-negative) cells detected by flow cytometry (representative of 3). (C) Western blot analysis confirming NFI-A knockdown in siNFI-A expressing HPCs in unilineage E culture. (D) Wright-Giemsa staining of vector- and siNFI-A–transduced cells. Percentage of blasts, erythroid (E), granulocytic (G), and monocytic/macrophage (Mo/Mac) cells (mean ± SEM values of 3 independent experiments). (E) Morphology of vector and siNFI-A cells at day 12 of E culture (representative field, original magnification ×400). See "Morphologic analysis" for more image information. (F) Number of BFU-E colonies generated by vector- and siNFI-A–infected HPCs (mean ± SEM values; n = 3).

status of the remaining viable cells (data not shown). NFI-A protein knockdown in siNFI-A expressing cells was confirmed by Western blot (Figure 2C). Moreover, E differentiation/maturation in siNFI-A cells was dramatically afflicted: at day 12, the residual cells were almost totally of granulocytic and monocytic type (Figure 2D-E). Similarly, clonogenic assays in E medium showed that siNFI-A transduction caused a drastic reduction of the BFU-E colony number (Figure 2F). These results indicate that NFI-A upmodulation is necessary to allow normal E differentiation/maturation of HPCs.

NFI-A accelerates erythroid differentiation of HPCs and it restores erythropoiesis in the presence of suboptimal or minimal erythropoietin (Epo) stimulus

We then hypothesized that the enforced overexpression of NFI-A may favor E differentiation, compared with empty vector cells. Indeed, lentiviral NFI-A overexpression in HPCs seeded in E culture (Figure 3Ai) resulted in an accelerated differentiation and maturation, as demonstrated by the increase of orthochromatic erythroblasts at day 8 (Figure 3Aii). Western blot analysis using anti-HA and anti-NFI-A antibodies confirmed the expression of exogenous NFI-A (Figure 3Aiii). In addition, NFI-A ectopic expression in K562 caused an increase in benzidine-stained cells and GPA expression in both baseline conditions and Ara-C-induced E differentiation with no significant change in cell growth rates (supplemental Figure 2Ai-iii).

In standard E culture, saturating levels of Epo (3 U/mL) are required to induce optimal erythroblast expansion and differentiation/maturation.[20,26] We hypothesized that NFI-A overexpression may restore erythropoiesis in the presence of a suboptimal or minimal Epo stimulus. To test this hypothesis, we supplemented E culture with a low or minimal Epo concentration, corresponding, respectively, to 1:20 (0.15 U) and 1:100 (0.03 U) of the saturating Epo level. Compared with control cells, NFI-A–transduced HPCs seeded in Epo 0.15 U medium displayed a similar proliferation rate (Figure 3Bi) while exhibiting enhanced differentiation/maturation as indicated by erythroblast morphology (Figure 3Bii), GPA expression, and β-globin mRNA level (Figure 3Biii). Interestingly, NFI-A enforced expression also increased BFU-E colony formation (Figure 3Biv). When Epo was lowered to 0.03 U, cell expansion was blocked (Figure 3Ci): importantly, erythroid cells were not present in control culture, whereas NFI-A overexpressing cells matured to the terminal stage, as shown by the increase of GPA^+ cells (Figure 3Cii, supplemental Figure 2B) and morphology analysis (Figure 3Ciii-iv).

We conclude that NFI-A overexpression in HPCs promotes E differentiation and maturation while inducing a more mature E phenotype in K562 cells. Furthermore, NFI-A overexpression restores erythroblast development in E culture supplemented with a suboptimal or minimal Epo stimulus.

NFI-A downmodulation is necessary to permit granulocytic differentiation/maturation

To examine the functional role of NFI-A in the G lineage, HPCs transduced with a lentivirus encoding NFI-A were seeded in G culture. Control cells were transduced with the empty vector. Cells expressing ectopic NFI-A had reduced viability (Figure 4Ai-ii) with no detectable differences in the cell cycle status (data not shown) and showed a delayed entry in the G pathway (Figure

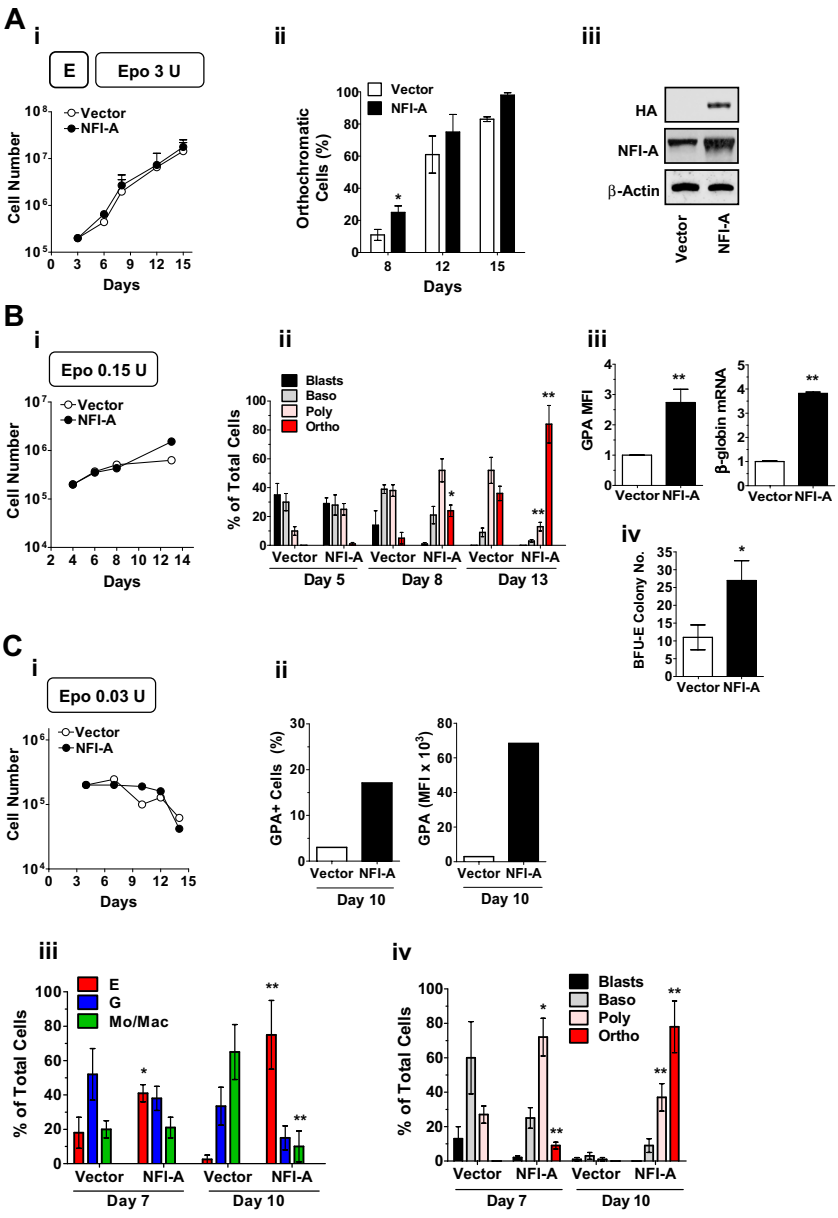

Figure 3. NFI-A overexpression favors differentiation and overcomes erythropoietin (Epo) dependence of erythroid (E) culture. (Ai) Growth curve of vector- and NFI-A–transduced HPCs in standard unilineage E culture (Epo 3 U/mL; mean ± SEM values; n = 3). (ii) Percentage of orthochromatic cells at sequential stages of E culture generated by vector- and NFI-A–expressing HPCs (mean ± SEM values; n = 3). (iii) Western blot showing ectopic expression of HA-tagged NFI-A in NFI-A–infected HPCs in E culture at day 8. (Bi) Growth curve (a representative experiment of 3 is shown) and (ii) morphologic evaluation (mean ± SEM values; n = 3) of E differentiation of vector- and NFI-A–transduced HPCs seeded in E culture with suboptimal amounts of Epo (0.15 U). (iii) Increase of GPA mean fluorescence intensity (MFI) (mean ± SEM values; n = 3) and real-time PCR showing β-globin mRNA expression (mean ± SEM values from 2 independent infections). (iv) Number of BFU-E colonies plated in Epo 0.15 clonogenic medium (mean ± SEM values of 2 paired experiments). (Ci) Growth curve of vector- and NFI-A–transduced HPCs in culture supplemented with minimal amounts of Epo (0.03 U). A representative experiment of 3 is shown. (ii) Percentage of GPA$^+$ cells (left) and GPA MFI (right) at day 10. A representative experiment of 3 is shown. (iii-iv) Morphology analysis of vector- and NFI-A–infected HPCs (mean ± SEM values; n = 3).

4Aiii). NFI-A cells displayed a significant reduction of G-CSFR mRNA (Figure 4Bi) and total protein expression (Figure 4Bii, supplemental Figure 3A) in addition to a strong decrease in myeloid markers CD11b and CD14/15 (Figure 4Ci-ii). In clonogenic G assay, vector-transduced HPCs generated a significant number of CFU-G colonies of large size; whereas in cultures of NFI-A infected cells, almost all G clones were abortive (Figure 4D). In the HL-60 cell line, ectopic expression of NFI-A decreased the RA effect on G differentiation, as indicated by the lower level of differentiation markers (CD11b, CD15, and G-CSFR; supplemental Figure 3B-C), thus in line with previous observations on the promyelocytic leukemia NB4 cell line.[12]

NFI-A is a regulator of the erythro-granulocytic lineage decision

Based on the results thus far, we hypothesized that NFI-A levels may function in directing HPCs into the E or G differentiation pathway. To test the hypothesis, we developed a culture system allowing HPCs to undergo bilineage E + G differentiation/maturation (Figure 5). This culture system is stimulated by an appropriate mixture of E and G growth factors (including Epo 0.6 U/mL and G-CSF 500 U/mL, see "Cell culture" for more information): as a result, the proliferating cells are characterized by a balanced ratio of E and G cells undergoing differentiation and maturation up to the terminal stage while including a small monocytic contaminant.

HPCs subjected to NFI-A enforced expression or knockdown were seeded into the E + G bilineage culture. Here again, control cells were infected with empty vector. As shown in Figure 5Ai, NFI-A– and vector-transduced HPCs similarly proliferated and differentiated up to day 9. Thereafter, the E population significantly prevailed and matured more rapidly in NFI-A–overexpressing cells (Figure 5Aii-iii). HPCs infected with siNFI-A proliferated similarly to control cells up to day 9 but then showed a blockage of cell expansion (Figure 5Bi). Notably, the siNFI-A–transduced cells displayed a predominant G morphology coupled with a more rapid maturation to mature granulocytes (Figure 5Bii-iii). Analysis of lineage-specific surface markers (GPA for the E and an equimolar

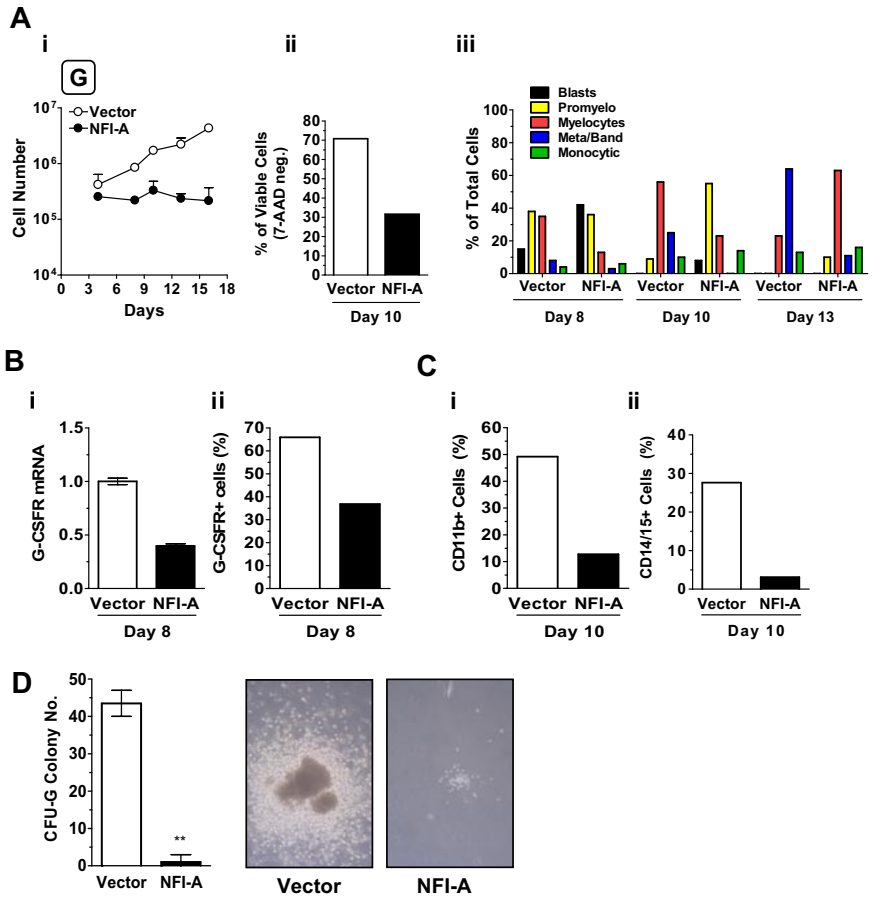

Figure 4. Ectopic expression of NFI-A blocks granulocytic (G) differentiation of HPCs. (Ai) Growth curve of unilineage G cultures transduced with vector or NFI-A lentivirus (mean ± SEM values of 3 independent experiments). (ii) The histogram shows the percentage of viable (or 7-amino-actinomycin D-negative) cells detected by flow cytometry (representative of 3). (iii) Wright-Giemsa staining of infected cells, showing the percentage of cells at various stages of differentiation. A representative experiment of 3 is shown. (Bi) Real-time PCR analysis of G-CSFR mRNA and (ii) flow cytometry analysis of total G-CSFR protein expression in vector and NFI-A cells at day 8. (C) Flow cytometry analysis of (i) CD11b and (ii) CD14/CD15 myeloid markers at day 10. (D) (Left) number of CFU-G colonies generated by transduced HPCs (mean ± SEM values; n = 3). (Right) Representative microphotographs of G colony or cluster in vector or NFI-A culture, respectively, at day 14. Original magnification ×100. See "Morphologic analysis" for more image information.

mix of CD14/CD15 for the G lineage) at day 9 confirmed the morphologic observations. NFI-A–infected cells express more GPA and no G markers, whereas siNFI-A–infected cells express with a greater intensity G markers and little or no GPA (Figure 5Ci). In addition, β-globin and G-CSFR mRNA (Figure 5Cii), along with G-CSFR protein expression analyzed by flow cytometry (Figure 5Ciii, supplemental Figure 4A) showed an opposite pattern of expression in the siNFI-A versus NFI-A cells compared with the vector cells confirming the lineage-specific prevalence. At day 9, macroscopic observation of the control cell pellet showed a central core of red E cells, surrounded by white G cells, whereas the siNFI-A pellet is entirely G-white and NFI-A overexpressing cells are almost entirely E-red, as confirmed by microscopic morphologic analysis of the same cell pellets (Figure 5D).

In a clonogenic E + G assay, GFP^+ colonies were scored after 14 to 18 days (Figure 5E). NFI-A–overexpressing cells showed an increased proportion of BFU-E colonies and a dramatic reduction in CFU-G colonies compared with vector colonies. In contrast, siNFI-A–infected HPCs showed an opposite distribution of colony types, with a predominance of CFU-Gs.

Altogether, these experiments indicate that NFI-A plays a key role in the erythro-granulocytic lineage decision at the level of HPCs and possibly early precursors.

A functional relationship between NFI-A levels and 2 lineage-associated genes: *β-globin* and *G-CSFR*

We then attempted to explore the mechanism of NFI-A action by screening possible *cis*-acting elements interacting with NFI-A within promoter regions of E- and G-specific genes.

We selected the β-globin promoter as a target of NFI-A during E differentiation because binding sites were noted in the proximal promoter region.[27] As expected, analysis of β-globin expression in E and G culture showed that the mRNA and protein level greatly increased in the E series (Figure 6A, supplemental Figure 5A) but was absent in the G lineage (Figure 6A). Using an HPLC assay, we observed that in E culture NFI-A–overexpressing cells showed an increased β-chain content at both early and intermediate days of differentiation (Figure 6Bi, supplemental Figure 5B). Conversely, real-time PCR showed a marked decrease of β-globin mRNA in siNFI-A cells (Figure 6Bii). Results in K562 cells were striking (Figure 6C, supplemental Figure 5C). In empty vector cells, β-globin was not detectable in both control cultures and after Ara-C-induced E differentiation, thus in line with previous reports.[28,29] Conversely, β-globin mRNA and protein were strongly induced in NFI-A–overexpressing cells in either control or Ara-C-treated cultures. γ-Globin and ϵ-globin were equally present in control vector and NFI-A cells, and both increased in a time-dependent manner on Ara-C treatment. Altogether, these data show that ectopic expression of NFI-A specifically induces β-globin expression, not only in E culture of HPCs, but also in K562 cells, which normally do not express β-globin.

Next, we focused on the G-CSFR, which contains 2 conserved putative NFI sites. In E culture, the G-CSFR mRNA and protein levels (Figure 6Di-ii) dropped down to untraceable levels at terminal stages. Conversely, in G culture, the G-CSFR mRNA and protein level progressively increased through late maturation (Figure 6Ei-ii). In E cells, lentiviral knockdown of NFI-A was similarly associated with marked upmodulation of G-CSFR total protein and G-CSFR surface expression (Figure 6Fi-ii). These

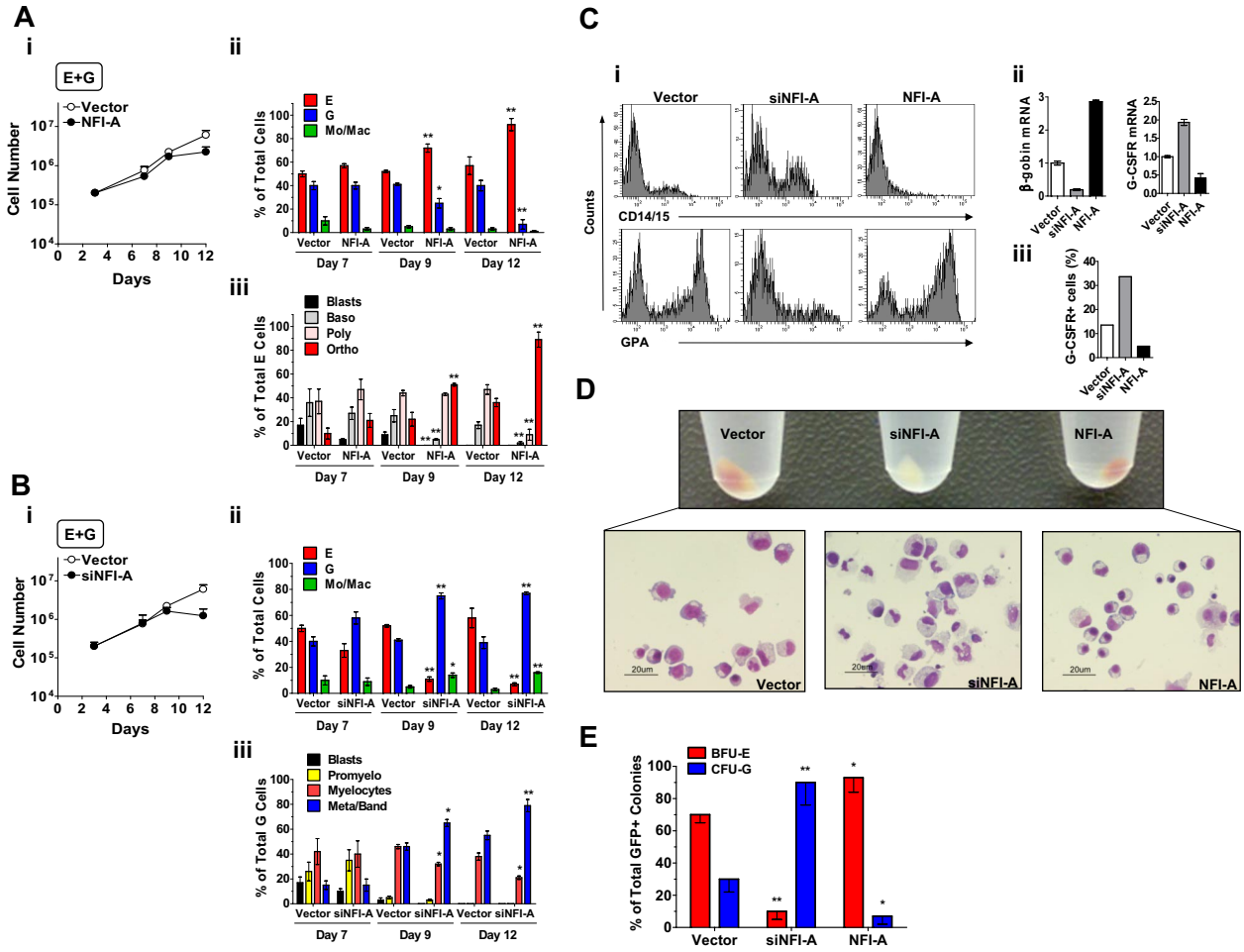

Figure 5. NFI-A regulates erythroid (E) versus granulocytic (G) lineage differentiation in bilineage E + G culture (mean ± SEM values from 3 independent experiments). (A) Ectopic expression of NFI-A promotes E and inhibits G differentiation/maturation. (i) Growth curve, (ii) morphology analysis of the cellular composition at sequential culture times, and (iii) differentiation/maturation of the E population of vector- and NFI-A–infected HPCs. (B) NFI-A knockdown blocks E and promotes G differentiation/maturation. (i) Growth curve, (ii) morphology analysis at sequential culture times, and (iii) differentiation/maturation of the G population in culture of vector- and siNFI-A–infected HPCs. (C) Lineage-specific marker expression at early stage (day 9) of culture. (i) Representative flow cytometry analysis of vector-, siNFI-A–, and NFI-A–infected cells using the erythroid GPA and the myeloid CD14/CD15 markers, (ii) β-globin and G-CSFR mRNA detected by real-time PCR, and (iii) percentage of cells expressing G-CSFR detected by flow cytometry (day 7). (D) Macroscopic and morphologic changes of vector-, siNFI-A–, and NFI-A–infected cells at day 9 of E + G culture. (Top) Macroscopic view of cellular pellets centrifuged from vector culture (mixed population, erythroid red cells in the center and peripheral myeloid-white cells in the surrounding ring), siNFI-A culture (only myeloid cells), and NFI-A culture (predominance of red cells). (Bottom) Representative morphology fields (original magnification, ×400). See "Morphologic analysis" for more image information. (E) E + G clonogenic activity of HPCs transduced with vector, siNFI-A, or NFI-A viruses. Histograms represent the relative GFP$^+$ BFU-E and CFU-G colony distribution. GFP$^+$ colony numbers were: vector BFU-E 34.3 ± 7, CFU-G 14.3 ± 5; siNFI-A BFU-E 4.6 ± 1.5, CFU-G 31 ± 9; NFI-A BFU-E 29.3 ± 6, CFU-G 3.5 ± 1 (mean ± SEM values from 3 paired experiments).

results were confirmed in HL-60 cells induced by RA treatment into G differentiation: NFI-A ectopic expression repressed the G-CSFR mRNA and surface protein expression. On the contrary, siNFI-A infection caused an induction of G-CSFR receptor protein level in HL-60 cells (supplemental Figure 3C-D).

NFI-A directly activates β-globin and represses G-CSFR proximal promoters, exhibiting a dual transcriptional activity in a lineage-specific context

Because of the functional role of NFI-A in β-globin induction, we attempted to map the in vivo binding of endogenous NFI-A to the β-globin promoter using chromatin-immunoprecipitation (ChIP). Computational analysis by Chip-Mapper, Alibaba 2.1 and MatInspector Professional software programs[30-32] revealed 3 potential NFI-binding sites in the β-globin proximal promoter region (Figure 7A): specifically, phylogenetic footprinting showed site 1 to be embedded in a highly evolutionary conserved region (supplemental Figure 6A). Consequently, NFI-A chromatin occupancy in primary cells (physiologic binding) was determined using genomic DNA isolated from CD34$^+$ HPCs, terminal E cells (E culture, day 14), and intermediate G cells (G culture, day 7) and immunoprecipitated using an NFI-A antibody. DNA was analyzed by multiplex PCR using primers specific for the promoter region containing the NFI-A–binding sites and a UR as an internal control. The linear range of amplification was confirmed by serial dilution of input DNA (supplemental Figure 7A). Figure 7B shows that NFI-A at these sites was present in CD34$^+$ HPCs and greatly enriched in terminal E cells, characterized by elevated levels of both NFI-A and β-globin. Intermediate G cells, which lack NFI-A protein, were used as a negative control (Figure 7B, supplemental Figure 7Bi). We further extended ChIP analysis in K562 cells using real-time PCR in parallel with the multiplex PCR approach to asses NFI-A binding. ChIP was performed in vector- and NFI-A–transduced K562 cells in the absence or presence of Ara-C. As shown consistently by the 2 independent methods, only NFI-A–transduced cells show NFI-A binding to the β-globin promoter, and

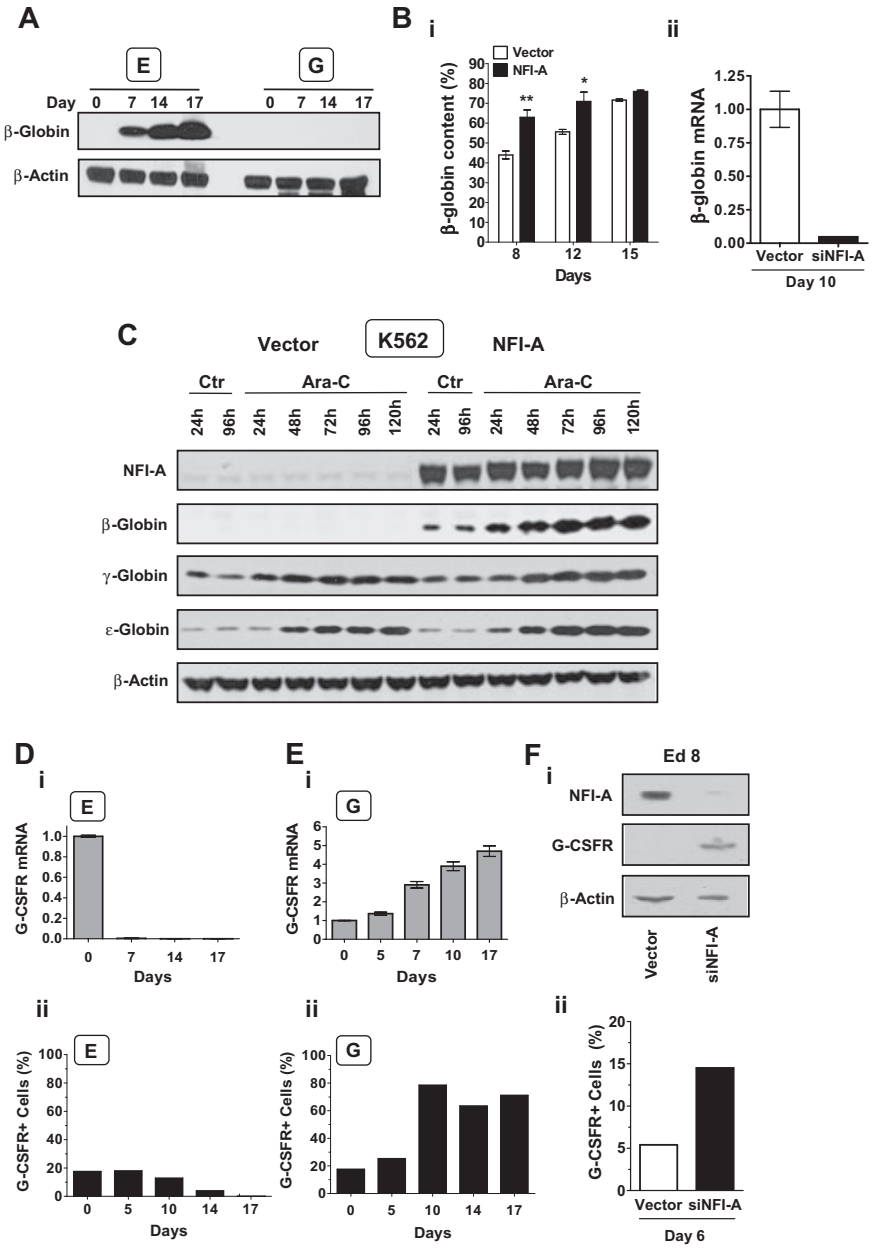

Figure 6. A functional relationship between NFI-A and 2 lineage-associated genes: *β-globin* and *G-CSFR.* (A) Immunoblot detection of β-globin at sequential stages of E and G culture. (B) (i) HPLC analysis of globin-chain content in unilineage E culture of HPCs transduced with empty vector or NFI-A. The β-globin chain content is expressed as the percentage of β-globin/non–α-globin chain content (ie, β/β + γ). Mean ± SEM values (n = 3). (ii) Real-time PCR of β-globin mRNA expression in siNFI-A–infected versus empty vector HPCs in E culture at day 10 (mean ± SEM values; n = 3). (C) Western blot analysis of β-globin, γ-globin, ε-globin, and NFI-A protein expression in control (Ctr) and Ara-C–treated vector- and NFI-A–transduced K562 cells. (Di) G-CSFR mRNA during E culture detected by real-time PCR (normalized mean ± SEM values; n = 3) and (ii) percentage of G-CSFR$^+$ cells detected by flow cytometry that were permeabilized and stained with a PE-conjugated G-CSFR antibody. (Ei) G-CSFR mRNA during G culture, and (ii) percentage of G-CSFR$^+$ cells detected by flow cytometry. (Fi) Western blot analysis showing G-CSFR reactivation after NFI-A knockdown in siNFI-A–infected HPCs in unilineage E culture at day 8. (ii) Surface expression of G-CSFR detected by flow cytometry in siNFI-A infected E cells at day 6.

this occupancy increases in a time-dependent manner in the presence of Ara-C (supplemental Figure 8A,Ci-ii), complementing the trend observed in primary cells. As expected, real-time ChIP analysis in the HL-60 cell line shows no significant binding over the course of RA treatment (supplemental Figure 8E).

To assess the contribution of individual NFI-A sites in β-globin transcription, we designed promoter-luciferase fusion constructs containing the wild-type β-globin promoter and NFI-A site-specific mutants (Figure 7A). Figure 7C shows that cotransfection of HB-Wt with a plasmid encoding NFI-A in K562 cells led to an approximately 3-fold increase in transcription with respect to HB-Wt alone. In contrast, HB-Mut1 abolished transcriptional induction even in the presence of ectopic NFI-A. HB-Mut3 responded to NFI-A to a lesser extent, whereas HB-Mut2 behaved similarly to HB-Wt. The mutant construct, containing 3 mutated sites (HB-Mut1, Mut2, Mut3), exhibited no transcriptional induction on NFI-A ectopic expression, as observed for HB-Mut1. In conclusion, the results indicate that NFI-A binds to and activates the β-globin promoter through primarily site 1 and secondarily site 3.

The G-CSFR promoter contains 2 conserved putative NFI-binding sites (supplemental Figure 6B). As a result, we performed multiplex ChIP analysis of the promoter using primers including both sites (Figure 7D). Genomic DNA from CD34$^+$ HPCs, intermediate E cells (E day 7), and intermediate G cells (G day 7) was immunoprecipitated using an NFI-A antibody. As shown in Figure 7E and supplemental Figure 7Bii, we found binding of NFI-A to the G-CSFR sites in CD34$^+$ HPCs and E cells, but not in G cells. Binding of NFI-A to G-CSFR sites within NFI-A–transduced K562 cells was observed by multiplex and real-time PCR and increased with time on exposure to Ara-C (supplemental Figure 8B,Di-ii). On the contrary, in the HL-60 cell line, NFI-A is present on the G-CSFR promoter in both vector- and NFI-A–transduced control cells, and rapidly falls off in vector cells on RA treatment, whereas its occupancy is only slightly reduced in NFI-A–overexpressing cells on RA treatment (supplemental Figure

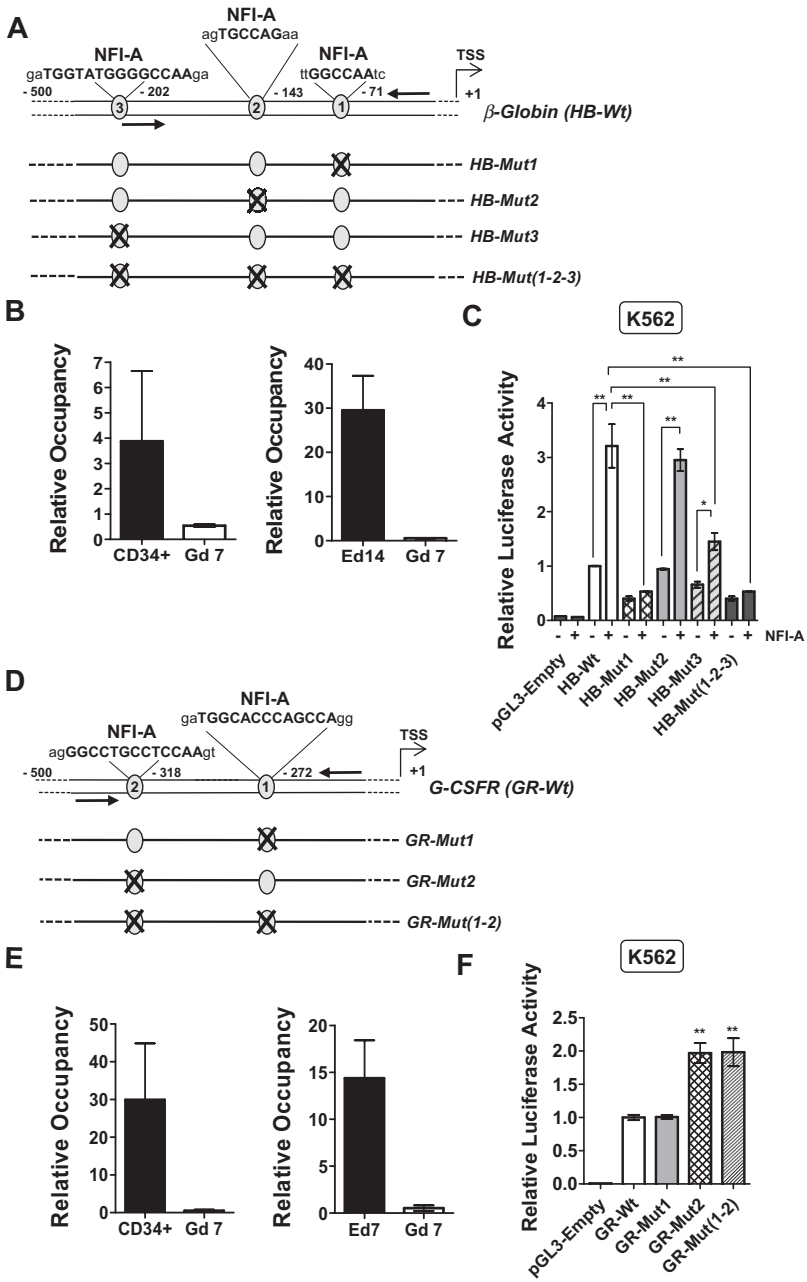

Figure 7. Antithetic effects of NFI-A on the β-globin and G-CSFR promoters in vivo. (A) Schematic representation of the β-globin proximal promoter. NFI-A DNA-binding site sequences are highlighted in bold characters. TSS indicates the transcriptional start site; arrows, the position of the primers used for the ChIP analysis. Mutant sites are numbered according to their vicinity to the TSS. (B) Relative quantification of NFI-A occupancy on the β-globin promoter. Chromatin was immunoprecipitated with an NFI-A antibody, and the bound DNA was analyzed by multiplex PCR using specific primers corresponding to the β-globin promoter region containing the NFI-A binding sites and an unrelated intergenic genomic region (UR) as an internal control. Histograms represent the mean ± SEM from 3 independent DNA preparations; PCR analyses were repeated at least 3 times. (C) Promoter assay showing a positive role of NFI-A in β-globin proximal promoter activation. Wild-type and mutant constructs were assayed for transcriptional activity relative to the endogenous NFI-A or in a cotransfection with an NFI-A–expressing plasmid. The firefly luciferase values were normalized to the Renilla luciferase values for each transfection, and the relative luciferase activity is represented as relative fold induction over the HB-Wt transfection (mean ± SEM values from 4 independent transfections). Each reading was repeated at least 2 times. (D) Schematic representation of the NFI-A binding sites on the G-CSFR promoter. (E) Relative quantification of NFI-A occupancy on the G-CSFR promoter. Chromatins were immunoprecipitated with an NFI-A antibody, and the bound DNA was analyzed by multiplex PCR using specific primers corresponding to the G-CSFR promoter region containing the NFI-A binding sites and an unrelated intergenic genomic region (UR) as an internal control. Histograms represent the mean ± SEM from 3 independent DNA preparations; multiplex PCR analysis was repeated at least 3 times. (F) Promoter assay showing NFI-A repressive activity on the G-CSFR promoter performed in K562 cells. Wild-type or mutant promoter constructs were transfected, and firefly luciferase activity was normalized to Renilla luciferase activity for each transfection. The relative luciferase activity is represented as relative fold induction over the GR-Wt transfection. Data represent mean ± SEM from 3 independent transfections. Each reading was repeated at least 2 times.

8F). To further demonstrate that NFI-A transcriptionally represses the G-CSFR promoter, we performed a promoter assay in K562 cells, using a wild-type promoter construct and site-specific mutants (Figure 7D). As shown in Figure 7F, the basal activity of the G-CSFR wild-type promoter construct (GR-Wt) was enhanced by mutating site 2 (GR-Mut2), as shown by a rescue of transcription of approximately 2-fold. The mutant construct bearing a mutation in site 1 (GR-Mut1) did not affect its transcriptional activity; conversely, the double-mutant construct (GR-Mut1, -Mut2) behaved similarly to GR-Mut2. In conclusion, we postulate that NFI-A binds and transcriptionally represses the G-CSFR promoter, specifically through site 2, whereas site 1 is inactive.

Discussion

Our studies indicate that NFI-A plays a major role in the control of the erythroid-granulocytic lineage decision at the level of HPCs. NFI-A accumulation during initial E differentiation results in progressive activation of *β-globin* gene transcription, coupled with repression of *G-CSFR*, thus channeling HPCs and early precursors into the E lineage and shutting off their G potential. Conversely, NFI-A suppression in early granulopoiesis activates G-CSFR transcription and impedes β-globin expression, thereby directing HPCs and early precursors into the G pathway.

As a model system, we used unilineage E and G cultures of human HPCs: these assays recapitulate the in vivo differentiation/maturation of these hematopoietic series, hence allowing analysis of lineage-specific cells at discrete sequential stages of erythropoiesis and granulopoiesis.[20,23] The expression of NFI-A, although low in early HPC differentiation, was either sharply up-regulated or fully suppressed in later stages of E or G culture, respectively. A similar pattern has been observed for other TFs controlling lineage specification, such as GATA-1,[33] PU.1,[34] and C/EBPα[35]: all are expressed at low levels in "primed" HSCs/HPCs, whereas their

upmodulation in later stages is critical to promote lineage(s)-specific differentiation program(s) and to antagonize the expression of genes specific for the other series.

NFI-A accumulation is necessary for both E differentiation and suppression of the G potential. In E culture, siNFI-A–transduced HPCs were incapable of E differentiation but generated predominantly myeloid cells. This is presumably the result of the presence of small amounts of IL-3 and GM-CSF in the E medium: these 2 cytokines display a pro-survival activity on granulomonocytic cells.[18,36] Furthermore, GM-CSF stimulates M-CSF release in monocytes,[37] giving rise to a positive autocrine feedback loop. Conversely, HPCs transduced with NFI-A in G culture displayed a block in G differentiation.

NFI-A is not only necessary for E differentiation/maturation but is also capable of driving it. During normal erythropoiesis, Epo binds to the EpoR and activates signaling cascades, resulting in antiapoptotic effects and proliferation coupled with E differentiation/maturation.[38] In suboptimal E culture, because of a low or minimal Epo stimulus, NFI-A overexpression was able to restore E differentiation/maturation: this suggests that NFI-A may directly target key molecules involved in the E gene program, independently of EpoR signaling.

Altogether, NFI-A upmodulation exerts sharp positive effects on erythropoiesis, whereas its downmodulation is permissive for granulopoiesis. Indeed, the results obtained in E + G liquid phase and clonogenic culture of HPCs indicate that NFI-A upmodulation or downmodulation governs the erythro-granulocytic lineage branchpoint, directing precursor cells into the E or G fate, respectively. Consequently, we hypothesized that NFI-A may exert these actions through transcriptional control of genes playing pivotal functions in the E or G program: indeed, a bioinformatic screen suggested that the β-globin and G-CSFR promoters were potential NFI-A targets.

NFI-A overexpression in E culture resulted in a significant increase of the β-globin content in erythroblasts. In the erythroleukemic K562 cells, incapable of synthesizing β-globin even on Ara-C induced E differentiation,[28] ectopic expression of NFI-A induced a marked expression of β-globin. These results indicate a tight correlation between NFI-A levels and β-globin expression. Identifying new players involved in the transcriptional regulation of *β-globin* gene is potentially of clinical significance because mutations in the gene or promoter *cis*-elements are relevant in β-thalassemias. We observed that NFI-A specifically binds the β-globin proximal promoter, primarily at position −73 to −78, and activates transcription. This NFI-A–binding site overlaps with the CCAAT element, which also binds to other factors and is 1 of 3 elements required for maximal transcription of the β-globin promoter.[39] Interestingly, a recently described case of β^{++}-thalassemia (mild β-thalassemia intermedia) was linked to a mutation of −73 (A to T) within the conserved CCAAT box.[40]

NFI-A is a novel negative transcriptional regulator of G-CSFR expression, which plays a crucial role in the production and function of granulocytes.[41] Knockdown of NFI-A in E culture led to activation of G-CSFR, whereas NFI-A transduction in G culture blocked the receptor expression. We found that NFI-A binds to a *cis*-element located between nucleotides −318 and −334 in the G-CSFR promoter and represses its transcription in reporter and functional assays. So far, only a few transcriptional regulators of this receptor have been discovered; some (eg, PU.1 and C/EBPα) have been extensively characterized,[42,43] whereas the contribution of others (eg, AP-1 and AP-2, GF-1) still needs to be clarified.[44] It is noteworthy that the G-CSFR is also expressed in human monocytes and directly modulates inflammatory cytokine secretion.[45] In acute promyelocytic leukemias bearing leukemogenic fusion proteins, G-CSFR function is disrupted[46]: NFI-A knockdown may provide an attractive therapeutic approach, possibly in combination with ATRA + G-CSF differentiation therapy.[46]

In ChIP experiments, we observed that chromatin occupancy by NFI-A at β-globin and G-CSFR sites increases with E differentiation. This is seemingly because of the rise of NFI-A concentration. In addition, other components may be involved, such as the chromatin status, interacting factors bound to nearby *cis*-acting elements, and the number and/or affinity of motif features.[47] Further studies will be required to determine the mechanism of action of NFI-A on these promoters, as well as to identify other possible NFI-A targets playing a significant role in the E and G differentiation program.

Recent studies identified NFI-A as a major component of regulatory pathways controlling RA-induced leukemic G differentiation and monocyte development. In both cases, NFI-A expression was suppressed by lineage-specific microRNAs, the granulocytic miR-223, and the monocytic miR-424, respectively, controlled by the C/EBPα and PU.1 TFs.[12,13] Whereas these studies indicated a role of NFI-A in myeloid differentiation, the mechanism of these actions was not elucidated, in that no NFI-A target gene was identified. Interestingly, miR-223 is sharply downmodulated during normal E differentiation (results not shown): hypothetically, this shutdown may add to the strong transcriptional induction of NFI-A expression.

TFs involved in hematopoietic lineage specification are part of cell-specific networks, participating in positive and negative cross-regulations at the transcriptional and posttranscriptional level.[48] This report uncovers that NFI-A is a novel piece of this network: ongoing studies aim to further delineate the interlink of NFI-A with other known TFs and circuitries.

Acknowledgments

The authors thank A. Cerio and A. D'Angiò for technical assistance, V. Michetti and M. Blasi for editorial assistance, and Dr Richard Gronostajski for sharing NFI reagents.

This work was supported by the Italy USA Oncology Program and the Biotechnology Program, Istituto Superiore di Sanità (C.P.); Associazione Italiana per la Ricerca sul Cancro (C.P., C.N., I.B.), University "La Sapienza," and Ministry for University and Research (PRIN, C.N., I.B.); EU project SIROCCO (LSHG-CT-2006-037900), and ESF project "NuRNASu," Centro di Eccellenza Biologia e Medicina Molecolare (I.B.). L.M.S. is supported by a fellowship from the University of Rome "La Sapienza."

Authorship

Contribution: L.M.S. and A.S. designed and performed research, analyzed and interpreted data, and wrote the manuscript; E.P. performed research and analyzed data; M. Ballarino, O.M., S.S., N.F., G.C., M.L.D.M., and A.F. performed research; M. Biffoni performed flow cytometric analysis; G.M., M.G., and I.B. contributed vital new reagents or analytical tools; and C.P. and C.N. coordinated the research and wrote the manuscript.

Conflict-of-interest disclosure: The authors declare no competing financial interests.

Correspondence: Cesare Peschle, Istituto di Ricovero e Cura a Carattere Scientifico Multimedica, Via Gaudenzio Fantoli 16/15, Milan, 20138, Italy; e-mail: cesare.peschle@iss.it; or Clara Nervi, University of Rome "La Sapienza" & San Raffaele Biomedical Park Foundation, Via di Castel Romano 100, Rome, 00128, Italy; e-mail: clara.nervi@uniroma1.it.

References

1. Orkin SH, Zon LI. Hematopoiesis: an evolving paradigm for stem cell biology. *Cell.* 2008;132: 631-644.
2. Loose M, Swiers G, Patient R. Transcriptional networks regulating hematopoietic cell fate decisions. *Curr Opin Hematol.* 2007;14:307-314.
3. Iwasaki H, Akashi K. Myeloid lineage commitment from the hematopoietic stem cell. *Immunity.* 2007; 26:726-740.
4. Tenen DG, Hromas R, Licht JD, Zhang DE. Transcription factors, normal myeloid development, and leukemia. *Blood.* 1997;90:489-519.
5. Cantor AB, Orkin SH. Transcriptional regulation of erythropoiesis: an affair involving multiple partners. *Oncogene.* 2002;21:3368-3376.
6. Arinobu Y, Mizuno S, Chong Y, et al. Reciprocal activation of GATA-1 and PU.1 marks initial specification of hematopoietic stem cells into myeloerythroid and myelolymphoid lineages. *Cell Stem Cell.* 2007;1:416-427.
7. Pina C, May G, Soneji S, Hong D, Enver T. MLLT3 regulates early human erythroid and megakaryocytic cell fate. *Cell Stem Cell.* 2008;2: 264-273.
8. Buitenhuis M, Verhagen LP, van Deutekom HW, et al. Protein kinase B (c-akt) regulates hematopoietic lineage choice decisions during myelopoiesis. *Blood.* 2008;111:112-121.
9. Lin YL, Wang YH, Lee HJ. Transcriptional regulation of the human TR2 orphan receptor gene by nuclear factor 1-A. *Biochem Biophys Res Commun.* 2006;350:430-436.
10. Emi Y, Ueda K, Ohnishi A, Ikushiro S, Iyanagi T. Transcriptional enhancement of UDP-glucuronosyltransferase form 1A2 (UGT1A2) by nuclear factor I-A (NFI-A) in rat hepatocytes. *J Biochem.* 2005;138:313-325.
11. Gronostajski RM. Roles of the NFI/CTF gene family in transcription and development. *Gene.* 2000;249:31-45.
12. Fazi F, Rosa A, Fatica A, et al. A minicircuitry comprised of microRNA-223 and transcription factors NFI-A and C/EBPalpha regulates human granulopoiesis. *Cell.* 2005;123:819-831.
13. Rosa A, Ballarino M, Sorrentino A, et al. The interplay between the master transcription factor PU.1 and miR-424 regulates human monocyte/macrophage differentiation. *Proc Natl Acad Sci U S A.* 2007;104:19849-19854.
14. Schechter AN. Hemoglobin research and the origins of molecular medicine. *Blood.* 2008;112: 3927-3938.
15. Gabbianelli M, Testa U, Massa A, et al. HbF reactivation in sibling BFU-E colonies: synergistic interaction of kit ligand with low-dose dexamethasone. *Blood.* 2003;101:2826-2832.
16. Stamatoyannopoulos G. Control of globin gene expression during development and erythroid differentiation. *Exp Hematol.* 2005;33:259-271.
17. Demetri GD, Griffin JD. Granulocyte colony-stimulating factor and its receptor. *Blood.* 1991; 78:2791-2808.
18. Barreda DR, Hanington PC, Belosevic M. Regulation of myeloid development and function by colony stimulating factors. *Dev Comp Immunol.* 2004;28:509-554.
19. Testa U, Fossati C, Samoggia P, et al. Expression of growth factor receptors in unilineage differentiation culture of purified hematopoietic progenitors. *Blood.* 1996;88:3391-3406.
20. Felli N, Fontana L, Pelosi E, et al. MicroRNAs 221 and 222 inhibit normal erythropoiesis and erythroleukemic cell growth via kit receptor down-modulation. *Proc Natl Acad Sci U S A.* 2005;102: 18081-18086.
21. Ballarino M, Morlando M, Pagano F, Fatica A, Bozzoni I. The cotranscriptional assembly of snoRNPs controls the biosynthesis of H/ACA snoRNAs in Saccharomyces cerevisiae. *Mol Cell Biol.* 2005;25:5396-5403.
22. Bonci D, Cittadini A, Latronico MV, et al. "Advanced" generation lentiviruses as efficient vectors for cardiomyocyte gene transduction in vitro and in vivo. *Gene Ther.* 2003;10:630-636.
23. Ziegler B, Testa U, Condorelli G, Vitelli L, Valtieri M, Peschle C. Unilineage hematopoietic differentiation in bulk and single cell culture. *Stem Cells.* 1998;16[Suppl 1]:51-73.
24. Labbaye C, Spinello I, Quaranta MT, et al. A three-step pathway comprising PLZF/miR-146a/CXCR4 controls megakaryopoiesis. *Nat Cell Biol.* 2008;10:788-801.
25. Fontana L, Pelosi E, Greco P, et al. MicroRNAs 17-5p–20a-106a control monocytopoiesis through AML1 targeting and M-CSF receptor up-regulation. *Nat Cell Biol.* 2007;9:775-787.
26. De Maria R, Zeuner A, Eramo A, et al. Negative regulation of erythropoiesis by caspase-mediated cleavage of GATA-1. *Nature.* 1999;401:489-493.
27. Jones KA, Kadonaga JT, Rosenfeld PJ, Kelly TJ, Tjian R. A cellular DNA-binding protein that activates eukaryotic transcription and DNA replication. *Cell.* 1987;48:79-89.
28. Watanabe T, Mitchell T, Sariban E, Sabbath K, Griffin J, Kufe D. Effects of 1-beta-D-arabinofuranosylcytosine and phorbol ester on differentiation of human K562 erythroleukemia cells. *Mol Pharmacol.* 1985;27:683-688.
29. Luisi-DeLuca C, Mitchell T, Spriggs D, Kufe DW. Induction of terminal differentiation in human K562 erythroleukemia cells by arabinofuranosylcytosine. *J Clin Invest.* 1984;74:821-827.
30. Marinescu VD, Kohane IS, Riva A. The MAPPER database: a multi-genome catalog of putative transcription factor binding sites. *Nucleic Acids Res.* 2005;33:D91-D97.
31. Grabe N. AliBaba2: context specific identification of transcription factor binding sites. *In Silico Biol.* 2002;2:S1-S15.
32. Cartharius K, Frech K, Grote K, et al. MatInspector and beyond: promoter analysis based on transcription factor binding sites. *Bioinformatics.* 2005;21:2933-2942.
33. Pan X, Ohneda O, Ohneda K, et al. Graded levels of GATA-1 expression modulate survival, proliferation, and differentiation of erythroid progenitors. *J Biol Chem.* 2005;280:22385-22394.
34. Laslo P, Spooner CJ, Warmflash A, et al. Multilineage transcriptional priming and determination of alternate hematopoietic cell fates. *Cell.* 2006;126: 755-766.
35. Radomska HS, Huettner CS, Zhang P, Cheng T, Scadden DT, Tenen DG. CCAAT/enhancer binding protein alpha is a regulatory switch sufficient for induction of granulocytic development from bipotential myeloid progenitors. *Mol Cell Biol.* 1998;18:4301-4314.
36. Fleetwood AJ, Cook AD, Hamilton JA. Functions of granulocyte-macrophage colony-stimulating factor. *Crit Rev Immunol.* 2005;25:405-428.
37. Horiguchi J, Warren MK, Kufe D. Expression of the macrophage-specific colony-stimulating factor in human monocytes treated with granulocyte-macrophage colony-stimulating factor. *Blood.* 1987;69:1259-1261.
38. Socolovsky M. Molecular insights into stress erythropoiesis. *Curr Opin Hematol.* 2007;14:215-224.
39. Gordon CT, Fox VJ, Najdovska S, Perkins AC. C/EBPdelta and C/EBPgamma bind the CCAAT-box in the human beta-globin promoter and modulate the activity of the CACC-box binding protein, *EKLF. Biochim Biophys Acta.* 2005;1729: 74-80.
40. Chen XW, Mo QH, Li Q, Zeng R, Xu XM. A novel mutation of −73(A–>T) in the CCAAT box of the beta-globin gene identified in a patient with the mild beta-thalassemia intermedia. *Ann Hematol.* 2007;86:653-657.
41. Ward AC. The role of the granulocyte colony-stimulating factor receptor (G-CSF-R) in disease. *Front Biosci.* 2007;12:608-618.
42. Smith LT, Hohaus S, Gonzalez DA, Dziennis SE, Tenen DG. PU.1 (Spi-1) and C/EBP alpha regulate the granulocyte colony-stimulating factor receptor promoter in myeloid cells. *Blood.* 1996;88: 1234-1247.
43. Friedman AD. C/EBPalpha and the G-CSF receptor gene: partners in granulopoiesis? *Blood.* 2001;98:2291-2292.
44. Seto Y, Fukunaga R, Nagata S. Chromosomal gene organization of the human granulocyte colony-stimulating factor receptor. *J Immunol.* 1992;148:259-266.
45. Saito M, Kiyokawa N, Taguchi T, et al. Granulocyte colony-stimulating factor directly affects human monocytes and modulates cytokine secretion. *Exp Hematol.* 2002;30:1115-1123.
46. de Figueiredo LL, de Abreu e Lima RS, Rego EM. Granulocyte colony-stimulating factor and leukemogenesis. *Mediators Inflamm.* 2004;13:145-150.
47. Johnson KD, Kim SI, Bresnick EH. Differential sensitivities of transcription factor target genes underlie cell type-specific gene expression profiles. *Proc Natl Acad Sci U S A.* 2006;103:15939-15944.
48. Graf T. Differentiation plasticity of hematopoietic cells. *Blood.* 2002;99:3089-3101.